

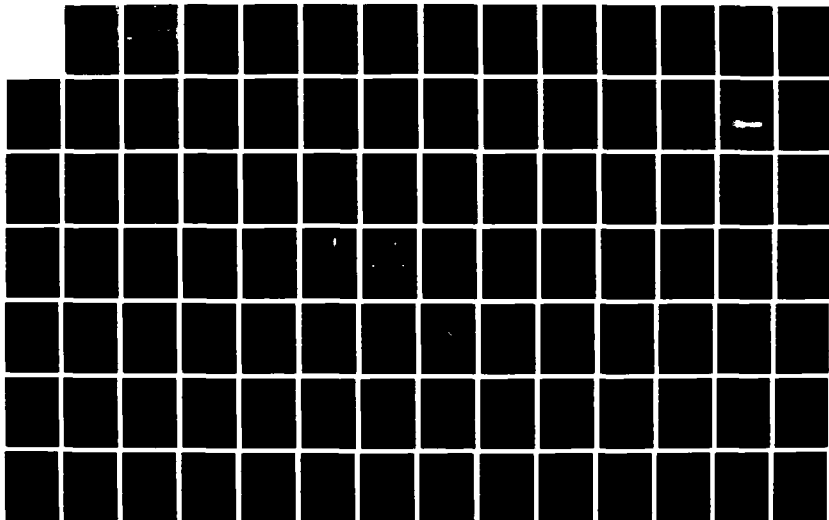
1/2

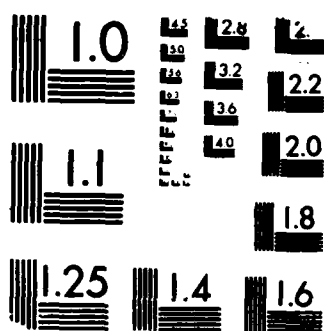
UNCLASSIFIED

F29601-85-K-0050

F/G 20/11

NL





MICROCOPY RESOLUTION TEST CHART
 (NBS 1963-A)

DTIC FILE COPY

2

AFWL-TR-86-104

AFWL-TR-
86-104

AD-A193 595

BEHAVIOR OF SAND/CONCRETE INTERFACES UNDER DYNAMIC LOADS

Robert L. Bigelis
Harold C. Sorensen

Washington State University
Pullman, WA 99163

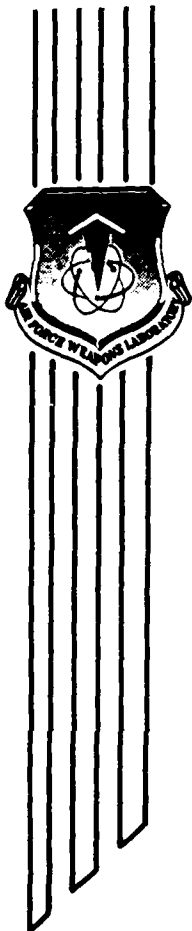
DTIC
ELECTE
MAY 31 1988
S H D

April 1988

Final Report

Approved for public release; distribution unlimited.

AIR FORCE WEAPONS LABORATORY
Air Force Systems Command
Kirtland Air Force Base, NM 87117-6008



This thesis was prepared by Washington State University, Pullman, Washington, under Contract F29601-85-K-0050, Job Order 8809131A with the Air Force Weapons Laboratory Kirtland Air Force Base, New Mexico. Douglas R. Seemann (NTES) was the Laboratory Project Officer-in-Charge.

When Government drawings, specifications, or other data are used for any purpose other than in connection with a definitely Government-related procurement, the United States Government incurs no responsibility or any obligation whatsoever. The fact that the Government may have formulated or in any way supplied the said drawings, specifications, or other data, is not to be regarded by implication, or otherwise in any manner construed, as licensing the holder, or any other person or corporation; or as conveying any rights or permission to manufacture, use, or sell any patented invention that may in any way be related thereto.

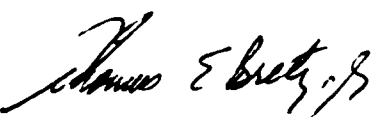
This report has been authored by a contractor of the United States Government. Accordingly, the United States Government retains a nonexclusive, royalty-free license to publish or reproduce the material contained herein, or allow others to do so, for the United States Government purposes.

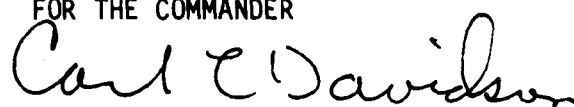
This report has been reviewed by the Public Affairs Office and is releasable to the National Technical Information Service (NTIS). At NTIS, it will be available to the general public, including foreign nationals.

If your address has changed, if you wish to be removed from our mailing list, or if your organization no longer employs the addressee, please notify AFWL/NTES, Kirtland AFB, NM 87117-6008 to help us maintain a current mailing list.

This thesis has been reviewed and is approved for publication.


DOUGLAS R. SEEMANN
Project Officer


THOMAS E. BRETZ, JR.
Lt Col, USAF
Chief, Applications Branch

FOR THE COMMANDER

CARL L. DAVIDSON
Col, USAF
Chief, Civil Engineering
Research Division

DO NOT RETURN COPIES OF THIS REPORT UNLESS CONTRACTUAL OBLIGATIONS OR NOTICE ON A SPECIFIC DOCUMENT REQUIRES THAT IT BE RETURNED.

UNCLASSIFIED
SECURITY CLASSIFICATION OF THIS PAGE

AD A193 395

REPORT DOCUMENTATION PAGE				
1a. REPORT SECURITY CLASSIFICATION Unclassified		1b. RESTRICTIVE MARKINGS		
2a. SECURITY CLASSIFICATION AUTHORITY		3. DISTRIBUTION/AVAILABILITY OF REPORT		
2b. DECLASSIFICATION/DOWNGRADING SCHEDULE		Approved for public release; distribution unlimited.		
4. PERFORMING ORGANIZATION REPORT NUMBER(S)		5. MONITORING ORGANIZATION REPORT NUMBER(S)		
		AFWL-TR-86-104		
6a. NAME OF PERFORMING ORGANIZATION Washington State University	6b. OFFICE SYMBOL (if applicable)	7a. NAME OF MONITORING ORGANIZATION Air Force Weapons Laboratory		
6c. ADDRESS (City, State, and ZIP Code) Pullman, WA 99163		7b. ADDRESS (City, State, and ZIP Code) Kirtland Air Force Base, NM 87117-6008		
8a. NAME OF FUNDING/SPONSORING ORGANIZATION	8b. OFFICE SYMBOL (if applicable)	9. PROCUREMENT INSTRUMENT IDENTIFICATION NUMBER F29601-85-K-0050		
8c. ADDRESS (City, State, and ZIP Code)		10. SOURCE OF FUNDING NUMBERS		
		PROGRAM ELEMENT NO. 62601F	PROJECT NO. 8809	TASK NO. 13
		WORK UNIT ACCESSION NO. 1A		
11. TITLE (Include Security Classification) BEHAVIOR OF SAND/CONCRETE INTERFACES UNDER DYNAMIC LOADS				
12. PERSONAL AUTHOR(S) Bigelis, Robert L. and Sorensen, Harold C.				
13a. TYPE OF REPORT Final	13b. TIME COVERED FROM Apr 85 to Jul 86	14. DATE OF REPORT (Year, Month, Day) 1988, April	15. PAGE COUNT 150	
16. SUPPLEMENTARY NOTATION Thesis				
17. COSATI CODES			18. SUBJECT TERMS (Continue on reverse if necessary and identify by block number)	
FIELD	GROUP	SUB-GROUP	Finite Elements Shear Transfer	
12	01		Interfaces	
20	11		Relative Motions	
19. ABSTRACT (Continue on reverse if necessary and identify by block number)				
<p>The objective of this research effort was to conduct an experimental program to determine the dynamic shear response of dry sand/concrete interfaces. A series of dynamic direct shear interface tests was performed using Yuma and McCormick Ranch sands in contact with concrete. Each concrete specimen was cast against a plywood form. These experiments were conducted using various values of normal stress, shearing velocity, and sand density.</p> <p>Results obtained from the experiments indicate that peak strength of the interface was not rate dependent, while residual strength decreased with increasing shearing velocity.</p> <p>Interface strength was found to be 100 to 108 percent of the strength of the surrounding sand. Theoretically, the interface strength is limited by the strength of the sand. This discrepancy is attributed to experimental error.</p> <p style="text-align: right;">(over)</p>				
20. DISTRIBUTION/AVAILABILITY OF ABSTRACT <input checked="" type="checkbox"/> UNCLASSIFIED/UNLIMITED <input type="checkbox"/> SAME AS RPT <input type="checkbox"/> DTIC USERS			21. ABSTRACT SECURITY CLASSIFICATION	
22a. NAME OF RESPONSIBLE INDIVIDUAL Douglas Seemann			22b. TELEPHONE (Include Area Code) (505) 846-6473	22c. OFFICE SYMBOL NTES

DD FORM 1473, 84 MAR

83 APR edition may be used until exhausted.
All other editions are obsolete.

SECURITY CLASSIFICATION OF THIS PAGE

UNCLASSIFIED

UNCLASSIFIED

SECURITY CLASSIFICATION OF THIS PAGE

19. ABSTRACT (Continued)

It is recommended that the strength of a dry sand/rough concrete interface be modelled using a Mohr envelope with a friction angle of 90 to 100 percent of the friction angle of the sand. This Mohr envelope should also be modified to model the curved envelope of typical sands when large ranges of normal stress are anticipated.

It is also recommended that postfailure response be modelled by a perfectly plastic model when high magnitude normal stresses are considered. While postfailure softening was found to be dependent on sand density and deformation rate, as well as normal stress when low magnitude normal stresses were applied, a near plastic behavior was observed beyond normal stresses of 2.5 MPa.

Accession For	
NTIS GRA&I	<input checked="checked" type="checkbox"/>
DTIC TAB	<input type="checkbox"/>
Unannounced	<input type="checkbox"/>
Justification	
By	
Distribution/	
Availability Codes	
Dist	Avail and/or Special
A-1	



UNCLASSIFIED

SECURITY CLASSIFICATION OF THIS PAGE

ACKNOWLEDGMENTS

I'd like to take this opportunity to thank the entire faculty and staff of the Department of Civil and Environmental Engineering for their guidance during my tenure at Washington State University.

I would also like to thank Dr. Timothy J. Ross and Mr. Doug Seemann of the Air Force Weapons Laboratory for providing this research opportunity.

Numerous individuals deserve mention and thanks for assistance in the experimental portion of this project: Dr. Richard Fragaszy for his soil Mechanics expertise, Ronald Galbraith for his help in pouring the concrete specimens and foundations, Bob Falk for his knowledge of the structures lab and hydraulic actuator system, and technicians Bill Elliot, Tom Weber, and Bob Lentz for their assistance with the machine work and the electronics of the testing devices.

I am also thankful to my parents, Mr. and Mrs. Charles F. Bigelis, for their love and support during my stay in Pullman.

Finally, I would like to thank the following people for their friendship and support: Steve Miller, Bill Bigelis, Kent Leyde, and Yosie and Lee Blakeslee.

BEHAVIOR OF SAND/CONCRETE INTERFACES UNDER DYNAMIC LOADS

Abstract

by Robert Lynn Bigelis, M.S.
Washington State University
December 1986

Chair: Harold C. Sorensen

The objective of this research effort was to conduct an experimental program to determine the dynamic shear response of dry sand/concrete interfaces. A series of dynamic direct shear interface tests was performed using Yuma and McCormick Ranch sands in contact with concrete. Each concrete specimen was cast against a plywood form. These experiments were conducted using various values of normal stress, shearing velocity, and sand density.

Results obtained from the experiments indicate that peak strength of the interface was not rate dependent, while residual strength decreased with increasing shearing velocity.

Interface strength was found to be 100% to 108% of the strength of the surrounding sand. Theoretically, the interface strength is limited by the strength of the sand. This discrepancy is attributed to experimental error.

It is recommended that the strength of a dry sand/rough concrete interface be modelled using a Mohr envelope with a friction angle of 90% to 100% of the friction angle of the sand. This Mohr envelope should also be modified to model

the curved envelope of typical sands when large ranges of normal stress are anticipated.

It is also recommended that post-failure response be modelled by a perfectly plastic model when high magnitude normal stresses are considered. While post-failure softening was found to be dependent on sand density and deformation rate, as well as normal stress when low magnitude normal stresses were applied, a near plastic behavior was observed beyond normal stresses of 2.5 MPa.

TABLE OF CONTENTS

	Page
ACKNOWLEDGMENTS.....	iii
ABSTRACT.....	v
LIST OF TABLES.....	ix
LIST OF FIGURES.....	x
LIST OF SYMBOLS.....	xiii
CHAPTER	
1 INTRODUCTION.....	1
2 LITERATURE REVIEW.....	4
2.1 Dynamic Tests of Granular Materials....	4
2.2 Soil/Concrete Interface Tests.....	7
3 ANALYTICAL MODELLING BY THE FINITE ELEMENT METHOD.....	16
3.1 Theoretical Interface Behavior.....	16
3.2 Finite Element Techniques.....	21
4 EXPERIMENTAL PROGRAM AND METHODS.....	25
4.1 Overview.....	25
4.2 Soil and Concrete Specimens.....	26
4.3 Standard Laboratory Soil Tests.....	28
4.4 Soil/Concrete Interface Tests.....	30
4.4.1 Direct Shear Test Device.....	30
4.4.2 Instrumentation.....	38
4.4.3 Operation of Test Device.....	41
4.5 Summary of Experimental Program.....	46

5	EXPERIMENTAL RESULTS.....	47
	5.1 Standard Laboratory Soil Tests.....	47
	5.2 Soil/Concrete Interface Tests.....	49
	5.2.1 Stress-Deflection Curves.....	51
	5.2.2 Failure Criterion.....	61
	5.2.3 Post-failure Response.....	65
	5.3 Measurement of Soil Deformation.....	71
6	CONCLUSIONS AND RECOMMENDATIONS.....	75
	6.1 Summary of Previous Literature.....	75
	6.2 Conclusions.....	75
	6.3 Recommendations.....	78
	REFERENCES.....	82
	APPENDIX Data Plots from Sand/Concrete Interface Tests.....	85

LIST OF TABLES

	Page
2.1 Parameters of Previous Tests of Rate Dependent Soil Behavior.....	6
4.1 Sand Density Statistics for Sand/Concrete Interface Tests.....	44
5.1 Results from Relative Density Tests.....	48
5.2 Rate Effect on Interface Friction Angle from Sand/Concrete Interface Tests.....	61
5.3 Friction Angles and Strength Ratios from the Dense Sand Tests.....	64

LIST OF FIGURES

	Page
1.1 Typical Soil/Structure Interaction Problem: Blast Load Conditions.....	2
2.1 Cylindrical Testing Device for Soil/Structure Interaction (from Brummonds and Leonards).....	9
2.2 Torsional Shear Ring Device (from Huck).....	11
2.3 Bi-linear Failure Surface for Dry Ottawa Sand/ Rough Concrete Interface (from Huck).....	13
2.4 Test Data from Dry Ottawa Sand/Rough Concrete Interface Test using a Normal Stress of 2.76 MPa (from Huck).....	13
3.1 Typical Shear Response of Dense and Loose Dry Sand at Low Confining Pressures (from Dunn).....	17
3.2 Various Mohr Failure Envelopes for Sands (from Bishop).....	19
3.3 Various Methods of Modelling the Failure Envelope of Dry Sand/Concrete Interfaces.....	20
3.4 Finite Element Techniques for Modelling Soil/ Structure Interaction.....	22
3.5 Interface Failure Envelope Currently in Use at the Air Force Weapons Laboratory.....	24
4.1 Geometry of Typical Concrete Specimen.....	27
4.2 Geometry of Sand/Concrete Direct Shear Device.....	32
4.3 Cross Section of Sand/Concrete Direct Shear Device.....	33
4.4 Configuration of Testing Device.....	35
4.5 Displacement vs. Time for Shearing Velocities of 2.54, 25.4, and 254. mm/second.....	37
4.6 Non-linear Response of Actuator Displacement at Shearing Velocity of 254 mm/second.....	37
4.7 Data Acquisition System.....	39
4.8 Cross Section Normal to Direction of Displacement..	42

5.1	Results of Mechanical Grain Size Distribution Tests for Yuma Sand and McCormick Ranch Sand.....	48
5.2	Results of Direct Shear Experiments for Yuma Sand McCormick Ranch Sand.....	50
5.3	Comparison of Inertial Effects to the Response from a Sand/Concrete Interface Test (V=254. mm/sec).....	50
5.4	Stress vs. Deflection For Dense Yuma Sand/Concrete Tests, V=2.54 mm/sec, 1st Repetition.....	52
5.5	Stress vs. Deflection For Dense Yuma Sand/Concrete Tests, V=2.54 mm/sec, 2nd Repetition.....	52
5.6	Stress vs. Deflection For Dense Yuma Sand/Concrete Tests, V=25.4 mm/sec, 1st Repetition.....	53
5.7	Stress vs. Deflection For Dense Yuma Sand/Concrete Tests, V=25.4 mm/sec, 2nd Repetition.....	53
5.8	Stress vs. Deflection For Dense Yuma Sand/Concrete Tests, V=254. mm/sec, 1st Repetition.....	54
5.9	Stress vs. Deflection For Dense Yuma Sand/Concrete Tests, V=254. mm/sec, 2nd Repetition.....	54
5.10	Stress vs. Deflection For Loose Yuma Sand/Concrete Tests, V=2.54 mm/sec.....	55
5.11	Stress vs. Deflection For Loose Yuma Sand/Concrete Tests, V=254. mm/sec.....	55
5.12	Stress vs. Deflection For Dense McCormick Sand/Concrete Tests, V=2.54 mm/sec, 1st Repetition.....	56
5.13	Stress vs. Deflection For Dense McCormick Sand/Concrete Tests, V=2.54 mm/sec, 2nd Repetition.....	56
5.14	Stress vs. Deflection For Dense McCormick Sand/Concrete Tests, V=25.4 mm/sec, 1st Repetition.....	57
5.15	Stress vs. Deflection For Dense McCormick Sand/Concrete Tests, V=25.4 mm/sec, 2nd Repetition.....	57
5.16	Stress vs. Deflection For Dense McCormick Sand/Concrete Tests, V=254. mm/sec, 1st Repetition.....	58
5.17	Stress vs. Deflection For Dense McCormick Sand/Concrete Tests, V=254. mm/sec, 2nd Repetition.....	58

5.18 Stress vs. Deflection For Loose McCormick Sand/ Concrete Tests, $V=2.54$ mm/sec.....	59
5.19 Stress vs. Deflection For Loose McCormick Sand/ Concrete Tests, $V=254$ mm/sec.....	59
5.20 Mohr Envelopes for Yuma Sand/Concrete.....	61
5.21 Mohr Envelopes for McCormick Sand/Concrete.....	62
5.22 Method of Quantifying Post-Failure Response.....	66
5.23 Softening vs. Density for Yuma Sand/Concrete.....	67
5.24 Softening vs. Density for McCormick Sand/Concrete..	67
5.25 Softening vs. Normal Stress for Dense Yuma Sand/Concrete	68
5.26 Softening vs. Normal Stress for Dense McCormick Sand/Concrete	68
5.27 Softening vs. Velocity for Dense Yuma Sand/Concrete	69
5.28 Softening vs. Velocity for Dense McCormick Sand/Concrete	69
5.29 Interface Shear Band Deformation Theory (from Chen and Schreyer).....	72
5.30 Measured Deformation Pattern.....	74
6.1 Comparison of Observed Mohr Envelopes from This Research and from Huck.....	77
6.2 Recommended Method for Determining the Mohr Envelope of a Dry Sand/Rough Concrete Interface....	79

LIST OF SYMBOLS

A	= surface area of interface
f_{ϕ}	= interface strength ratio
F	= shear force
N	= normal force
V	= shearing velocity
P	= normal stress
α	= adhesion
c	= cohesion
δ	= interface friction angle
ϕ	= soil friction angle
τ	= shear stress
σ	= normal stress
ρ	= correlation coefficient
τ_s	= failure shear stress for sand
σ_s	= failure normal stress for sand, interface
τ_i	= failure shear stress for interface

CHAPTER 1

INTRODUCTION

The stress-strain behavior of soil/concrete interfaces during applications of impulsive loads is of considerable interest to structural engineers. Examples of these include structural foundation motion due to seismic shock, strength requirements of concrete piles during pile driving, and shear stress transfer to buried structural components subjected to blast loads. Of particular interest in this study are the effects of blast loads on dry sand/concrete interfaces, but the theories presented herein are basically the same for each of the three previous examples.

As can be seen in the example in Figure 1.1, a blast load on a buried silo structure will generate stress waves propagating through the structure and the surrounding soil mass. These two stress waves will travel at different speeds due to the differences in the properties of the materials. In general, the stress wave speed in concrete will be greater than the stress wave speed in soil. Thus, differential shear deformation at the interface will occur during the stress wave passage in the structure, and again during the stress wave passage in the surrounding soil mass.

The shear behavior for sand/concrete interfaces may be affected by a number of factors. These include applied

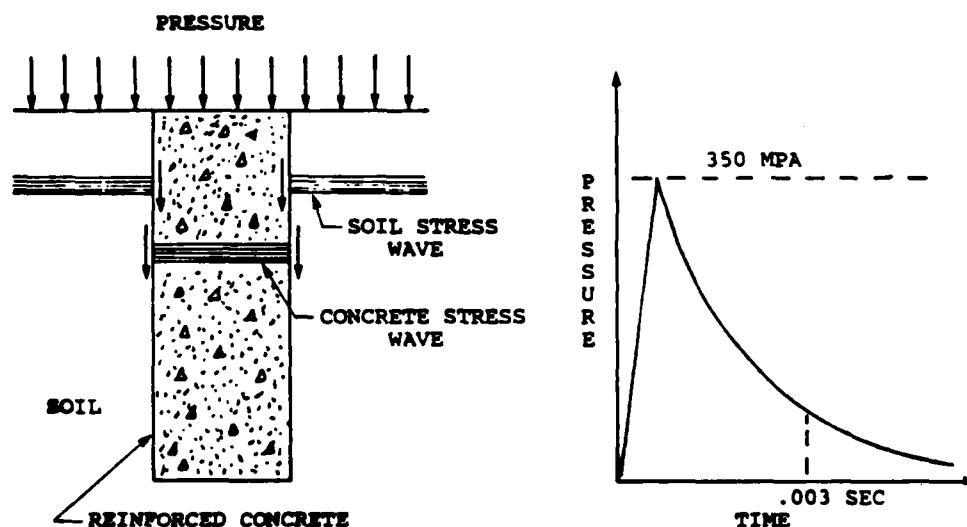


Figure 1.1 Typical Soil/Structure Interaction Problem: Blast Load Conditions

normal stress, soil density, water content of the soil, roughness of the concrete, soil particle diameter, loading rate, and individual material properties of the soil and concrete being modelled.

There has been a substantial amount of research conducted in the pre-failure to failure regime of stress-strain behavior of soil/structure interfaces, but post-failure response has not been discussed in the majority of these studies. While post-failure response is generally not a concern in conventional elastic analysis, both pre-failure behavior and post-failure behavior must be considered when high magnitude loads are involved. In addition, variations in the load rate have not been fully addressed. As noted previously, shear deformations induced by shock wave

propagation will occur at different rates due to the different wave speeds in the materials considered. This leads to the question of rate effects on interface behavior. The objective of this research is to conduct an experimental test program in order to determine the effects of load rate, normal pressure, and sand density on the pre-failure and post-failure shear response for sand/concrete interfaces.

The results of these experiments will be used to recommend appropriate soil/structure interaction parameters for use by personnel in the Civil Engineering Research Division at the Air Force Weapons Laboratory (AFWL), Kirtland Air Force Base, Albuquerque, New Mexico. Engineers at the AFWL use the computer program SAMSON2 to model soil/structure interaction. The SAMSON2 computer code is an explicit dynamic finite element program which uses sliding elements (or slidelines) to model dissimilar material interaction. Test results provided in this report will provide a better understanding of sand/concrete interface behavior.

CHAPTER 2

LITERATURE REVIEW

In order to properly present past research associated with dynamic soil/concrete interaction, this literature review is divided into two sections. The first section describes literature associated with the testing of sands under dynamic load conditions. Although soil behavior alone does not dictate the response of a soil/concrete interface, it is generally concluded by most researchers that the properties of the soil contribute most significantly to the interface response. The second section deals specifically with previous soil/media interaction testing programs.

2.1 Dynamic Tests of Granular Materials

In 1962 Whitman (24) published findings from an extensive test program concerned with the shear strength of sands under various loading rates. Triaxial tests with times to failure ranging from 5 minutes to 5 milliseconds were conducted using a hydraulic loading device. The 5 millisecond failure time corresponds to a deformation velocity of 3000 mm/sec. A total of 70 tests were performed on dry Ottawa 20-30 sand in both dense and loose states. The diameter of each specimen was 38 mm. The heights of the specimens ranged from 76 mm to 102 mm. A maximum confining pressure of 100 kPa was used. Results obtained from this study indicated that there is no strain rate effect on

strength in the range of 0.002% to 3% strain per sec, and a 2% to 10% increase in strength in the range of 3% to 420% strain per sec. In conclusion, Whitman stated that the change in friction angle is less than 10% for the loading rates which he used, and, that due to test uncertainties, this change is probably less than 5%.

Ito and Fujimoto (16) conducted a series of dynamic triaxial tests on air-dried Toyoura sands in 1980. The axial load was applied using a hydraulic actuator which produced strain rates up to 320% per second. For their tests this corresponds to a displacement rate of 370 mm/sec. The sand specimens which were tested had a diameter of 50 mm and a height 110 mm. Tests were conducted under confining pressures of 0.1, 0.2 and 0.3 MPa. Although there was considerable scatter in the results, Ito and Fujimoto reported that the strength at the highest strain rate was 10% to 20% higher than that produced at the lowest strain rate.

In 1984 Hungr and Morgenstern (15) performed a number of tests using a torsional shear ring device. This device could displace at a maximum velocity of 1000 mm/sec and could produce axial loads up to 200 kPa. Tests were performed on a number of different materials including polystyrene beads, two types of coarse sand, and a sand-rock flour mixture. Results of these tests showed that the

strength of the sands which were tested was not influenced by the shearing velocity.

Although a number of other researchers have conducted work in this area, these three publications give an indication as to the variation in results obtained from previous rate dependent strength tests on granular materials. A tabular summary of these and other test programs is shown in Table 1.1. Although all of the test results reported in this review range from a slight decrease

Table 2.1 Parameters of rate dependent tests¹

Author	Testing device	Materials tested	Maximum velocity mm/sec	Maximum stress kPa	Rate effect
Whitman 1962(24)	Triaxial	Ottawa sand	3000.	100	Slight
Healy 1963(13)	Torsional	Ottawa sand	30.0	63	Slight
Novosad 1964(19)	Torsional	Glass beads	500.0	2	None
Scarlett 1969(20)	Torsional	Sand	30.0	6	None
Bridgwater 1972(3)	Torsional	Glass beads	2000.	25	Yes
Ito 1980(16)	Triaxial	Toyoura sand	370.	300.	Yes
Hungr 1984(15)	Torsional	Sand and flour	1000.	200	None

1. Portions of this table were taken from Hungr(15).

in strength to a 20% increase in strength with increasing strain rate, it can be seen that the majority of these studies found slight to no rate dependent effects on the strengths of dry granular materials.

2.2 Soil/Concrete Interface Tests

In the review of previous soil/structure interaction testing programs, it was found that the majority of results were presented in the form of the ratio produced by dividing the interface friction angle by the friction angle of the soil tested, i.e.,

$$f_{\phi} = \delta / \phi$$

where f_{ϕ} = interface strength ratio, δ = interface friction angle, and ϕ = soil friction angle. This same nomenclature will be used in this review. Test results from previous work with dry sand and concrete will be emphasized in this presentation, since they are of primary interest in this study.

In 1961 Potyondy (20) performed a comprehensive testing program using a static direct shear device. Interface experiments were conducted using sand and clay in contact with several different construction materials including steel, concrete and wood. Concrete specimens with smooth and rough surfaces were used. The qualitative descriptions of smooth and rough are somewhat arbitrary, however, the common approach is to describe concrete as having a smooth surface when it has been poured against surfaces as rough or

less rough than steel and to describe concrete as having a rough texture when it has been poured against surfaces as rough or rougher than plywood. Potyondy's results indicate the strength ratios $f_\phi = 0.89$ for smooth concrete and $f_\phi = 0.99$ for rough concrete when dry sands are used.

A slightly weaker interface was found for the smooth concrete by Clough and Duncan (6) in 1971. The concrete surface was prepared by casting the concrete against a steel form. Using a direct shear device for experiments involving dry sand/concrete interfaces, they found a strength ratio (f_ϕ) equal to 0.83. Similar results were reported by Desai and Holloway (7) in 1972 and Desai (8) in 1976. Values for f_ϕ ranged from 0.87 to 0.89 for the various sand densities and surfaces which were tested by Desai using a static direct shear device.

In 1979 Kulhawy and Peterson (17) published the results of an extensive testing program for sand/concrete interfaces also using a static direct shear device. Four surface textures of concrete were used ranging from concrete poured against glass (very smooth) to concrete poured against sand (very rough). The sand specimens consisted of two types, a uniform sand and a well graded sand. Both soils were cohesionless. Results obtained from this test program indicated that f_ϕ values ranged from 0.78 to 1.00 for the smooth interfaces and from 0.93 to 1.00 for the rough

interfaces. A value for f_ϕ equal to 1.00 indicates soil failure near the concrete interface.

Brummond and Leonards (4) reported results for static and dynamic sand/structure interaction experiments conducted in 1973. The testing device, shown in Figure 2.1, consisted of a concrete test rod encased in a cylinder of sand. The rod was located along the center axis of the cylinder and the sand was confined by a rubber membrane. Each of the concrete rods which were tested were 29 mm in diameter and 356 mm in length. Interface normal stresses ranging from 8.62 kPa to 86.2 kPa were applied by creating a negative pressure within the membrane. Deformation velocities which were used in the test program were not reported. However,

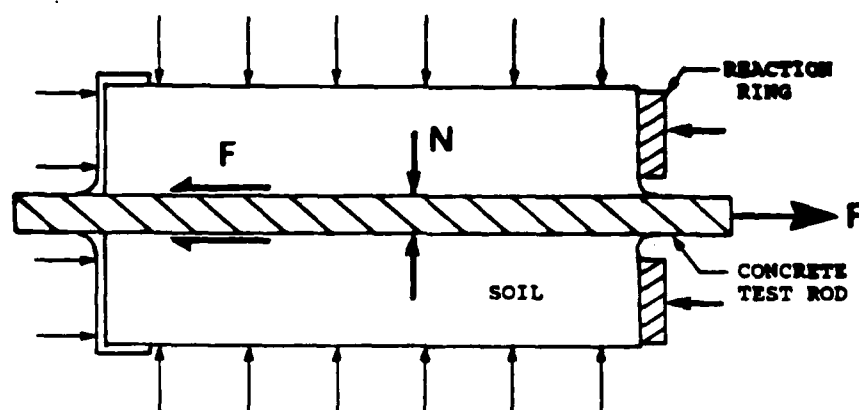


Figure 2.1 Cylindrical Testing Device for Soil/Structure Interaction (from Brummonds and Leonards)

Brummonds and Leonards did report that peak stress values occurred after approximately 5 minutes for static loading conditions and that peak stress values occurred within 1 to 2 milliseconds under dynamic loading conditions. Small piezoelectric gages were placed in the sample next to the test rod to detect any changes in the normal pressure during the dynamic experiments.

The sand specimens used by Brummond and Leonards consisted of a uniformly graded sand with $\phi = 40$ degrees and an angular sand with $\phi = 48$ degrees. Concrete rods with both smooth and rough surfaces were used. Results from these tests indicated that for the smooth concrete rods the average strength ratio (f_ϕ) was 0.76 for the static tests and 0.84 for the dynamic tests. For the rough concrete rods, the average strength ratio (f_ϕ) was 0.91 for the static tests and 0.98 for the dynamic tests. The results from these tests indicate that an increase in interface strength occurred for an increase in the load rate.

In 1974 Huck (14) introduced the use of the torsional shear ring device for soil/structure interaction experiments. This apparatus is shown in Figure 2.2. A uniform state of shear strain is produced throughout the interface plane with this type of device. Unlike the direct shear device, the interface surface area is constant for even very large values of shear strain.

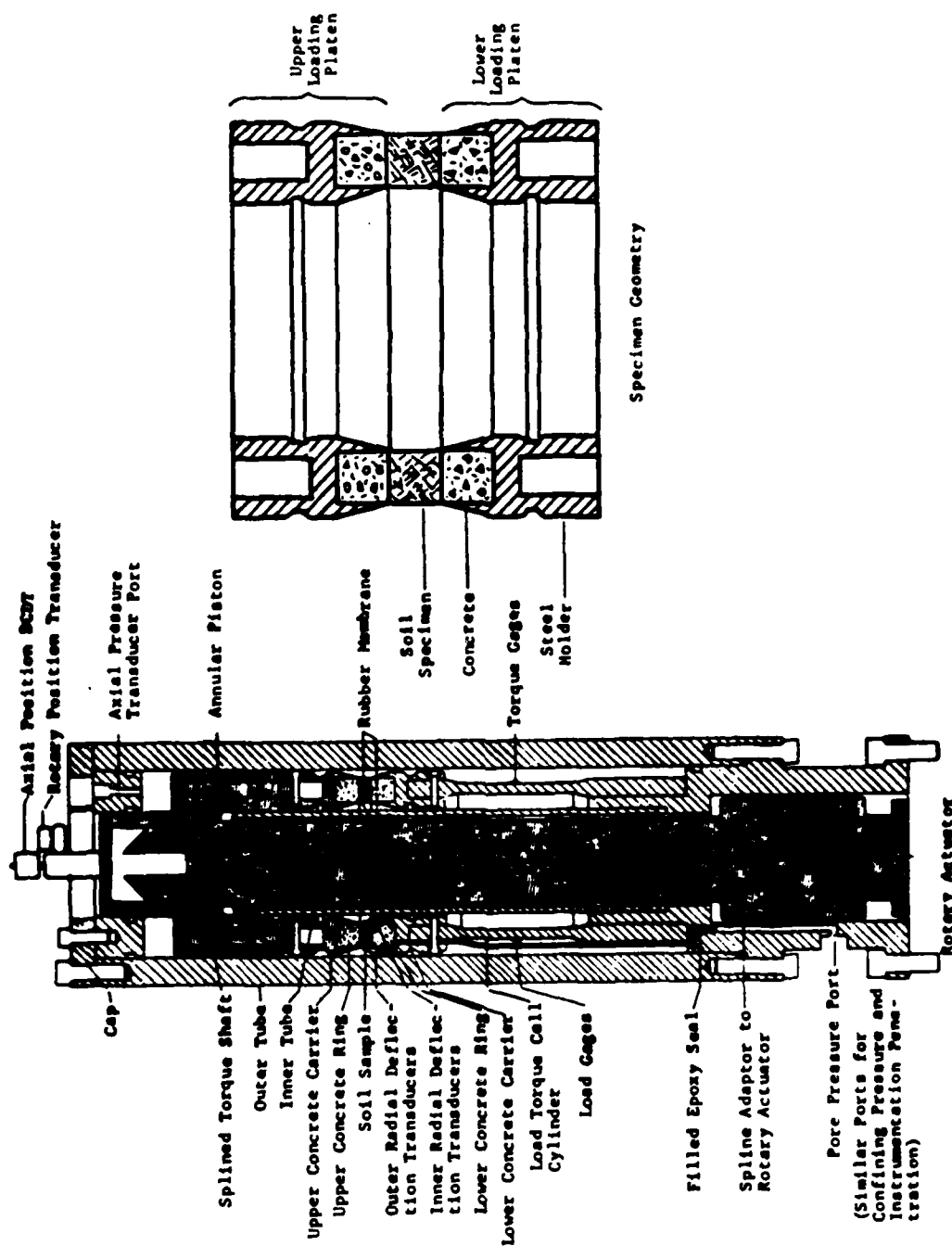


Figure 2.2 Torsional Shear Ring Device (from Huck).

Dynamic tests were conducted by Huck in which samples of sand and clay in contact with both smooth and rough surfaces of concrete were used. The sand which was used in these tests was an Ottawa 20-40 sand with a friction angle of $\phi = 40$ degrees. To place the sand in the test device, a "raining" procedure was used which produced a sand density of 1.78 g/cc. This corresponds to a relative density of 80%.

Normal pressures of 1.38, 2.76, 5.52 and 11.0 MPa were used in the experimental program. The normal loads were applied statically, and the specimen was dynamically sheared with the use of a hydraulic rotary actuator. Times to failure ranged from 4 to 7 milliseconds. Static tests were not conducted, and no attempt was made to control or vary the shearing velocity.

The results obtained from experiments performed by Huck on sand/rough concrete interfaces can be interpreted as a bi-linear failure surface model as shown in Figure 2.3. To explain this behavior, Huck theorized that failure of a sand/concrete interface could be separated into two failure modes. Under low normal stresses, soil failure occurred near the interface, but, under higher normal stresses the interface became weaker than the soil, and, thus, failure of the interface occurred. Although his discussion explains the test results which were reported, there was no visual evidence, such as photographs or personal observations,

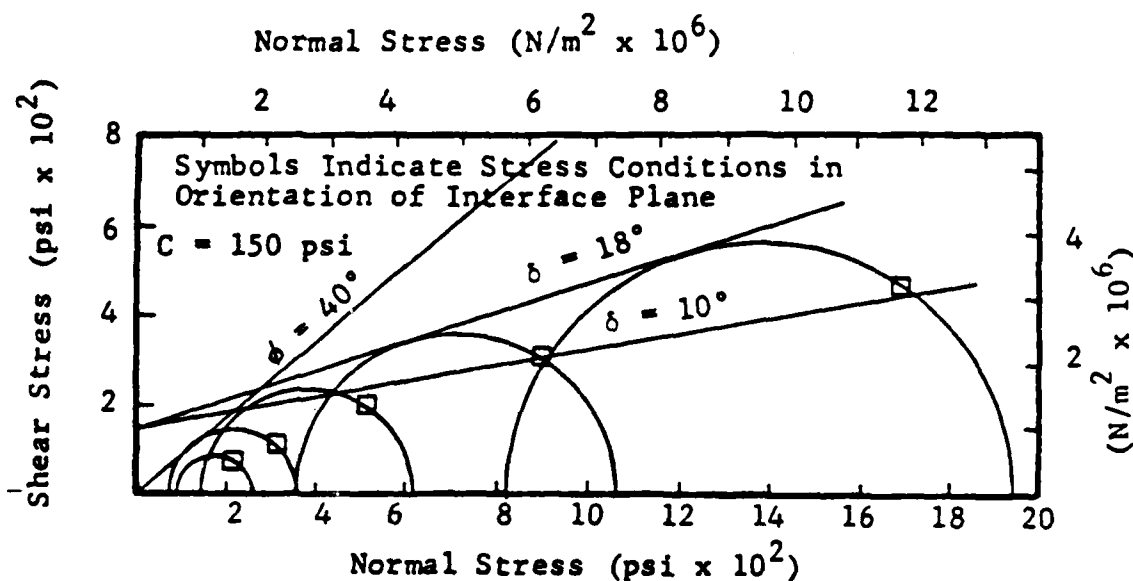


Figure 2.3 Bi-linear Failure Surface for Dry Ottawa Sand/Rough Concrete Interface (from Huck).

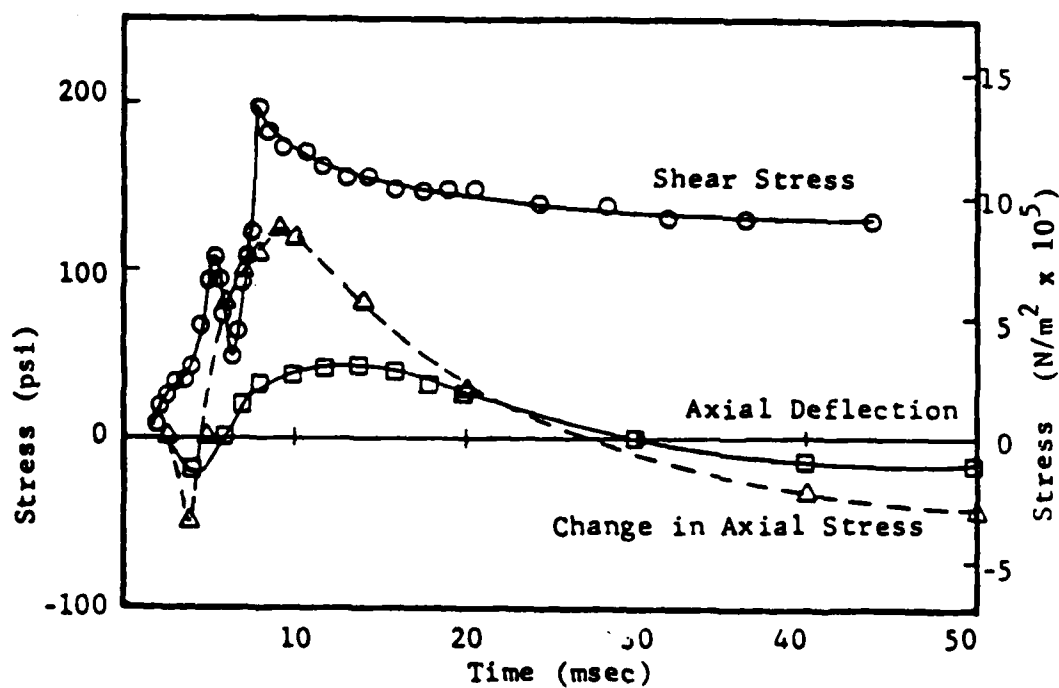


Figure 2.4 Test Data from Dry Ottawa Sand/Rough Concrete Interface Test using a Normal Stress of 2.76 MPa (from Huck).

given to support the concept that separate modes of failure actually occurred at the interface during the experiments.

It is not appropriate to compare the bi-linear failure curve reported by Huck to the strength ratio f_ϕ since the latter is based on a single linear relationship. But, using the data values from the experiments involving the lower normal pressures which were performed by Huck, a strength ratio (f_ϕ) of 0.50 was calculated by this author.

Post-failure response of Ottawa sand/rough concrete experiments conducted by Huck, shown for the 2.76 MPa test in Figure 2.4, indicates a general decrease and flattening of the shear stress curve as the relative deflection increases. This behavior is described as strain softening and is typical of the behavior of dense sands (11). But a further investigation of these data indicates that the normal stress decreases at a rate faster than the rate of decrease in the shear stress, thus indicating a condition of strain hardening, which is not typical of post-failure response of sand. No explanation was given by Huck for this behavior.

Finally, in 1985 Drumm and Desai (10) conducted a series of dynamic and static tests using Ottawa sand and concrete. The test device which was used was a modified direct shear device designed to allow for a more uniform shear stress distribution than the shear stress distribution produced by the standard direct shear test box. Dynamic

shearing loads were applied using a hydraulic actuator, and the maximum shearing velocity which was used produced failure after approximately 125 milliseconds. Drumm and Desai found that interface strength was independent of shearing velocity for the shearing velocities which were used. Therefore, strength ratios were reported only for the static tests. For a sand/smooth concrete interface, the strength ratio (f_{ϕ}) was found to be 0.93. No post-failure analysis was conducted by Drumm and Desai.

In summary, the results from various experimental studies using sand/concrete interfaces indicate that the interface strength ranges between 50% to 100% of the strength of the sand. If results reported by Huck are ignored, this range can be narrowed to 75% to 100% of sand strength. Effects of shearing velocity on interface strength reported by different researchers varied between no change to a 10% increase in strength with increasing shearing velocity.

CHAPTER 3

ANALYTICAL MODELLING BY THE FINITE ELEMENT METHOD

The finite element method is currently the most popular procedure for performing stress calculations in dynamic soil/structure interaction problems. In order to describe finite element techniques of interface modelling, a brief review of interface behavior shall be presented. The intent of this chapter is to briefly describe the expected results of the test program and to summarize current finite element methodologies used to model interface behavior.

3.1 Theoretical Interface Behavior

As indicated in previously mentioned literature, the shear response of a sand/concrete interface is very similar to the shear response of the surrounding soil mass. However, an important difference is that the interface strength is generally weaker than that of the soil. To better understand the behavior of sand/concrete interfaces, a review of typical shear behavior of sands will be presented.

For a given granular soil, the shear response will depend primarily on the density of the soil and the magnitude of the applied confining stress. Under low confining pressures, the stress-strain response of a sand is similar to the response shown by the stress-strain curves in Figure 3.1.

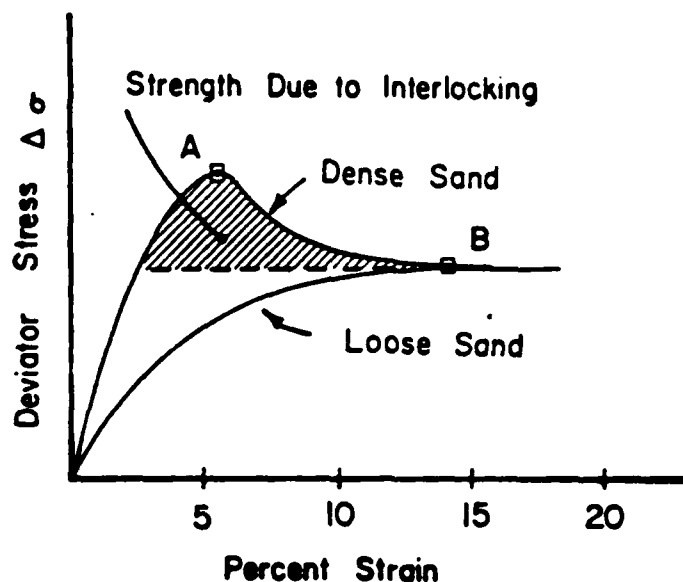


Figure 3.1 Typical Shear Response of Dense and Loose Dry Sand at Low Confining Pressures (from Dunn)

These two curves depict the results of shear strength tests which were performed using two different densities of sand. While both curves are nonlinear, each curve is markedly different. There is a pronounced peak in the stress-strain curve for the dense sample. As strain is increased beyond this peak, a decrease in stress is observed until a constant level of stress, referred to as the residual stress, is attained.

The peak in the stress-strain curve of the dense sand is attributed to particle interlocking. The post-peak decrease in stress is due to energy loss when particles release and pass by one another.

The loose sand sample on the other hand has no apparent peak, and the shear stress rises slowly to the same residual

value attained for the dense sample. Since the sample is tested in a loose state, the soil particles will not interlock and will simply pass by one another.

In both the dense sand and loose sand tests, the density of the sand sample will change during the performance of the test. Using an initially dense sand sample, the density will increase when shear displacement begins. However, as shearing proceeds further, the dense sample will decrease in density due to the dilation caused by particles rolling over one another. The loose sample on the other hand will only densify during shear deformation. Finally, at the residual stress value, point B in Figure 3.1, both sands will have the same final density.

These types of responses are only characteristic of sands which are tested at low confining pressures. Under greater magnitudes of confining pressure, a dense sand will begin to respond more like a loose sand. That is, the stress peak for a dense sand will become less pronounced as the magnitude of the confining stress is increased. This peak will eventually disappear at very high levels of confining stress. This response has been documented by a number of researchers (1,23).

High levels of confining stress will also affect the shape of the Mohr envelope (strength envelope) for dense sands as shown in Figure 3.2. Mohr envelopes are created by plotting shear stress values at failure (point A in Figure

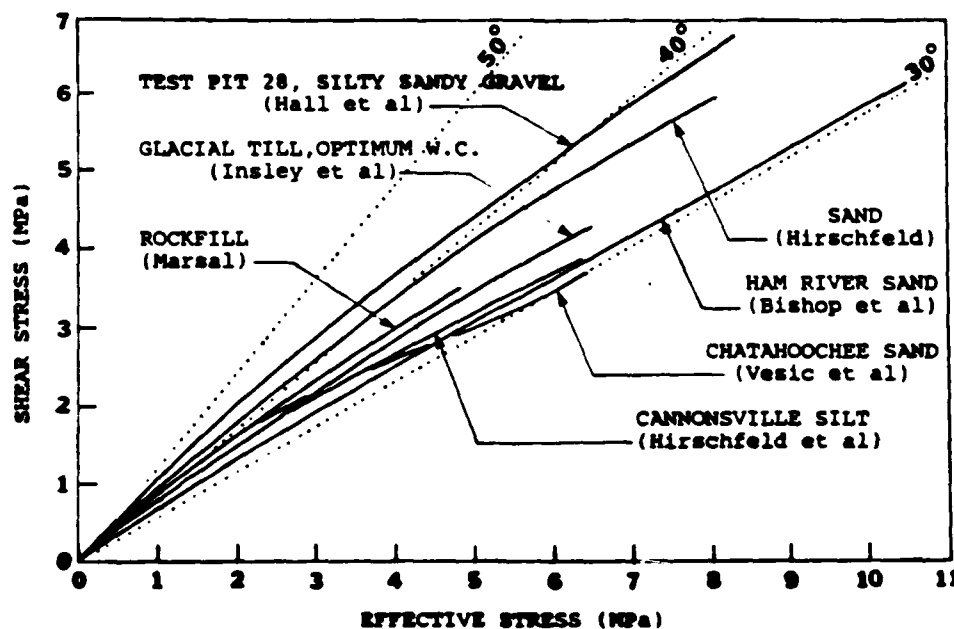


Figure 3.2 Various Mohr Failure Envelopes for Sands (from Bishop).

3.1 for the dense sand) against the normal stress at which the test was conducted. When the range of normal stress being considered is small, the Mohr envelope can be considered linear. Hence, a constant value for the friction angle is used. But when a large range of normal stress is considered the Mohr envelope for dense sands becomes slightly curved. This curvature is a result of particle crushing during shear displacement when the sand is subjected to high magnitude normal stresses.

As mentioned above, the interface strength is generally considered to be weaker than the strength of the surrounding soil mass. This weakened Mohr envelope, as shown in Figure

3.3, has been modelled by different methods. Under a low range of normal stress, Desai and others have used a linear relationship. Under greater ranges of normal stress, Huck suggests different modes of failure occur and a much weaker interface is observed. Another possible method would be to consider the curvature of the Mohr envelope for dense sands and reduce this envelope by some reduction factor. Results obtained from sand/concrete interface tests conducted in this research program will be compared to these three types

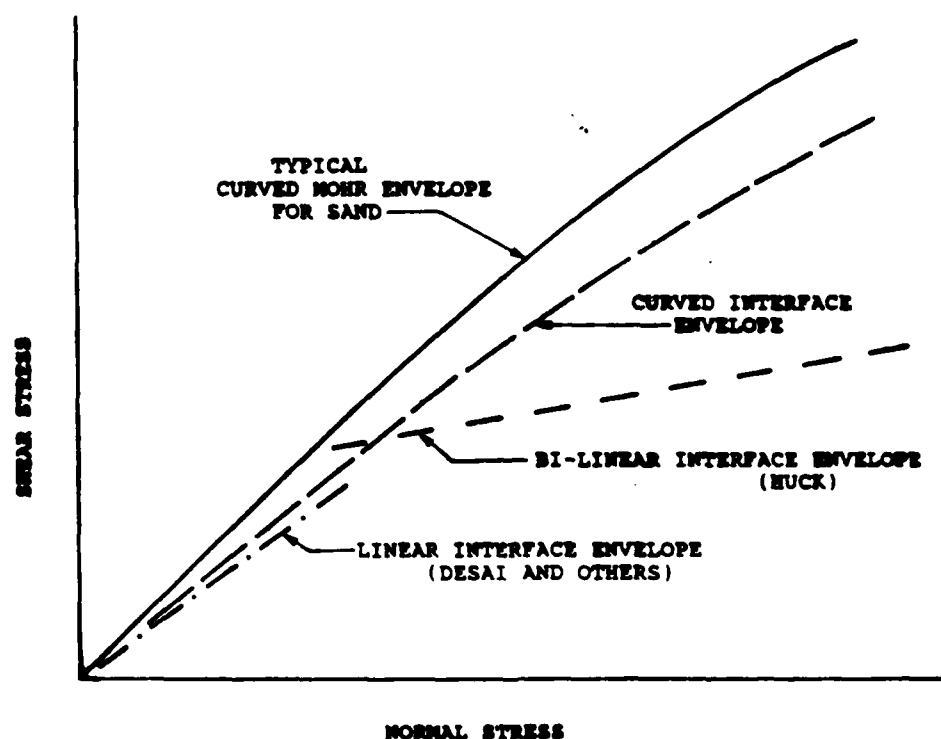


Figure 3.3 Various Methods of Modelling the Failure Envelope of Dry Sand/Concrete Interfaces

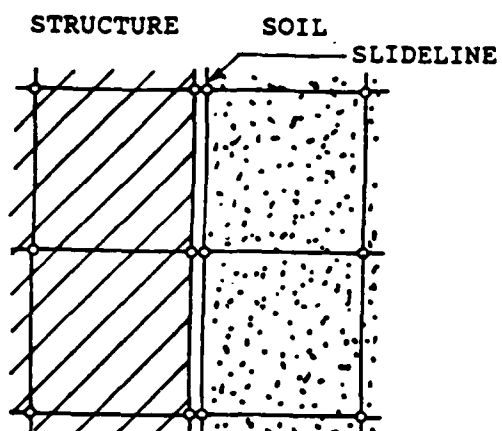
of weakened Mohr envelopes to determine which model most closely describes the actual behavior.

3.2 Finite Element Techniques

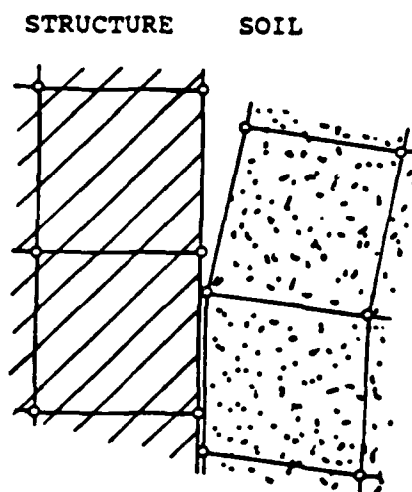
To model dynamic soil/structure interaction using finite elements, a method must be available that will model the large shear deformations that occur at dissimilar material interfaces. These deformations can be modelled with the use of the sliding element method or the interface element method. These two methods are depicted in Figure 3.4. The method of sliding elements allows adjacent elements to simply slide relative to each other. Interface elements on the other hand are elements which simulate the unique qualities of the interface. These interface elements are placed between the soil elements and the structural elements. For both of these methods, the movement of elements on either side of the interface will be governed by appropriate interface stress-strain models.

The method which currently exists in the SAMSON2 finite element code at the AFWL is the sliding element method. The interface between a number of sliding elements is commonly called a slideline. During an analysis, the nodes on opposite sides of the slideline are initially bonded, i.e., they are rigidly connected and can transfer shear and normal forces across the interface. Shear stresses and normal stresses are calculated for each node on the slideline and compared to stress values from a Mohr envelope during each

SLIDING ELEMENTS

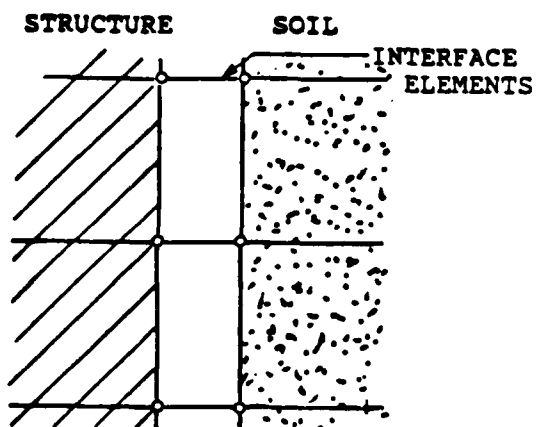


UNDISTORTED INTERFACE

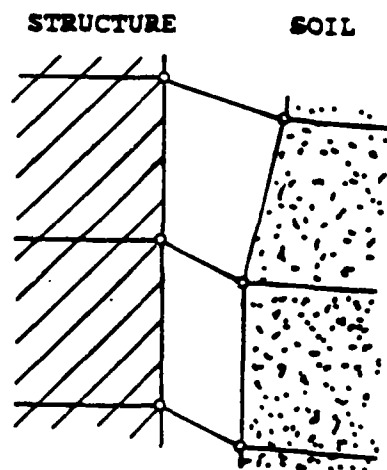


DISTORTED INTERFACE

INTERFACE ELEMENTS



UNDISTORTED INTERFACE



DISTORTED INTERFACE

Figure 3.4 Finite Element Techniques for Modelling Soil/Structure Interaction.

iteration of the explicit dynamic analysis. If the stress state at an interface node exceeds the Mohr envelope stress value, the node is released (failure), otherwise the node remains bonded to the slideline.

The movement of a node after it has been released will be dictated by the sign of the normal stress at the interface. If a tension state exists normal to the slideline at the point of the released node, the interface nodes will be allowed to separate. Nodes will move away from each other during the time step and a gap at the slideline will form. If a compressive normal stress state exists at the point of the released node, the elements will slide relative to one another according to a post-failure friction law. This procedure is continued throughout the analysis.

The Mohr envelope currently in use at the AFWL is the interface bi-linear failure criterion suggested by Huck (14) in 1974. This failure criterion is shown in Figure 3.5. Post-failure behavior is governed by a perfectly plastic model suggested by the Army Waterways Experiment Station in 1985 (25). This perfectly plastic model limits the transferable shear stress across the slideline to the limiting value associated with the bi-linear failure criterion.

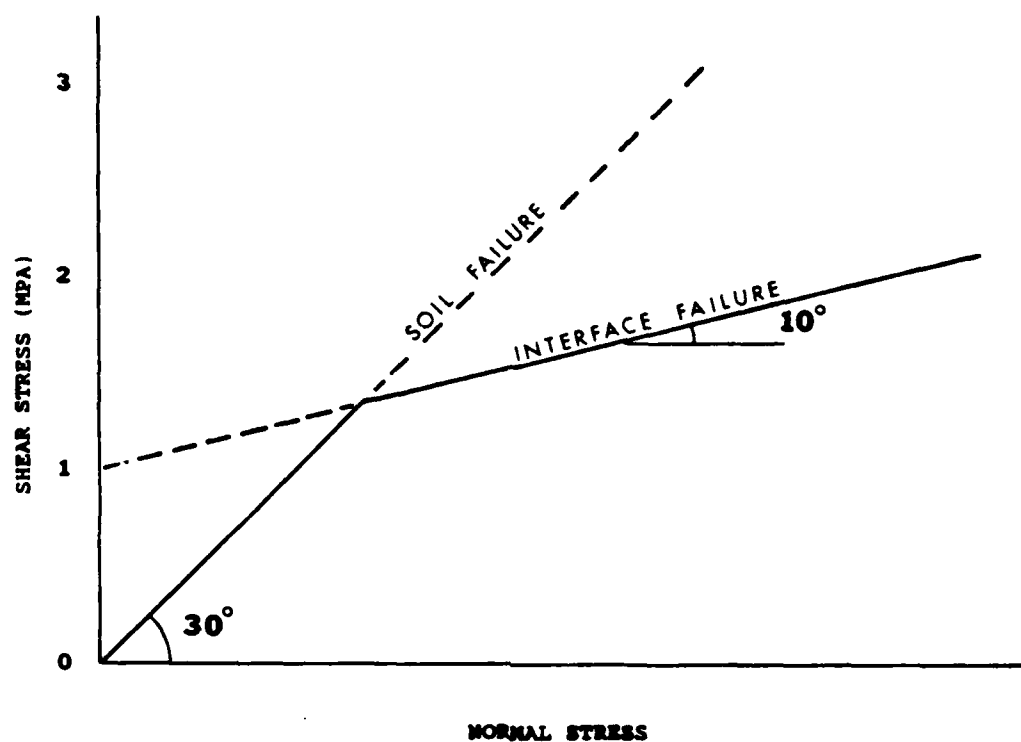


Figure 3.5 Interface Failure Envelope Currently in Use at the Air Force Weapons Laboratory.

CHAPTER 4

EXPERIMENTAL PROGRAM AND METHODS

4.1 Overview

The basic objective of this research is to conduct an experimental program to predict the failure criterion and post-failure response of a sand/concrete interface when subjected to dynamic shear loads. The quantification of the failure criterion will consist of the ratio $f_\phi = \delta/\phi$. Quantification of the post-failure response will consist of determining the amount of softening, or shear stress drop, after the peak failure stress occurs.

Friction angles are calculated by determining the least squares linear fit of the shear stress values versus normal stress data values at failure. The angle that this line makes with the normal stress axis, or horizontal axis, is the friction angle of the soil. The normal stress range used in this experimental program is small enough to assume a linear Mohr envelope.

Before proceeding, an important assumption must be explained. The most accurate procedure used to find the strength ratio (f_ϕ) would be to determine both ϕ and δ using a torsional shear ring device. However, for this research a simpler device was desired and, thus, direct shear devices were used to determine both ϕ and δ . It must be understood that direct shear devices tend to give slightly higher

values of friction angles than torsional devices (2), but the assumption is made herein that the ratio f_{ϕ} will be the same for both devices.

The experimental program which was developed includes three standard laboratory soil tests: mechanical grain size distribution, relative density and static direct shear. The program also includes tests for sand/concrete interfaces using a special dynamic direct shear device designed and built specifically for this research. Section 4.2 briefly describes the soil and concrete specimens which were used, while the procedures and devices used for the standard soil tests and the soil/concrete tests are described in sections 4.3 and 4.4, respectively.

4.2 Soil and Concrete Specimens

Two different soil types, Yuma sand and McCormick Ranch sand, are used in this test program. These two angular sands originated from the central region of New Mexico. In order to eliminate inaccuracies caused by the large grained particles and the small rocks in the samples, the sand was passed through a #12 U.S. Standard Sieve (diameter = 1.70 mm). The particles which did not pass the #12 sieve were discarded.

Because of the range of normal pressures used for the sand/concrete interface tests, it was decided, from review of previous testing programs (10), that the relatively soft outside surface of the concrete specimen would be worn off

after each test, thus changing the surface texture of the concrete specimens. For this reason a different concrete specimen was used for each test. It is believed that a new surface for each test would better simulate actual field conditions than that produced by using the same specimen over and over. Figure 4.1 shows the geometry of a typical specimen.

The concrete mix design consisted of a combination of 3.2 mm aggregate, sand, Type I and II Portland cement, and water. The mix was designed for a compressive strength of 40.0 MPa. Uniaxial compression tests on three cylinders produced an average 28-day compressive strength of 43.4 MPa.

The surface texture of each concrete specimen was that obtained by casting the concrete against an unsanded plywood form. This surface will be defined as having a rough texture.

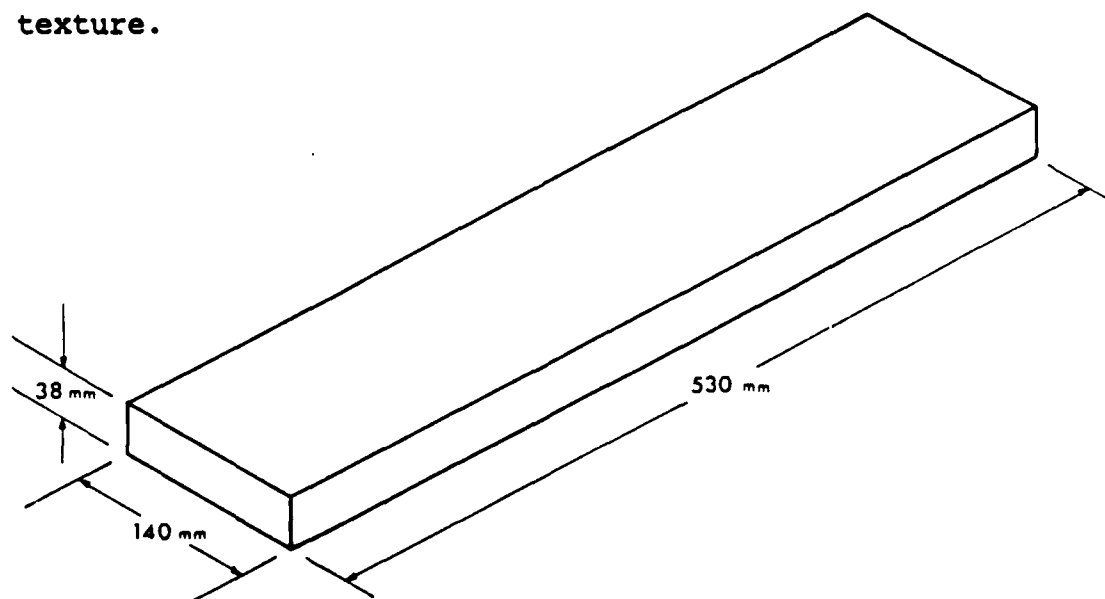


Figure 4.1 Geometry of Typical Concrete Specimen

4.3 Standard Laboratory Soil Tests

In order to identify the strength and classification of a soil, it is necessary to perform a number of standard laboratory tests. The tests used in this program include mechanical grain size distribution tests, relative density tests and static direct shear tests. Mechanical grain size distribution tests are used to determine the relative proportions of the different grain sizes which make up a given soil mass. The relative density test provides a range for the maximum and minimum densities that the soil might normally have in the field. The direct shear test is a convenient way to determine the Mohr envelope (strength) of a soil. Each test was performed on various oven dry samples of both Yuma sand and McCormick Ranch sand.

Each of the grain size distribution tests was performed according to procedures outlined by ASTM D421-58 and D422-63. Two grain size tests were performed for each sand type using a 1000 gram sample of sand for each test. This resulted in a total of four tests. It is reiterated here that the samples which were used had been previously passed through a #12 US Standard sieve. The difference between sample weight before testing and retained sample weight after testing produced an error of less than 1% for each test which was performed.

Each relative density test was performed according to the procedure outlined by ASTM D2049-69. The objective of

the relative density tests is to determine the minimum and maximum densities of the sand. To determine the maximum density of the sand, a sample was placed into a standard compaction mold in five layers. Each layer was densified by applying a static surcharge of approximately 55 kPa on the sample and then tapping the sides of the mold 200 times with a hard rubber mallet. After the five layers were placed, the sample was weighed and the density of the soil in the mold was calculated. To determine the minimum density of the sand, a sample was carefully spooned into the compaction mold in a single loose layer. The specimen was then weighed, and the density of the soil was calculated. Each minimum and maximum test was performed three times. The lowest minimum density and the highest maximum density obtained from these three tests were taken as the resulting minimum and maximum densities of the sand, respectively.

Each direct shear test was performed according to the procedure outlined by ASTM D3080-72. Direct shear tests were conducted by the use of an Engineering Equipment Laboratory (EEL) motorized direct shear machine. These tests were conducted at normal pressures of 0.325, 0.635 and 1.25 MPa and on sand samples with relative densities of approximately 80%. The densities which were used were 1.60 g/cc (79%) for Yuma sand and 1.52 g/cc (76%) for the McCormick Ranch sand. Sand samples were prepared for testing by placing a known weight of sand into the 63.5 mm

diameter shear box. These samples were placed in three layers, each layer being tamped 100 times with a 60 mm diameter load plate and plastic hammer. After sand placement, a static gravity normal load was applied and the sample was sheared. Shearing displacement proceeded at a rate of 1 mm/minute, and each sample was sheared to a full displacement of 10 mm. Shearing load and displacement were constantly monitored with the use on an x-y plotter.

4.4 Soil/Concrete Interface Tests

The primary work of interest in this project is the dynamic sand/concrete interface tests. Forty-eight tests were conducted using a dynamic direct shear device constructed for this research. Each test was performed to a full displacement of approximately 25 mm. Variable parameters for the sand/concrete interface test program are as follows:

2 soil types: Yuma and McCormick Ranch sands

2 densities: Dense and Loose

3 normal pressures: 0.690, 1.38 and 2.76 MPa

3 shear velocities: 2.54, 25.4 and 254. mm/second

The following subsections explain the dynamic shear device, the data aquisition system, and the test methods and procedures used during these tests.

4.4.1 Direct Shear Device

The direct shear device was designed to allow for the application of dynamic shear and static normal loads to a

soil/structure interface. The basic geometry and cross section of the device are shown in Figures 4.2 and 4.3. This device can accommodate a maximum sample height of 57 mm and a maximum concrete surface area of 426 cm². The longitudinal dimension of the sand confinement box is made considerably greater than the width dimension of the box so as to decrease the influence of the front and back confining walls on the shear strain distribution of the sand.

Most commercially available direct shear devices for soil come equipped with a mechanism to adjust the gap between the lower and upper shear boxes. For the soil/concrete direct shear device, this gap is adjusted by the raising or lowering of two movable plates. These plates are mounted on the front and back walls of the soil confining box as shown in Figure 4.3. After performing a number of trial tests, it was found that the interface was able to resist more shear stress before failure with a gap height of 0.5 mm than with the plates at the full height of 3.2 mm. To simulate the large shear strains inherent in soil/structure interaction, the gap was set at the full height of 3.2 mm. This gap height of 3.2 mm is approximately two times the value of the diameter of the maximum grain size in the soil, thus allowing soil failure to occur near the interface if the strength of the interface is found to be greater than the strength of the soil.

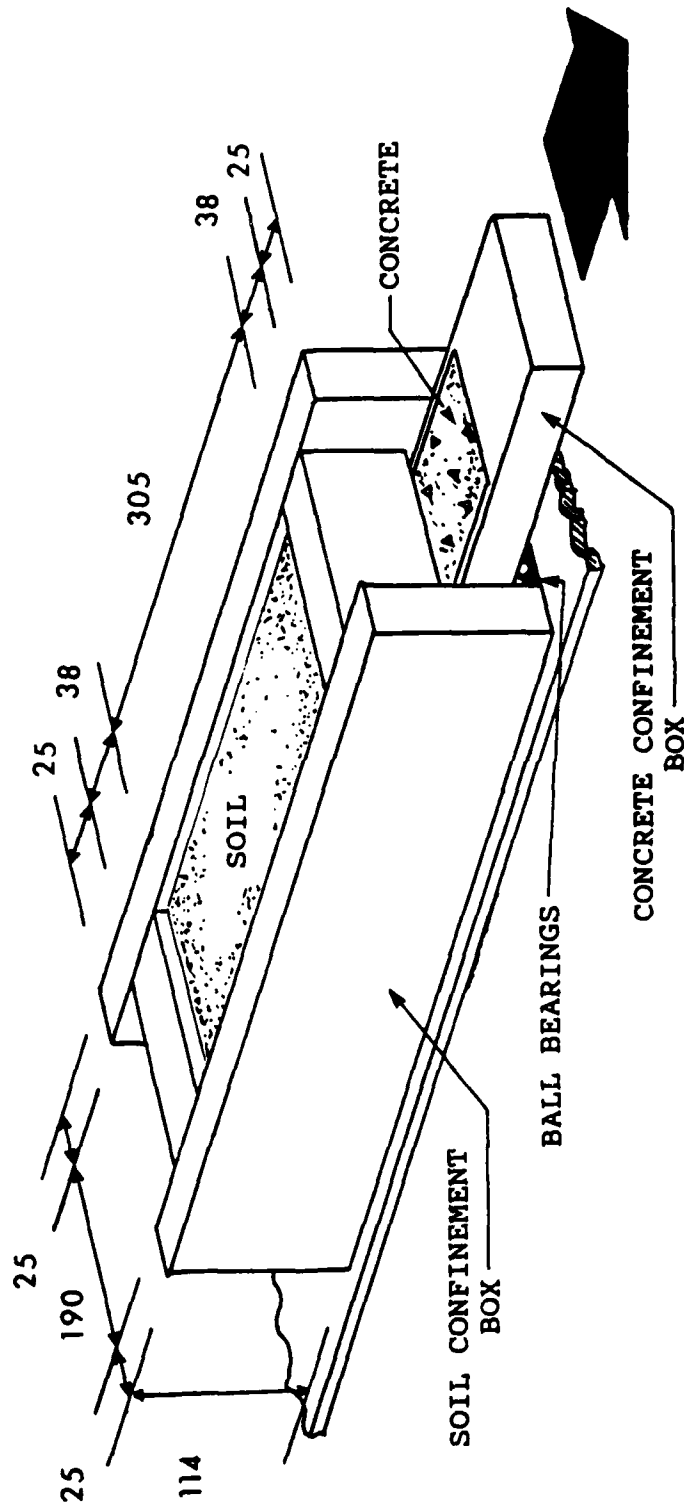


Figure 4.2 Geometry of Sand/Concrete Direct Shear Device.
(all dimensions in millimeters.)

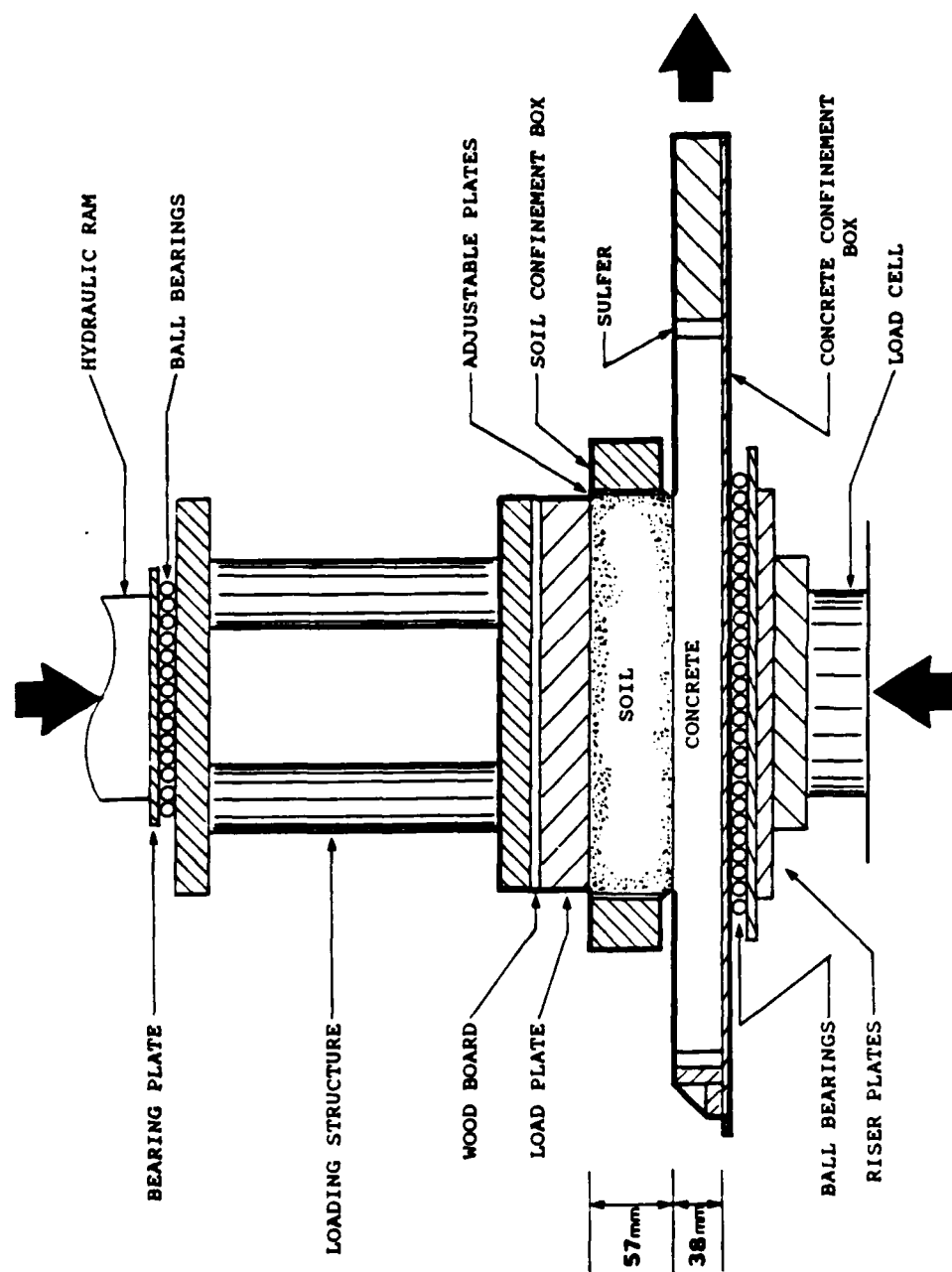


Figure 4.3 Cross Section of Sand/Concrete Direct Shear Device.

As can be seen in Figure 4.3 the concrete specimen is confined in a steel box with the use of steel brackets and a sulfur capping compound. The steel box is supported from below by 154, 13 mm diameter ball bearings. Shear load at the interface is measured by a load cell connected between the actuator shaft and the actuator extension shown in Figure 4.4. Typical values of friction coefficients for ball bearings range between 0.006 and 0.004 (9). Therefore, the shear load transferred by the ball bearings is negligible compared to the shear load transferred by the sand specimen.

The normal load on the concrete is measured by a load cell placed below the concrete confinement box. The soil confinement box is supported independently of the concrete confinement box, and, thus, the normal load cell will indicate only the total normal load applied to the concrete. However, it was determined that the hinge connecting the actuator to the actuator extension, shown in Figure 4.4, was supporting 2% of the applied normal load. This was corrected by recalibration of the data acquisition system.

Both the normal and shear loading devices, shown in Figure 4.4, use hydraulic oil pressure. The normal loading device is a Soiltest static loading ram with an ultimate capacity of 1100 kN. The dynamic shear loading device is an MTS hydraulic actuator with an ultimate capacity of 100 kN.

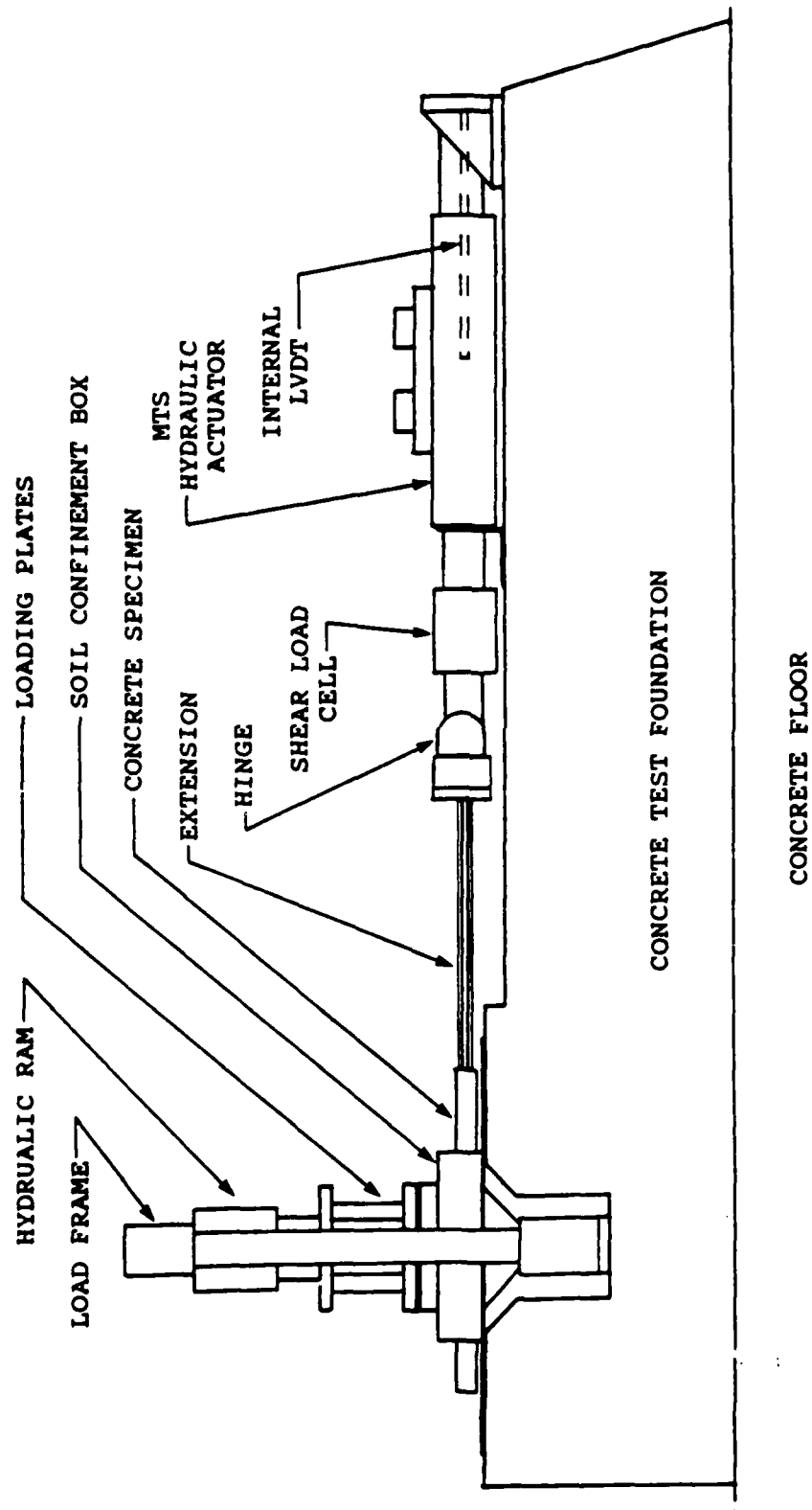


Figure 4.4 Configuration of Testing Device.

The displacement of the MTS actuator is controlled by a voltage signal and an analog feedback system.

The displacement voltage signal used for this research is a ramp function, or triangular wave function. This produces a constant velocity movement of the actuator. By changing the frequency of the triangular wave, the shearing velocity of the actuator can be adjusted. The three shearing velocities used for this testing program are shown in Figure 4.5.

During trial tests using the shear device, it was found that the displacement versus time response of the actuator was not completely linear when the shearing velocities of 254 mm/second were used. Displacement versus time curves of the actuator movement at $V=254$ mm/second are shown in Figure 4.6. In addition, it was also found that, as the static normal pressure increased, the time required for the actuator to reach full input velocity also increased. This nonlinearity is simply due to the fact that the pump driving the actuator could not supply sufficient oil flow to accelerate the actuator and the concrete specimen fast enough to produce the required velocity. The effect of this discrepancy is neglected since, for each test conducted, full velocity was reached before interface failure occurred.

To ensure proper alignment of the loading devices with the shear box a theodolite and an automatic level were used during the initial installation. To further ensure

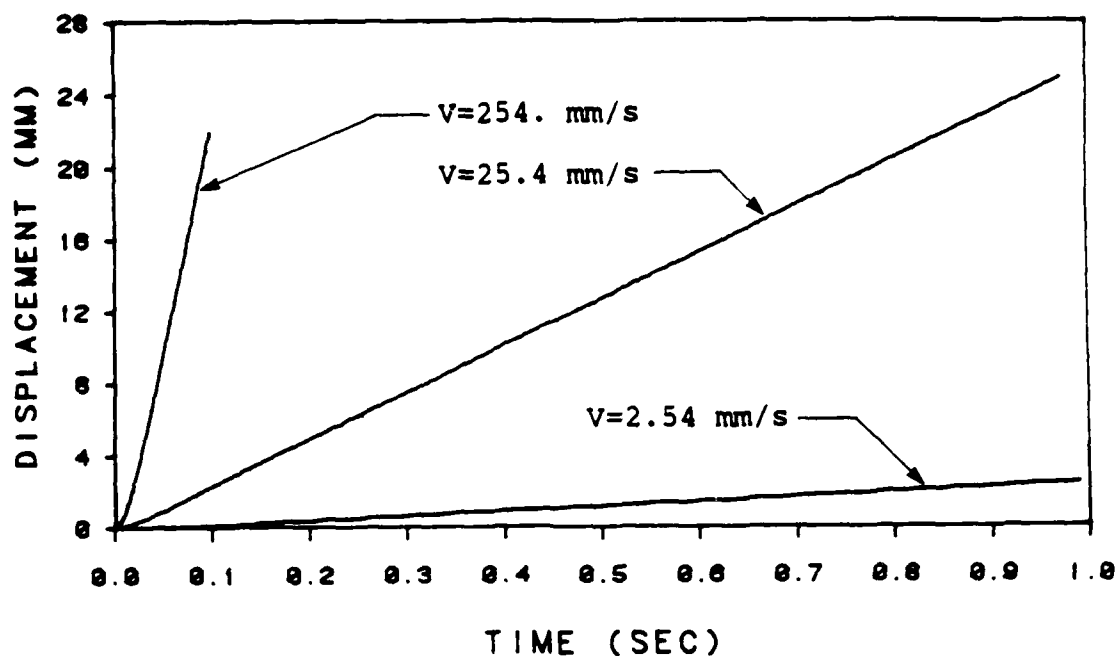


Figure 4.5 Displacement vs. Time for Shearing Velocities of 2.54, 25.4, and 254. mm/second.

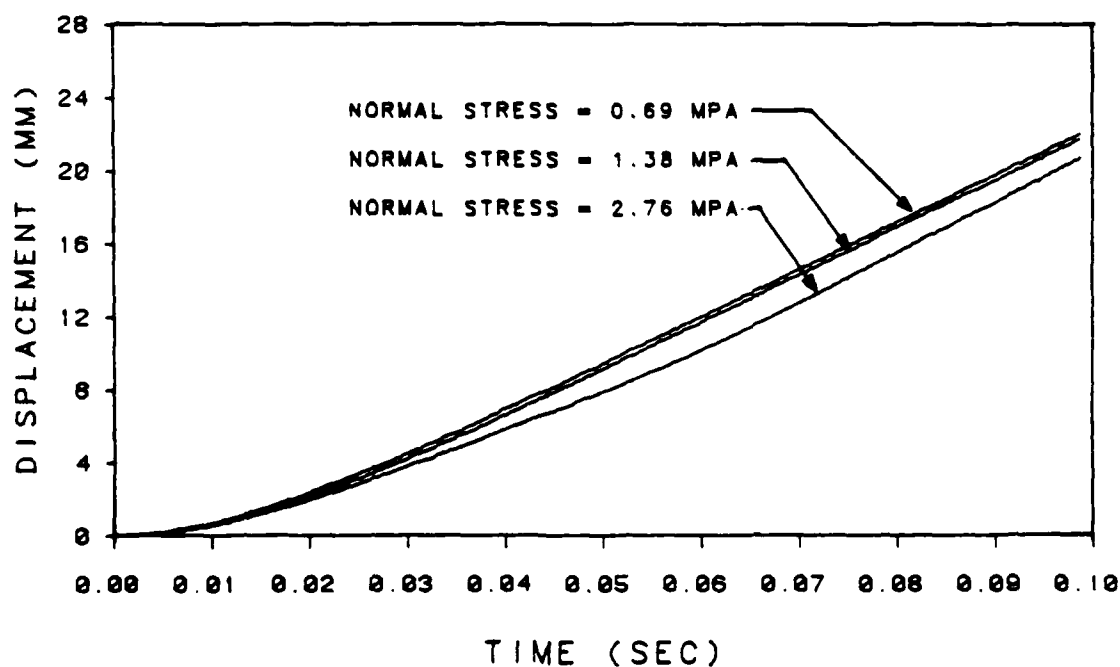


Figure 4.6 Non-Linear Response of Actuator Displacement at Shearing Velocity of 254. mm/second.

alignment, a series of trial tests were performed to ascertain the effect of conducting the test in opposite directions of displacement. If the device were misaligned, the results produced by displacing the concrete specimen in one direction would be different than results produced by displacing the concrete specimen in the opposite direction. No significant difference was observed in results from tests performed using opposite directions of displacement.

4.4.2 Instrumentation

Three variables were measured during each test: displacement, total shear load and total normal load. The displacement was measured by an LVDT located inside the hydraulic actuator. Total shear load was measured by an MTS 100 kN load cell which was connected between the actuator ram and the concrete specimen confinement box. Total normal load was measured by an Interface 222 kN load cell located below the concrete confinement box. The location of the normal load cell is shown in Figure 4.3, and the locations of the shear load cell and the LVDT are shown in Figure 4.4.

Each of the measuring devices mentioned above requires the use of conditioners to transform the measured response into a ± 10 volt scale. These conditioners are depicted in Figure 4.7 along with the remainder of the data acquisition system. Output voltage from the two MTS conditioners were quite noisy, and, therefore, the two signals which were output from these conditioners were

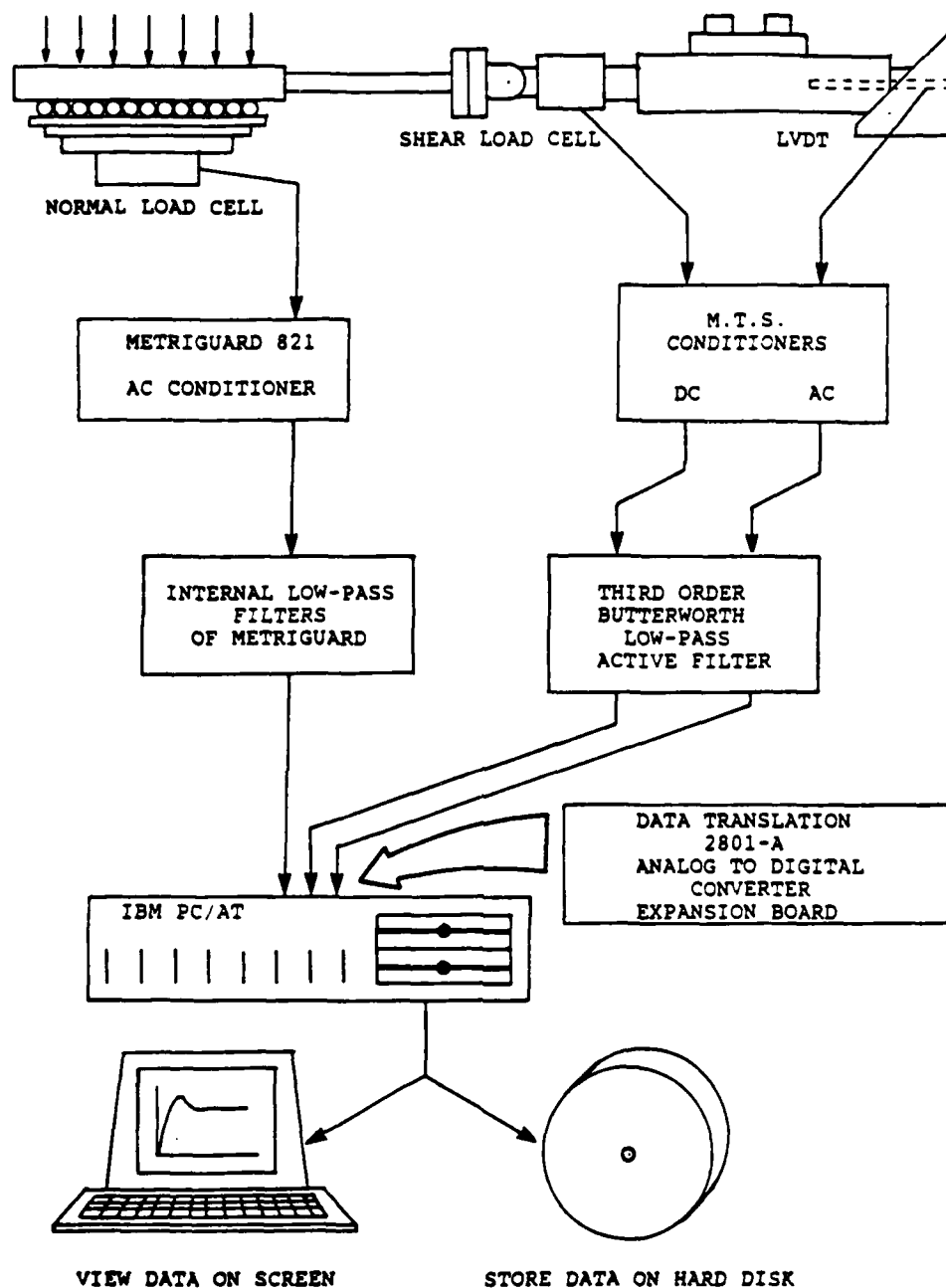


Figure 4.7 Data Aquisiton System.

passed through a 3rd order Butterworth active filter. Proper tests were performed with a digital oscilloscope to ensure that outputs from the conditioners and filters did not lag behind actual response of the soil/structure interface. Lagging response is commonly caused by excessive filtering.

The +/- 10 volt signals were connected to a Data Translation 2801-A Analog to Digital (A/D) converter board installed in an expansion slot of an IBM PC/AT. The A/D converter transforms an analog voltage signal into digital floating point numbers. These data values are stored in the computer memory after digitization. This particular board digitizes data as fast as 20,000 points per second. During each of the soil/concrete interface experiments a total of 330 points were obtained from each measuring instrument.

A question may be raised here as to why no axial deformation measurements were recorded. Axial expansion or axial contraction of the soil mass during shear testing is a result of shearing strain within the sample. However, shearing strain is not uniform throughout the cross-section of a direct shear device. Therefore, axial deformation will also not be uniform. In addition, shear friction from the sides of the box will constrain dilation and contraction of the soil near the walls. Because of the non-uniform axial deformation and the friction from the sidewalls, a recording of deformation at the top of the sample may not accurately

represent the axial deformations occurring in the sample. It was therefore decided that no axial deformations would be measured.

4.4.3 Operation of Test Device

The following chronological procedure was used for preparation and performance of each of the experiments. To begin preparation for a test, a concrete specimen was installed into the device. This was performed by sliding and fixing a specimen into the concrete confinement box connected to the actuator. To fix the specimen in the box, a steel bracket was bolted to the back slot of the box. This is shown in Figure 4.3. A tensile preload of 22 kN was then applied to the steel box and a sulfur capping compound was poured into the two gaps between the concrete specimen and the front and back stops of the concrete confinement box. After the sulfur compound had cooled, the confinement box was unloaded. This procedure rigidly fixed the concrete specimen into the box, thus allowing no relative deflection between the concrete confinement box and the concrete specimen during an actual test.

To ensure that sand particles did not travel between the concrete specimen and the sidewalls of the soil confinement box, a strip of electrical tape was placed over this gap. The gap and the tape are shown in Figure 4.8. The effect of the tape on the shear response of the interface was neglected.

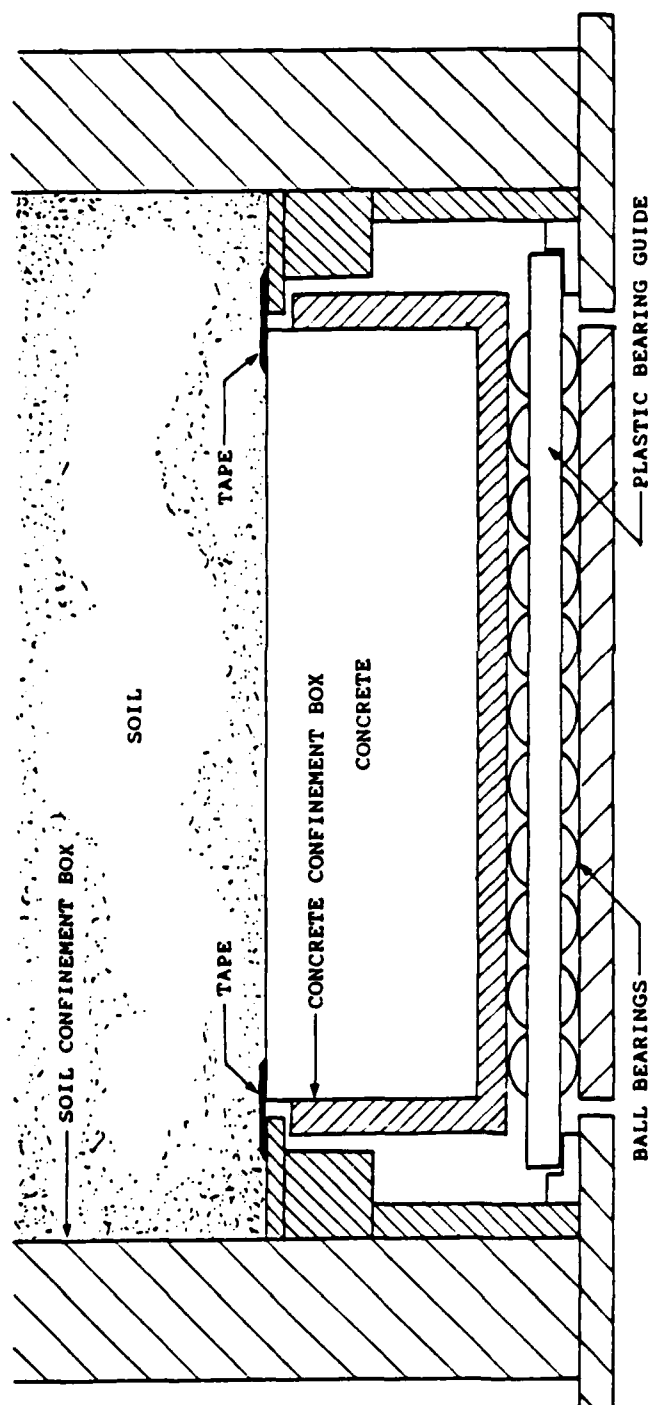


Figure 4.8 Cross Section Normal to Direction of Displacement.

Once the concrete specimen was installed, the width of the specimen was measured in order to calculate the surface area of the interface. The area of the specimen is used by the computer program to convert voltage values for load directly into shear stresses and normal stresses.

Occasionally the actuator would inadvertently displace when hydraulic pressure was initially applied. This was caused by voltage offsets developed during the period of time that the actuator system was shut down. To eliminate the possibility of sand sample disturbances caused by this movement, the hydraulic pressure was applied to the actuator before sample placement.

To account for tare weights, voltage offsets, etc., values of initial voltage levels must be measured so that these values may be subtracted out after performance of the test. This was accomplished by taking "zero" voltage readings with the A/D converter and storing these values in the computer memory.

Since two different densities of sand were used in this testing program, two different methods of sand placement were utilized. Each test was conducted with a sand sample height of 57 mm. For the low density tests, the sand was rained from a height of 20 cm. For the high density tests, the sand was rained from the same height but placed in three layers. After one third of the sand was placed into the box, a surcharge pressure of 7 kPa was applied to the sample

by the use of a thick steel plate. This plate was then tapped 200 times with a large rubber mallet. This procedure was repeated for each of the three layers. These methods for sand placement resulted in the mean and standard deviation densities listed in Table 4.1.

Table 4.1. Density statistics.

Sand	Low Density (g/cc)		High Density (g/cc)	
	Mean	Std. Dev.	Mean	Std. Dev.
Yuma	1.43	0.0204	1.60	0.0248
McCormick Ranch	1.35	0.0137	1.54	0.0156

After the sand was placed, a series of load plates were carefully placed on the sample. These load plates are shown in Figure 4.3. The load plates transfer force between the sample and the Soiltest load ram. This series of load plates consists of a 38 mm thick steel load platen, a 6 mm thick wood board, a load extension structure with a height of 270 mm, a layer of 13 mm diameter ball bearings, and a 6 mm thick load ram bearing plate. The ball bearings allow the stack of load plates to displace and rotate slightly without transferring moment and shear loads to the loading frame. Slight movements of the plates are expected during dynamic shearing due to nonhomogeneous soil strains throughout the sand sample cross-section.

Once the load plates were installed, the desired normal load was statically applied. Normal load magnitude was

monitored by a digital display of the output voltage from the normal load cell. When the normal load reached the desired magnitude, the A/D converter was manually triggered to begin digitizing the voltage signals from the measuring devices. The actuator controller was then manually triggered to begin displacing the actuator. Full displacement for each test was approximately 25 mm. Test duration varied between 10 seconds for the slow velocity tests to 0.10 second for the high velocity tests.

After the voltage versus time signals were digitized, the data acquisition program subtracted out the "zero" readings and then converted the resulting values into displacements, shear stresses, and normal stresses. These data files were then stored onto a hard disk. But, these data values also remained in core storage to be viewed graphically on the computer monitor so that the results could be interpreted immediately.

At the end of each test, the sand sample and concrete specimen were taken out and discarded. A careful procedure was followed to ensure that sand did not fall into the ball bearing support area below the concrete confinement box. This area was vacuumed thoroughly after each test.

4.5 Summary of the Test Program

The following is a summary of the test program. Qualitative descriptions of low, medium, and high for various densities, velocities, and normal pressures will be used in the following chapter.

1. Grain size distribution tests:

- 2 soil types: Yuma sand and McCormick Ranch sand
- 1000 gram sample of soil for each test
- 2 repetitions

Total of 4 tests.

2. Relative density tests:

- 2 soil types: Yuma sand and McCormick Ranch sand
- Maximum and minimum density tests
- 3 repetitions

Total of 12 tests.

3. Static direct shear tests of soil:

- 2 soil types: Yuma sand and McCormick Ranch sand
- 1 density: dense
- 3 normal pressures: 0.325, 0.635, and 1.25 MPa
- 2 repetitions

Total of 12 tests

4. Dynamic direct shear tests on sand/concrete interfaces:

- 2 soil types: Yuma sand and McCormick Ranch sand
- 2 densities: dense and loose
- High density tests:
 - 3 normal pressures: 0.690, 1.38, 2.76 MPa (low, medium, high)
 - 3 shear velocities: 2.54, 25.4, 254. mm/second (low, medium, high)
 - 2 repetitions
- Low density tests:
 - 3 normal pressures: 0.690, 1.38, 2.76 MPa
 - 2 shear velocities: 2.54 and 254. mm/second
 - 1 repetition

Total of 48 tests.

CHAPTER 5

EXPERIMENTAL RESULTS

5.1 Standard Laboratory Tests

The results of the mechanical grain size distribution tests for Yuma sand and McCormick Ranch sand are shown in Figure 5.1. Soil classifications resulting from these tests indicate that the Yuma sample is a well graded sand (SW-SM) and that the McCormick Ranch sample is a poorly graded sand (SP-SM). The sharp drop in the top portion of the distribution curve for the Yuma sand is attributed to the initial passing of the sample through a #12 sieve. The Yuma sand contained a significant percentage of particles larger than a #12 sieve. Thus the initial sieving significantly affected the top portion of the curve.

A comparison of results obtained from the relative density tests to typical textbook values of relative density (22) is shown in Table 5.1. Although the resulting maximum and minimum densities appear relatively low compared to these literature values, it should be noted that the textbook values given here are only typical values, and these typical values should not be considered as a range within which all density values for that particular classification of soil should exist. Performance of the relative density experiment has been criticized in the past by ASTM committee members (2) because of the poor

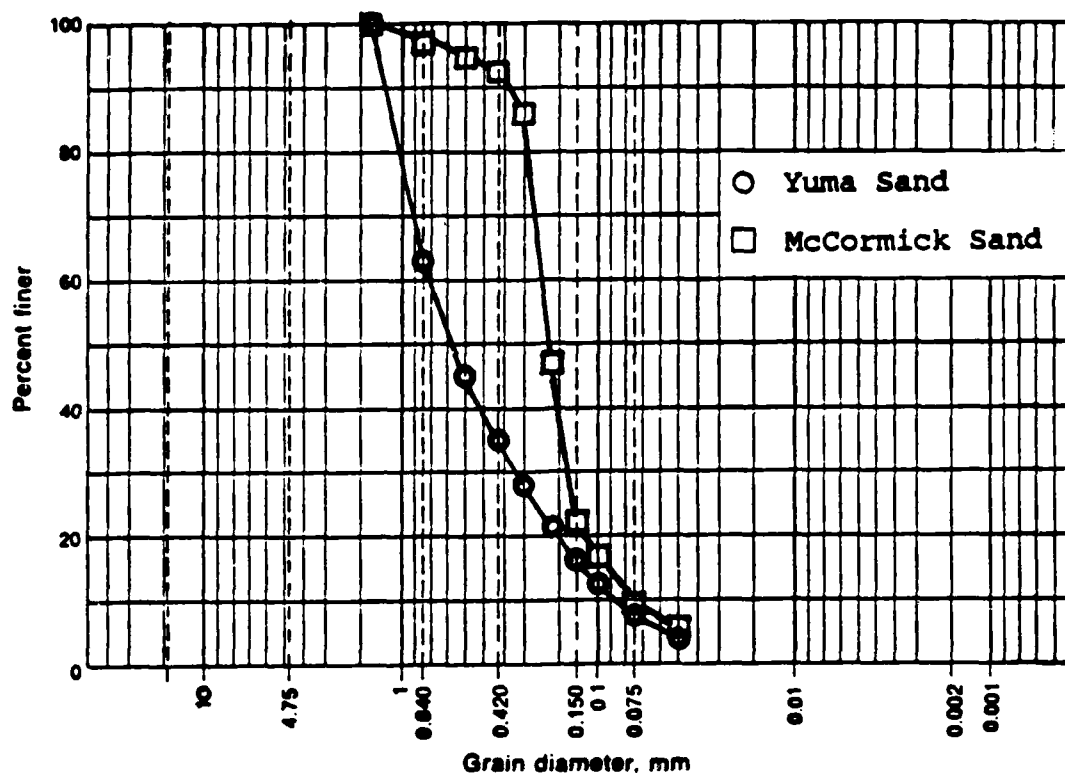


Figure 5.1 Results of Mechanical Grain Size Distribution Tests for Yuma Sand and McCormick Ranch Sand.

Table 5.1 Results of relative density tests.

Soil Description	Test Results		Typical values (2)	
	Min	Max	Min	Max
	(g/cc)		(g/cc)	
Yuma (Well graded angular sand)	1.36	1.68	1.53	1.98
McCormick (Uniform angular sand)	1.31	1.60	1.44	1.84

reproducibility of the test, but the test is still widely used.

Using the relative density test results the mean relative density values used in the sand/concrete test program were calculated: 26% and 79% for the loose and dense Yuma sand/concrete tests, respectively; 16% and 76% for the loose and dense McCormick sand/concrete tests, respectively.

To determine the friction angle of the soil, a least squares regression calculation was performed on the failure shear and normal stress values resulting from the static direct shear tests. This calculation fit the data to the equation $y=ax$. Figure 5.2 shows the resulting friction angles obtained from direct shear experiments performed on Yuma sand and McCormick sand.

The resulting friction angles for the dense samples of Yuma sand and McCormick sand are 43 degrees and 39 degrees, respectively. These values are within the limiting values given in standard textbooks for dense angular sands (11).

5.2 Sand/Concrete Interface Tests

Before performance of any of the sand/concrete interface experiments, it was necessary to determine the inertial effects on the measured response of the interface. Inertial loads are created by the acceleration of the 50 kg steel and concrete box at the beginning of each of the high velocity tests. Determination of the magnitude of these inertial loads was accomplished by performing free vibration

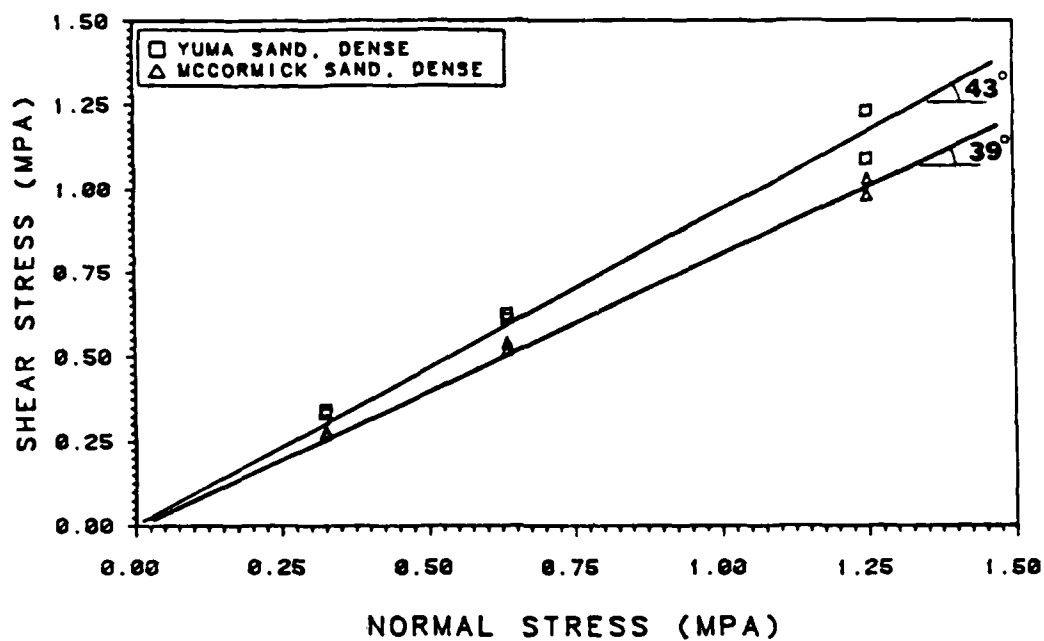


Figure 5.2 Results of Direct Shear Experiments for Yuma Sand and McCormick Ranch Sand.

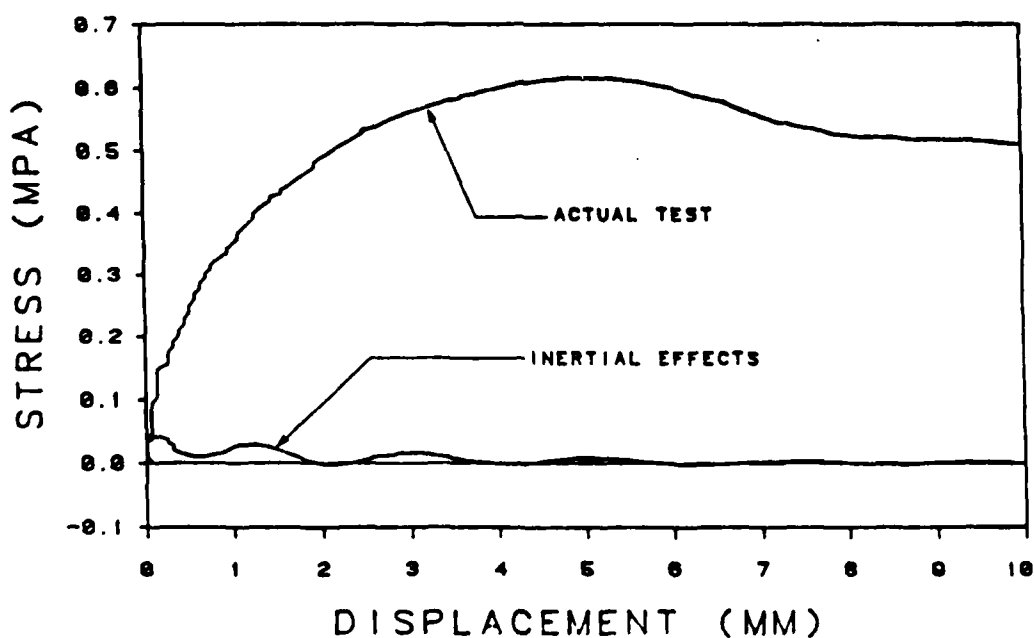


Figure 5.3 Comparison of Inertial Effects to the Response from a Sand/Concrete Interface Test.

experiments with the concrete specimen in place but with no soil sample placed in the soil confinement box. The loads measured by the shear load cell during free vibration tests were thus only the inertial loads. If the values of these inertial loads were found to be significant, these values could be subtracted out after each interface experiment.

A comparison between inertial effects recorded during free vibration tests and the actual measured response of a sand/concrete interface experiment is shown in Figure 5.3. The actual experiment was performed with McCormick Ranch sand at the lowest normal stress level of 0.69 MPa and at the highest shearing velocity of 254 mm/sec. As can be seen the inertial effects become almost insignificant by the time the peak shear stress in the actual test is attained. It should also be noted that the actual test appears to be influenced by these inertial effects only at the very beginning of the test where the acceleration magnitude is the greatest. After this initial influence, the sand specimen has damped out the transient response. It is concluded from this comparison that the inertial effects are insignificant and are, therefore, neglected.

5.2.1 Stress-Displacement Curves

The stress versus displacement curves for the dynamic tests of sand/concrete interfaces are shown in Figures 5.4 to 5.19. These curves are also shown in Appendix A at a smaller scale in order to provide greater detail. In each

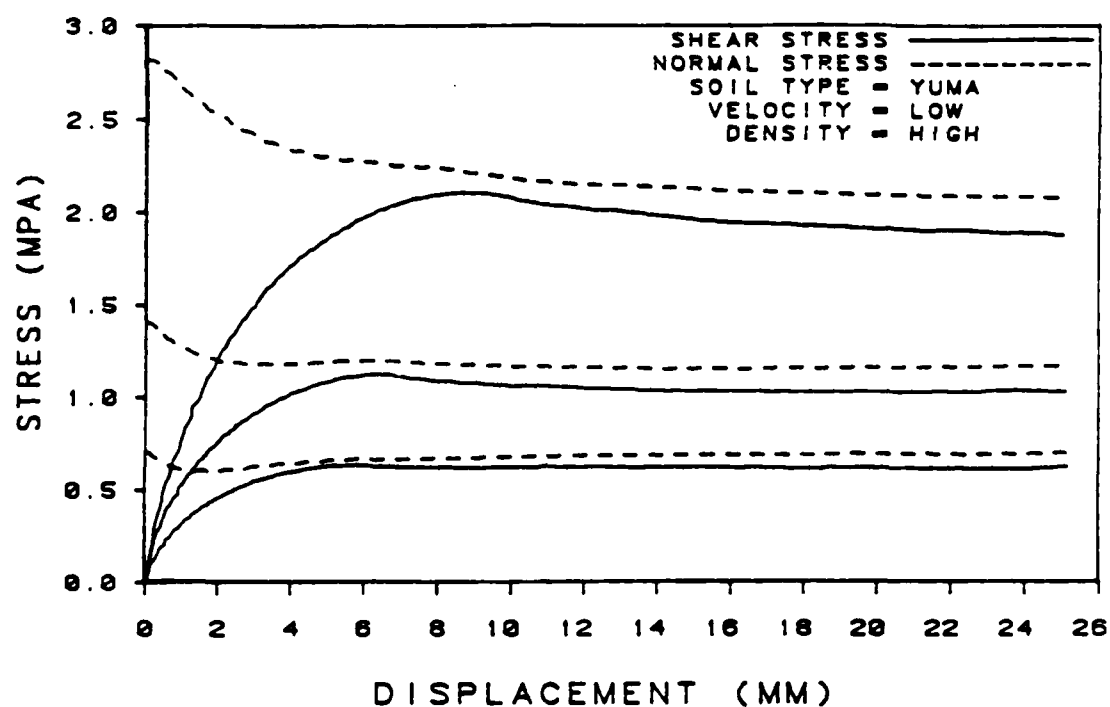


Figure 5.4 Stress vs. Deflection For Dense Yuma Sand/
Concrete Tests, $V=2.54$ mm/sec, 1st Repetition.

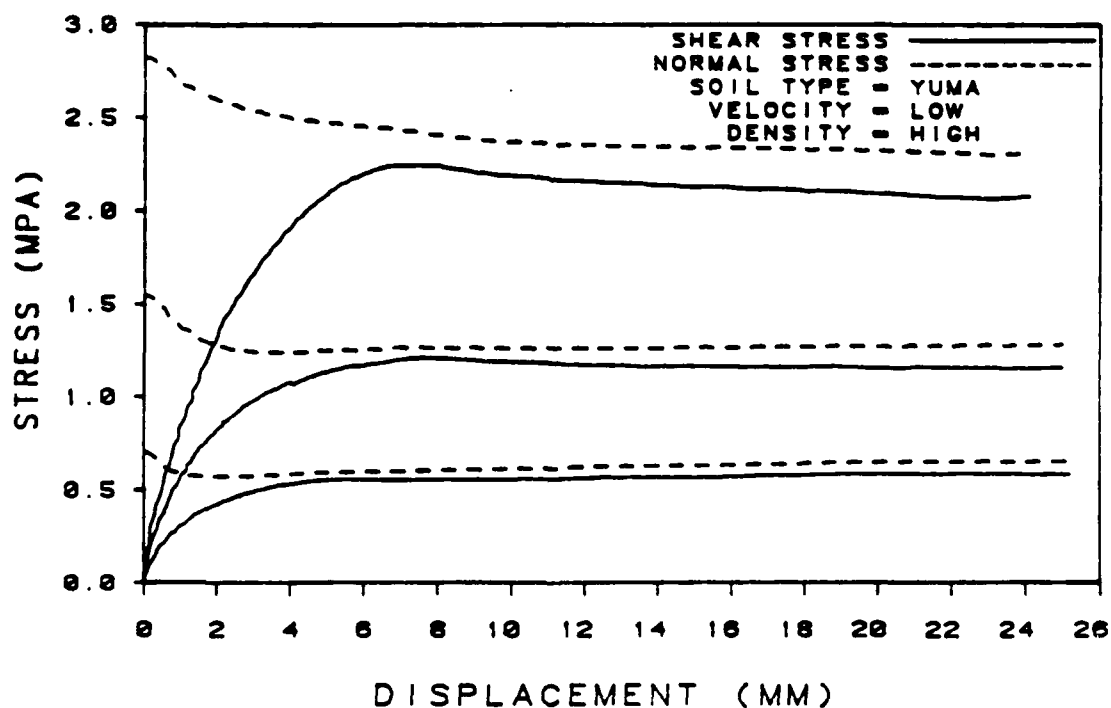


Figure 5.5 Stress vs. Deflection For Dense Yuma Sand/
Concrete Tests, $V=2.54$ mm/sec, 2nd Repetition.

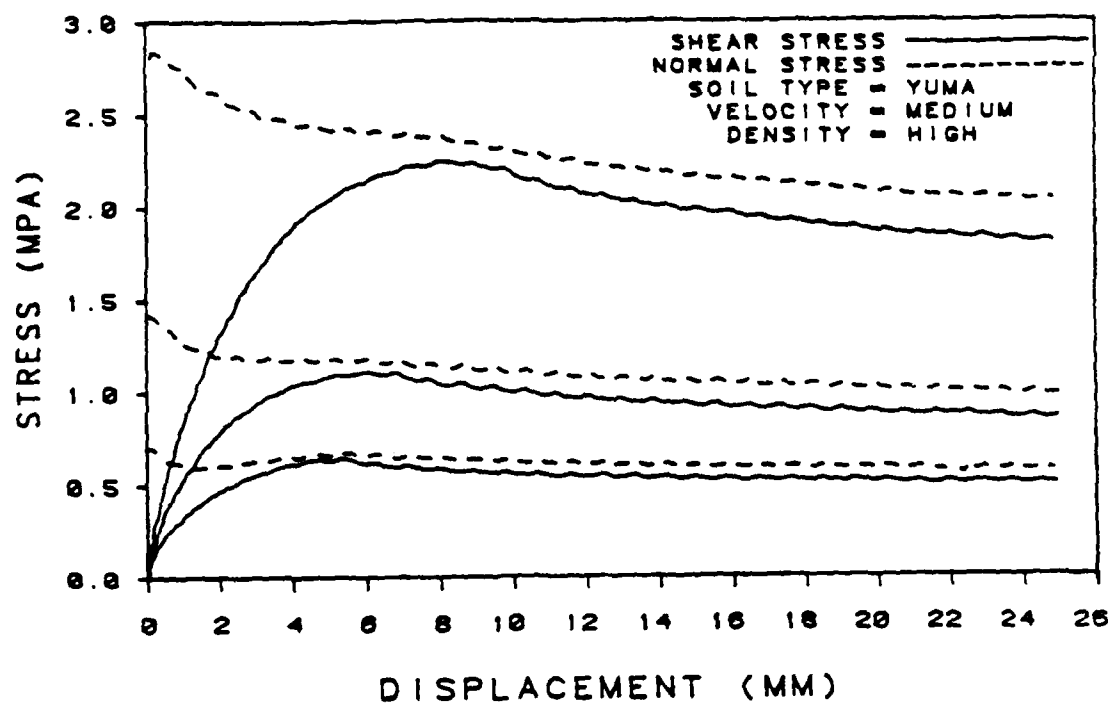


Figure 5.6 Stress vs. Deflection For Dense Yuma Sand/
Concrete Tests, $V=25.4$ mm/sec, 1st Repetition.

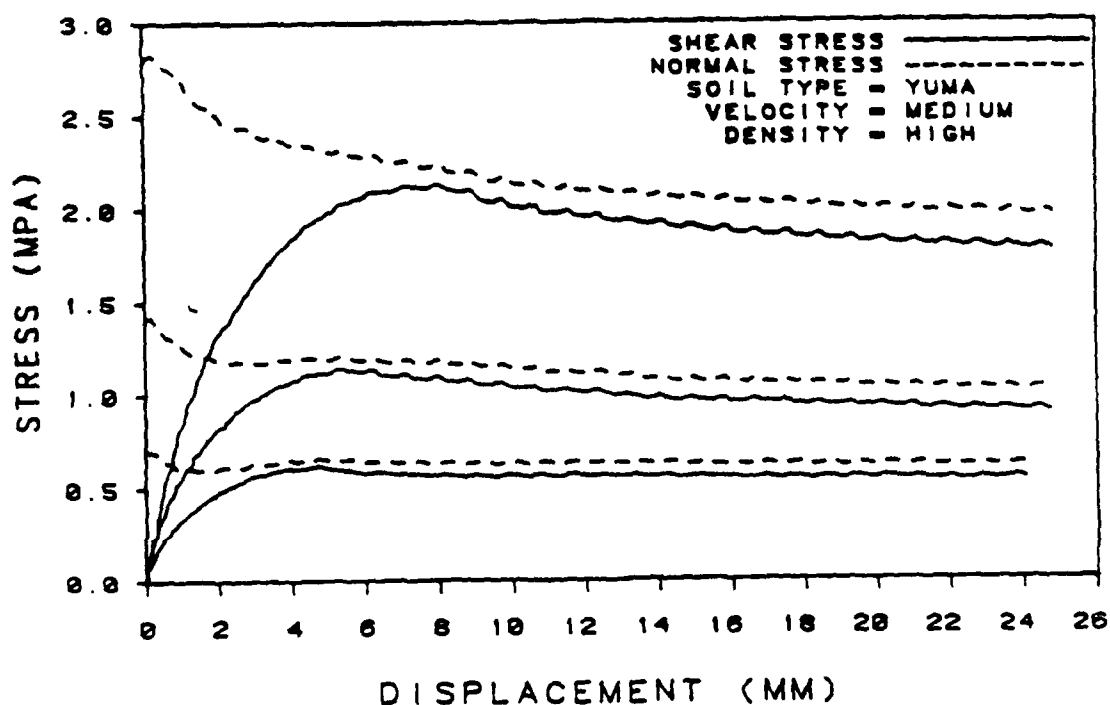


Figure 5.7 Stress vs. Deflection For Dense Yuma Sand/
Concrete Tests, $V=25.4$ mm/sec, 2nd Repetition.

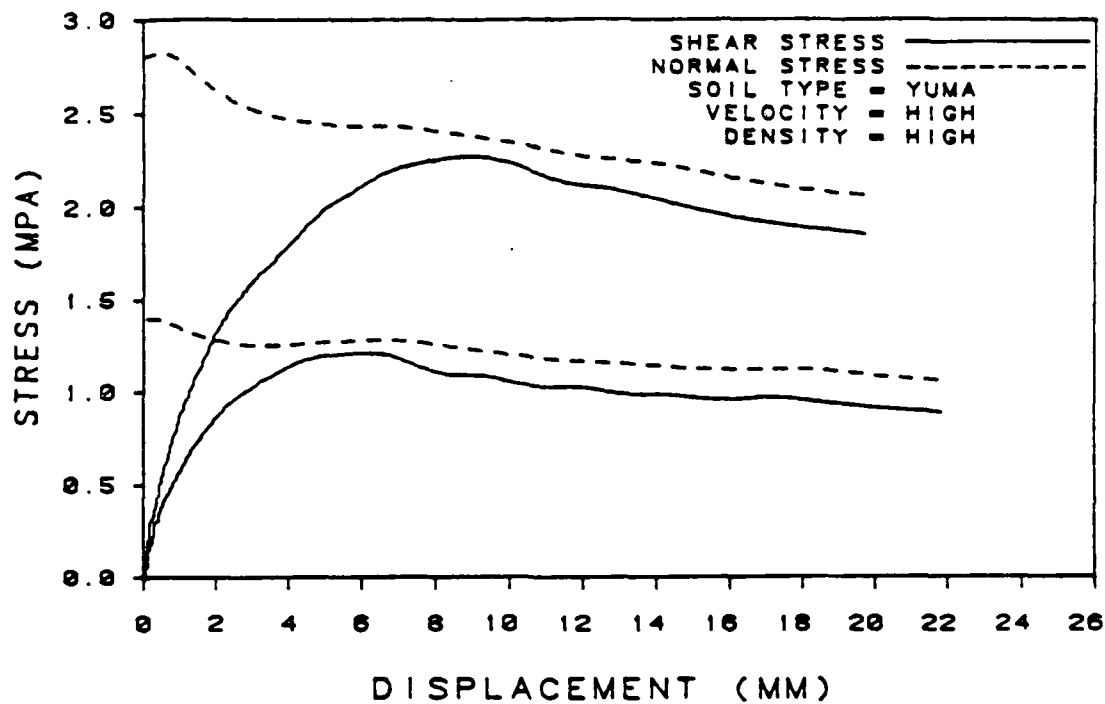


Figure 5.8 Stress vs. Deflection For Dense Yuma Sand/
Concrete Tests, V=254. mm/sec, 1st Repetition.

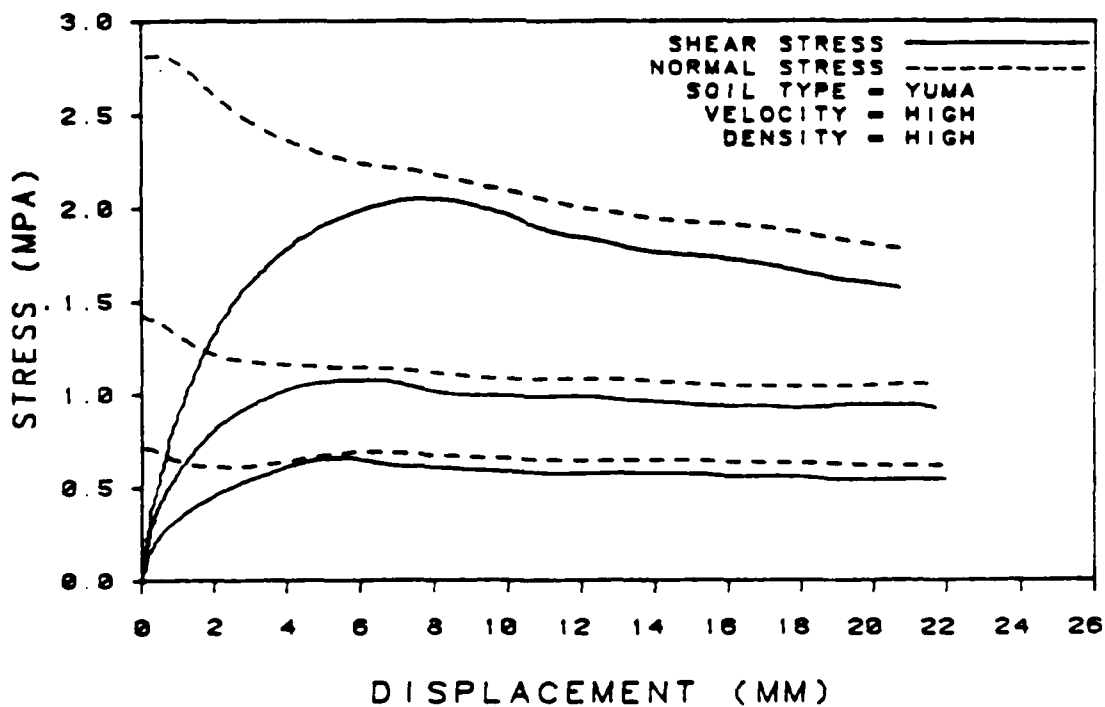


Figure 5.9 Stress vs. Deflection For Dense Yuma Sand/
Concrete Tests, V=254. mm/sec, 2nd Repetition.

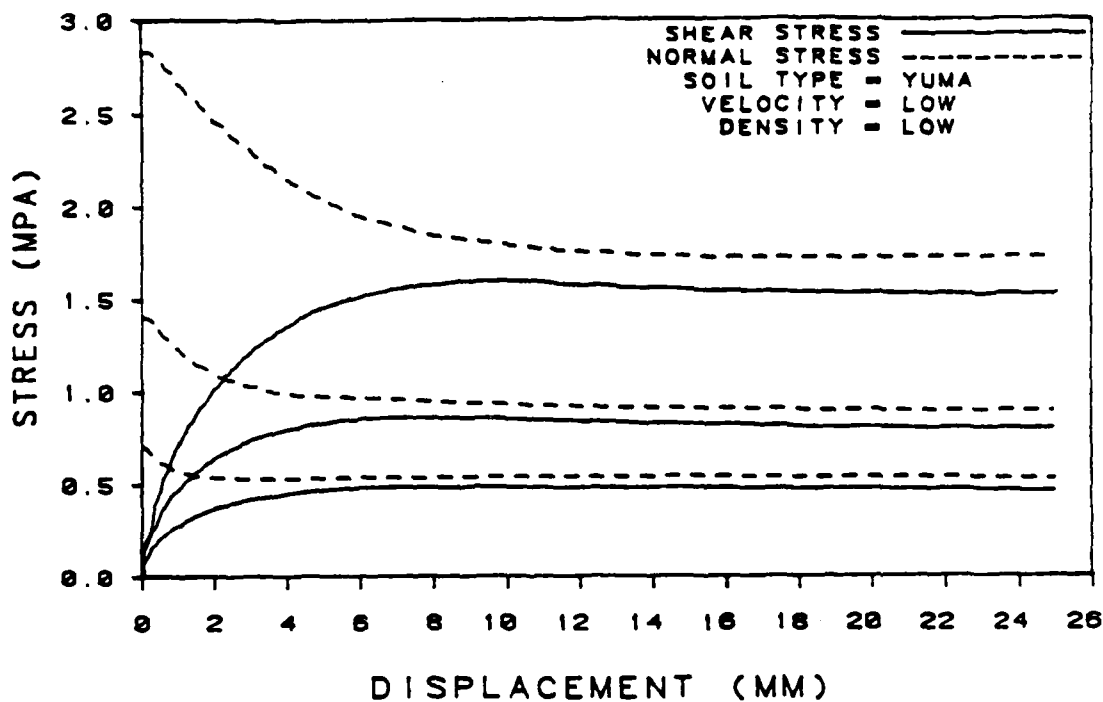


Figure 5.10 Stress vs. Deflection For Loose Yuma Sand/
Concrete Tests, $V=2.54$ mm/sec.

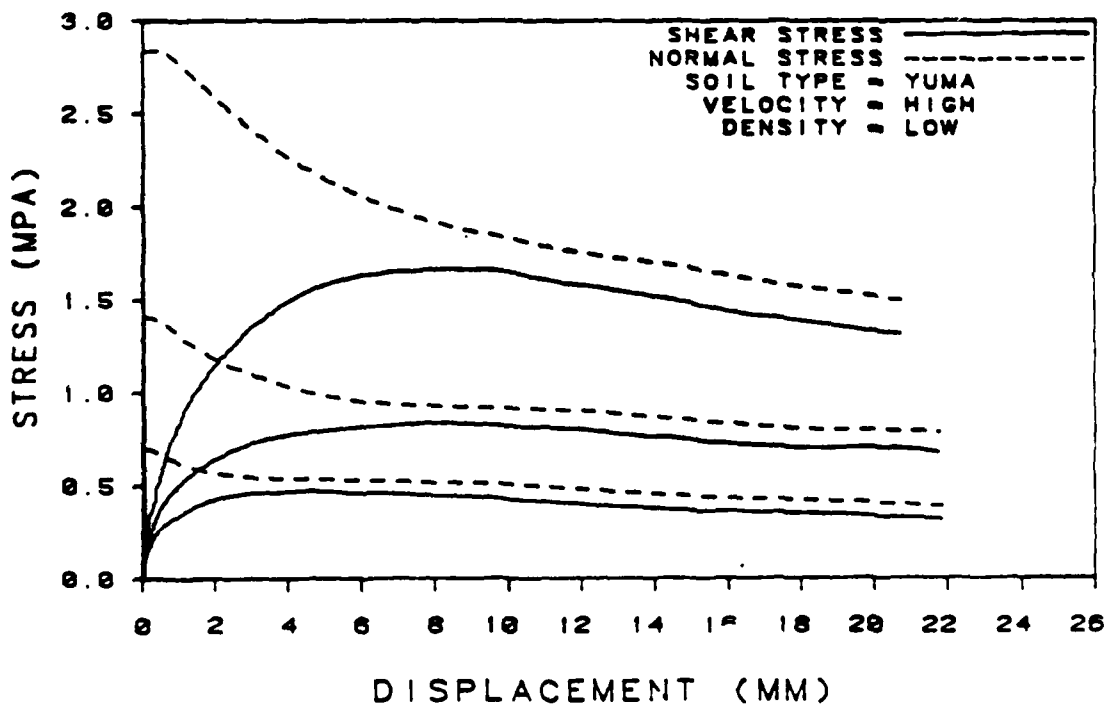


Figure 5.11 Stress vs. Deflection For Loose Yuma Sand/
Concrete Tests, $V=254.$ mm/sec.

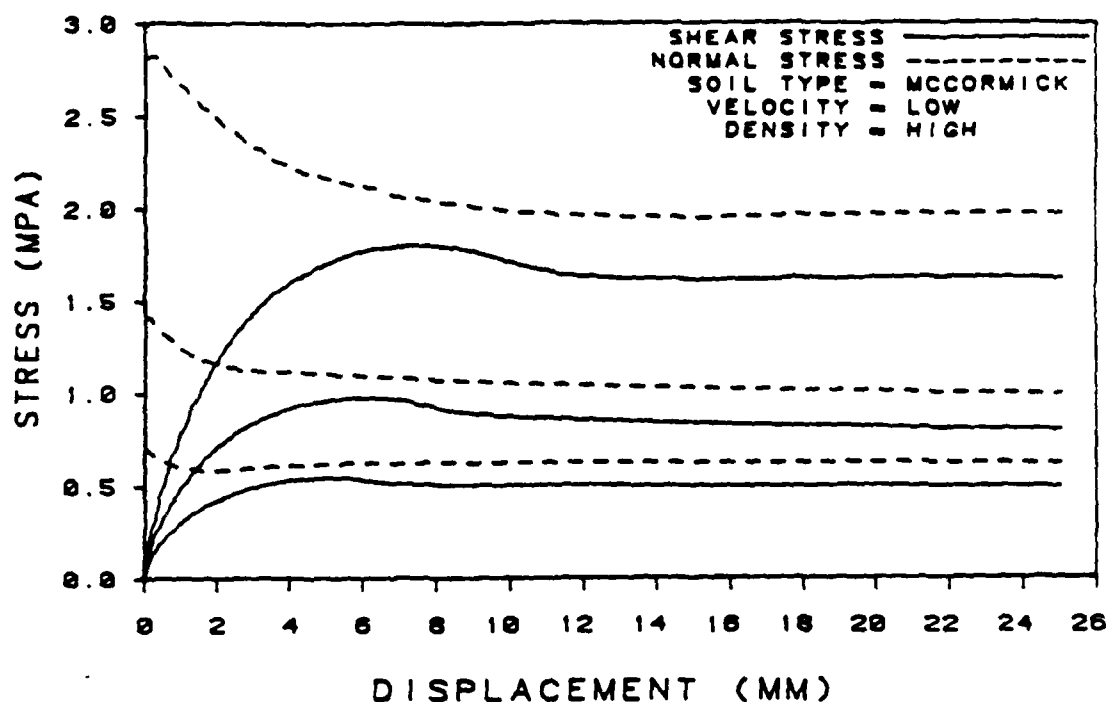


Figure 5.12 Stress vs. Deflection For Dense McCormick Sand/Concrete Tests, $V=2.54$ mm/sec, 1st Repetition.

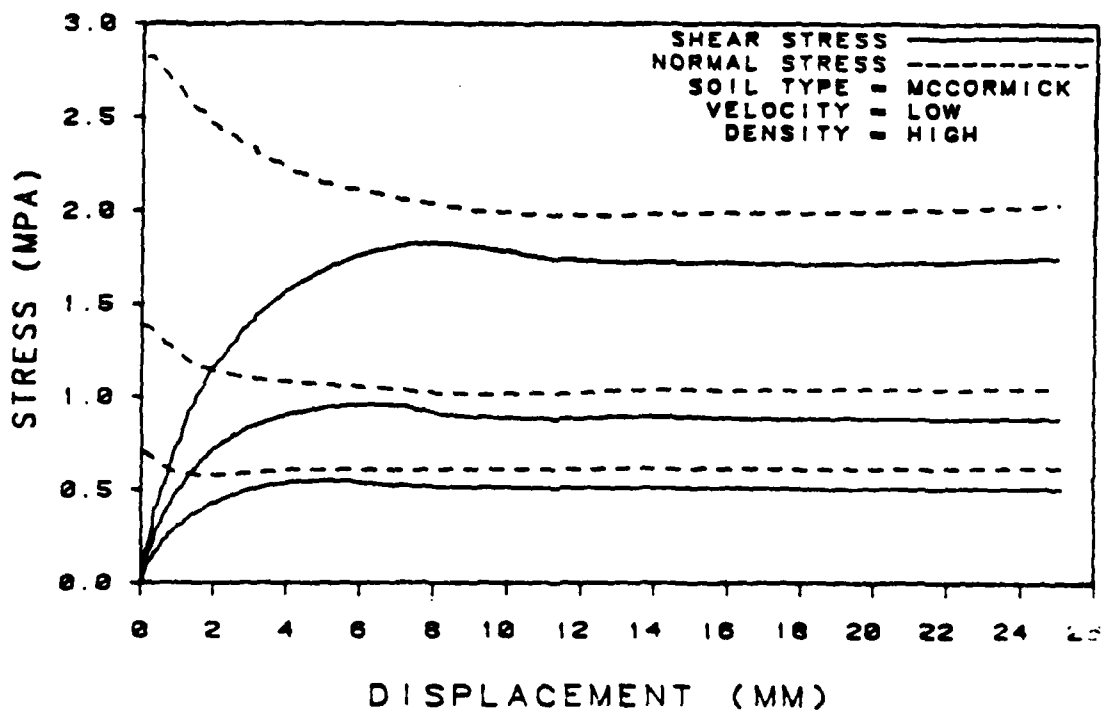


Figure 5.13 Stress vs. Deflection For Dense McCormick Sand/Concrete Tests, $V=2.54$ mm/sec, 2nd Repetition.

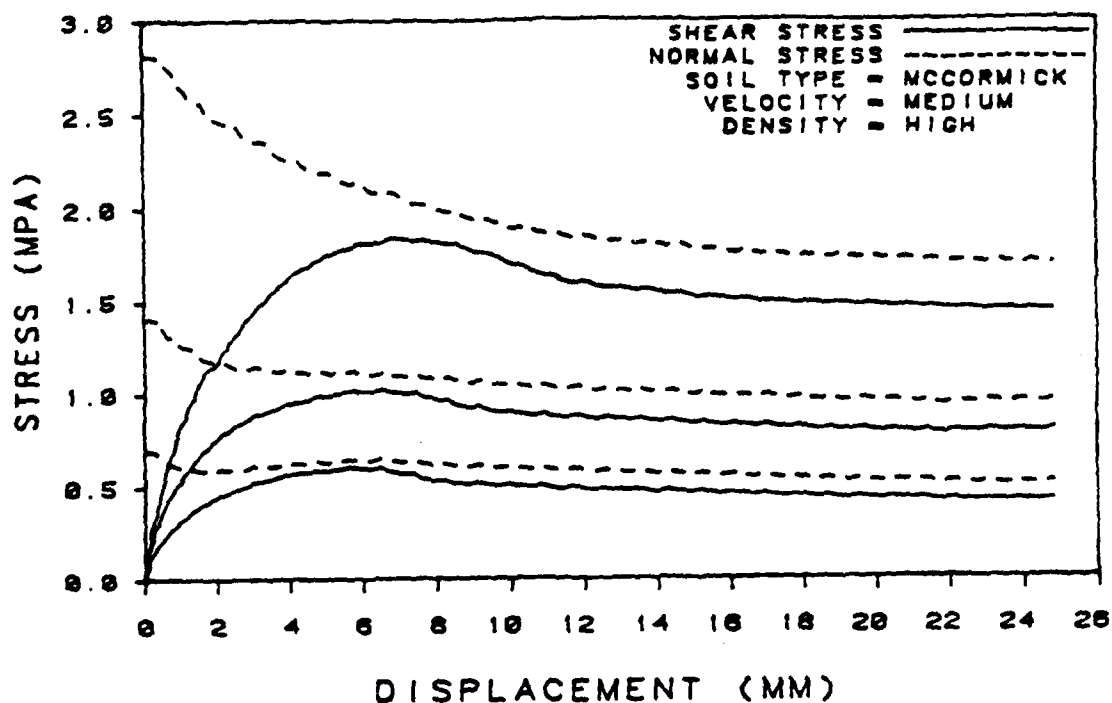


Figure 5.14 Stress vs. Deflection For Dense McCormick Sand/Concrete Tests, $V=25.4$ mm/sec, 1st Repetition.

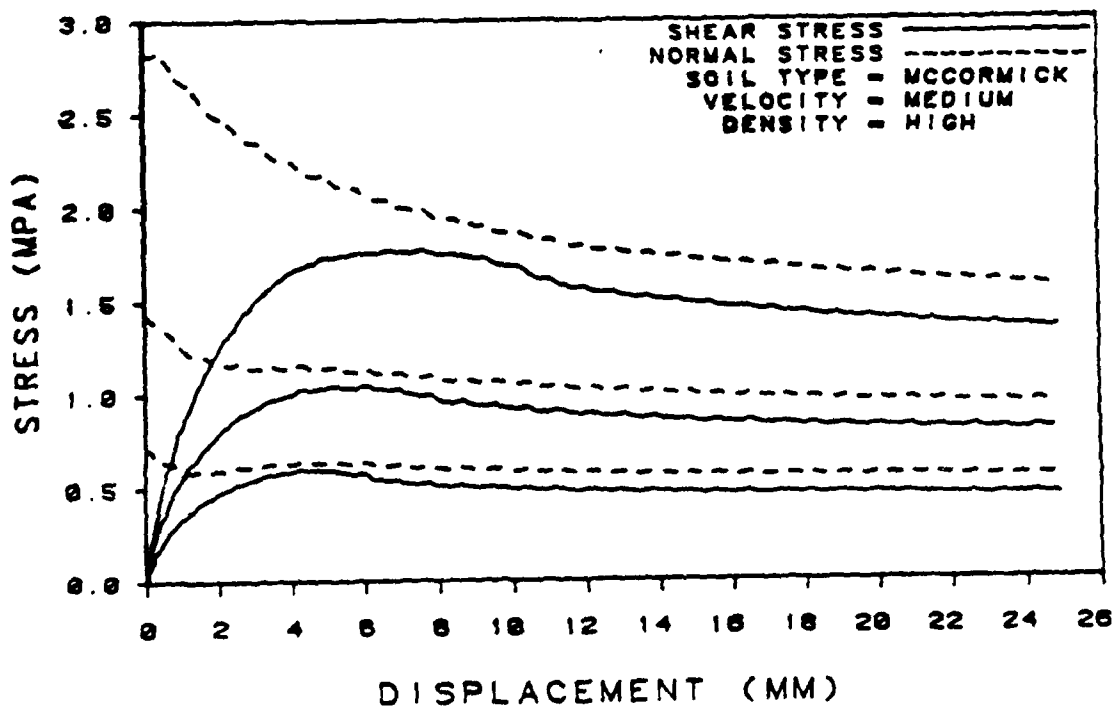


Figure 5.15 Stress vs. Deflection For Dense McCormick Sand/Concrete Tests, $V=25.4$ mm/sec, 2nd Repetition.

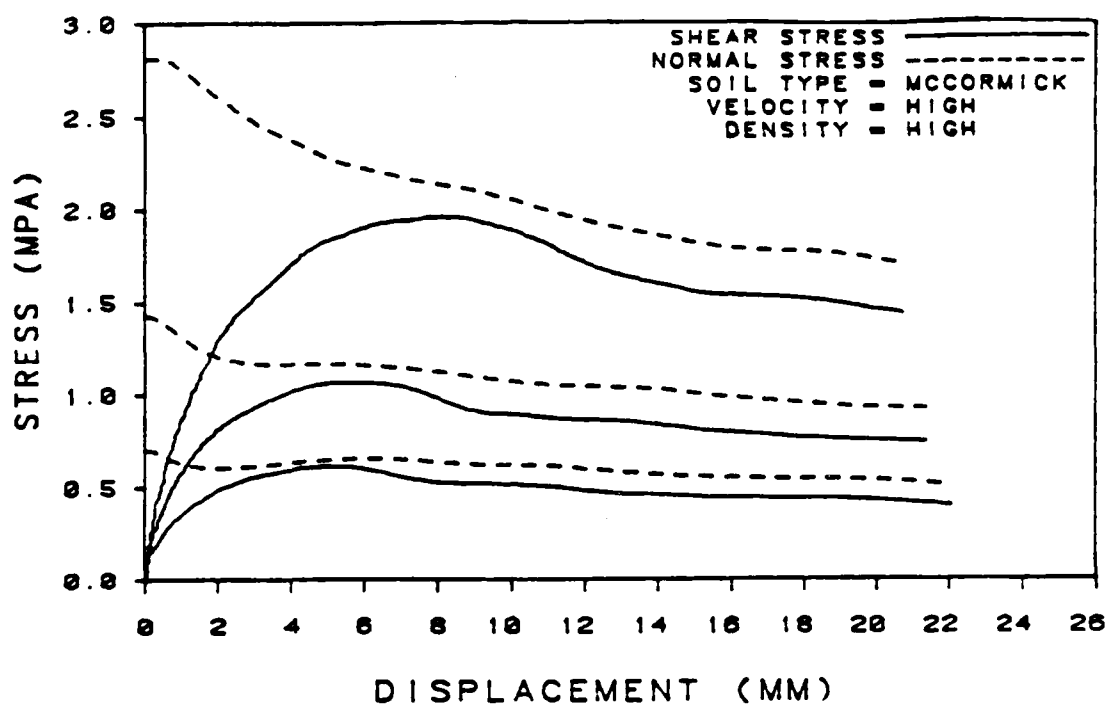


Figure 5.16 Stress vs. Deflection For Dense McCormick Sand/Concrete Tests, $V=254$. mm/sec, 1st Repetition.

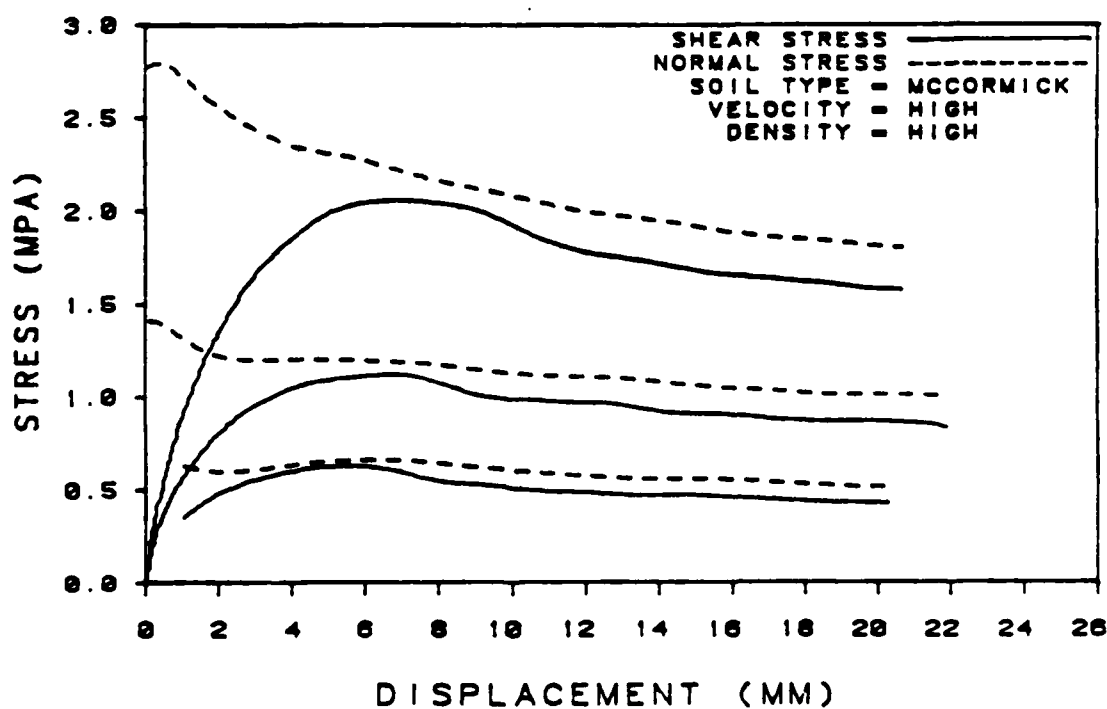


Figure 5.17 Stress vs. Deflection For Dense McCormick Sand/Concrete Tests, $V=254$. mm/sec, 2nd Repetition.

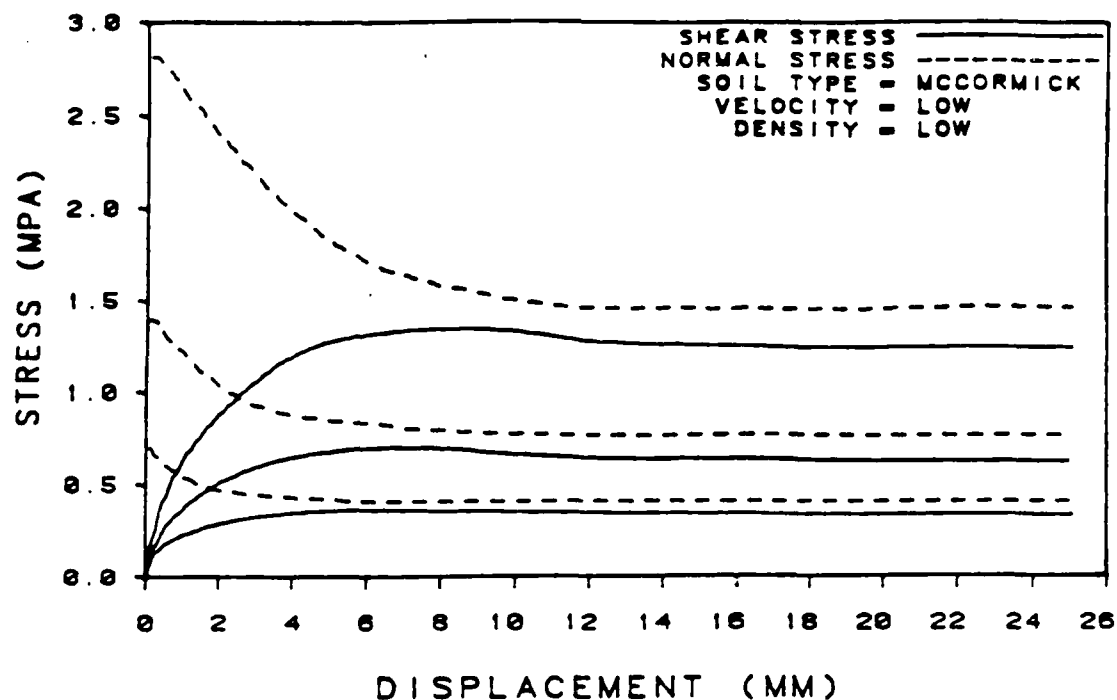


Figure 5.18 Stress vs. Deflection For Loose McCormick Sand/Concrete Tests, $V=2.54$ mm/sec.

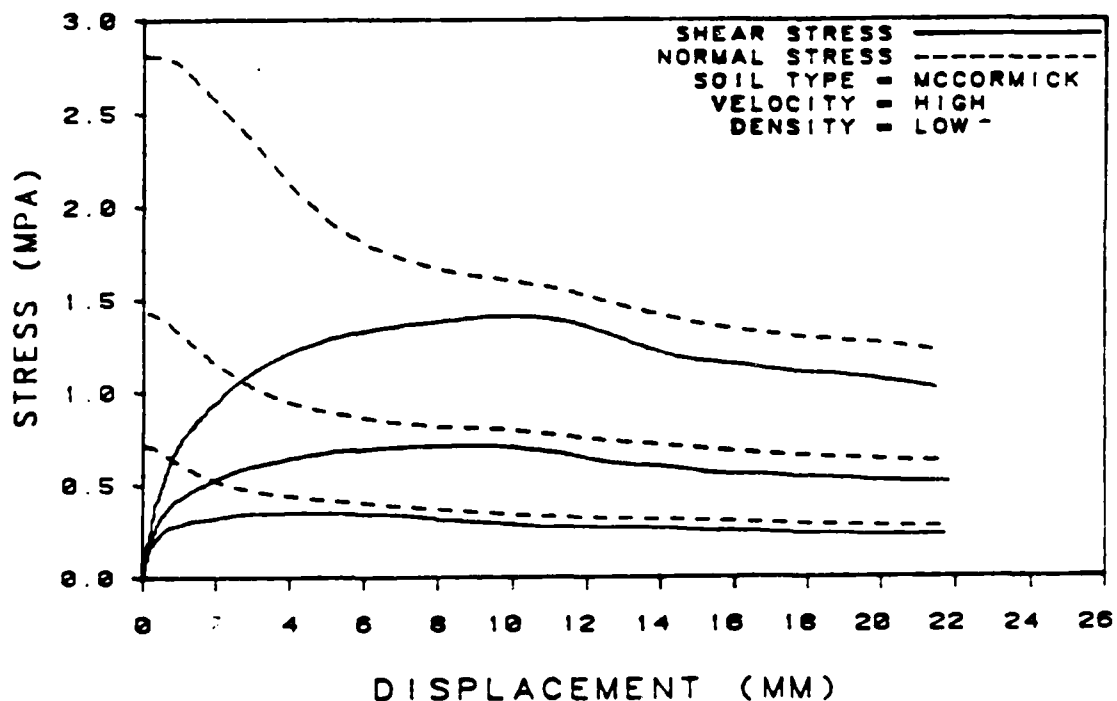


Figure 5.19 Stress vs. Deflection For Loose McCormick Sand/Concrete Tests, $V=254$ mm/sec.

of the plots the shear stress is represented by a solid line and the corresponding normal stress is the dashed line directly above it.

As shown by these curves, a decrease in the normal stress was observed during the initial stages of shear displacement in each of the experiments. This normal stress drop was caused by the inability of the static loading ram to keep up with the axial deformation rate of the soil sample. After the performance of the test, the normal pressure quickly returned to the original static level.

A closer observation of the behavior of the normal stress change during the experiments indicates typical axial deformation behavior for sands. Under the low confining pressure, 0.69 MPa, each of the dense sand samples contracts and then dilates due to particles rolling over one another. When subjected to higher confining pressures, 1.38 and 2.76 MPa, the dense samples only contracted. Experiments on loose sand/concrete interfaces indicated that during shear deformation only contraction of the samples occurred under each level of applied normal stress.

Shear deformation responses from these experiments are also typical for sands. For the high density experiments, the shear stress will rise nonlinearly to a peak value and will then soften to a residual stress value. For the low density tests the shear stress slowly rises to a constant value.

5.2.2 Failure Criterion

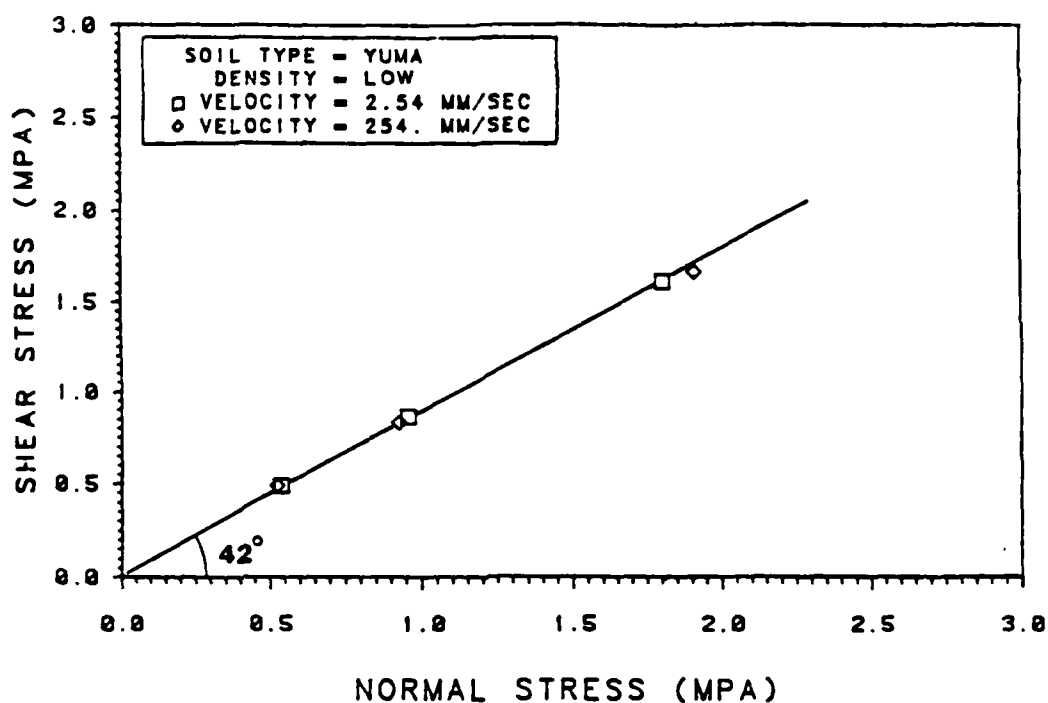
To evaluate the friction angle of the interface, the failure stresses, shear and normal, were determined for each experiment. These data were then used in a least squares regression analysis to determine the best fit to the equation $y=ax$. From this linear fit, a friction angle was calculated. Friction angles were determined for each soil type, shearing rate, and density.

As can be seen in Table 5.2 the friction angles obtained from the sand/concrete interface experiments were not affected by variations in shearing velocity. This is shown graphically for Yuma sand and McCormick Ranch sand in Figures 5.20 and 5.21, respectively. These results also indicate a slight decrease in the friction angle as the sample density is decreased.

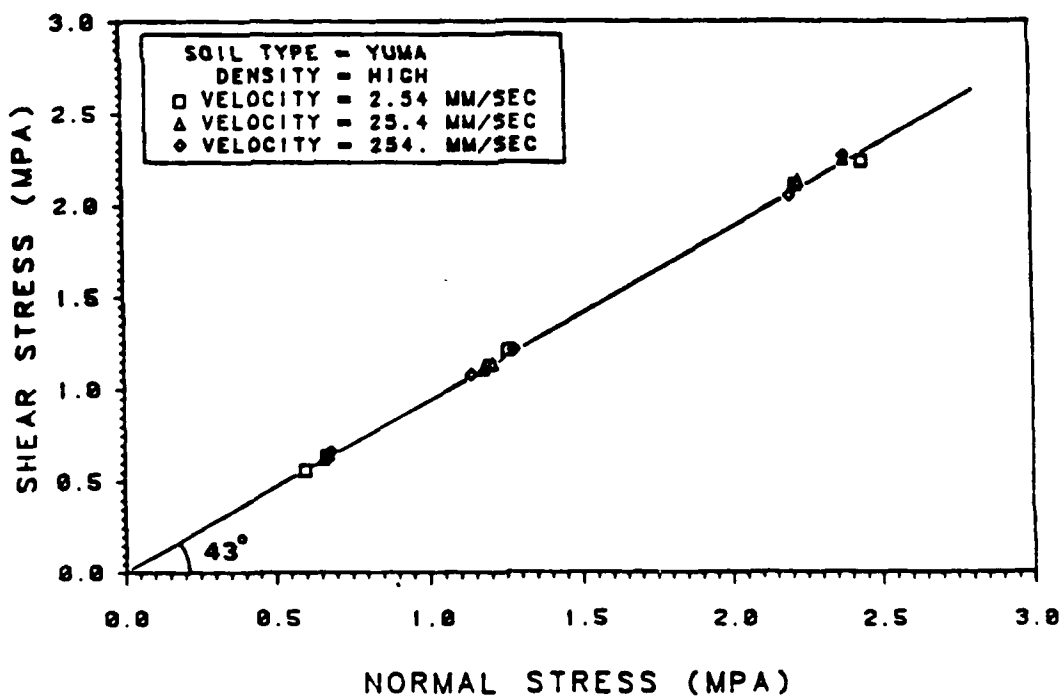
Table 5.2 Rate effect on interface friction angle from sand/concrete interface tests.

Soiltype		δ (degrees) for different displacement rates		
		2.54 mm/s	25.4 mm/s	254. mm/s
Yuma	(Dense)	43	43	43
	(Loose)	42	--	41
McCormick	(Dense)	42	42	43
	(Loose)	41	--	41

The strength ratios (f_ϕ) resulting from the dense sand/concrete experiments are shown in Table 5.3. The f_ϕ value of 1.08 for the McCormick sand/concrete interface

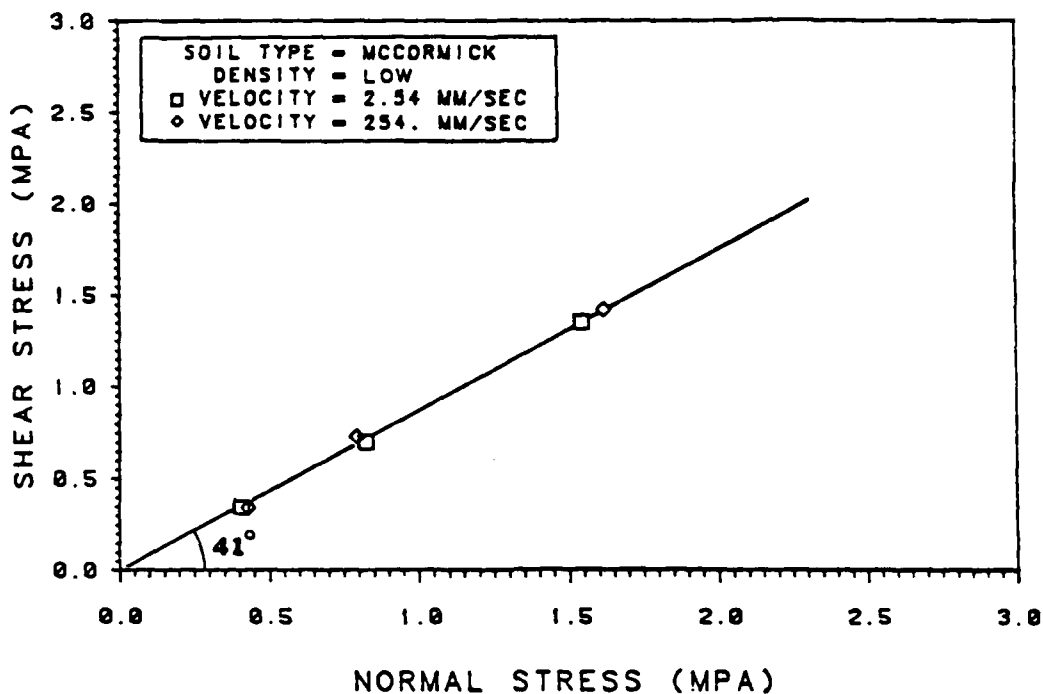


a. Mean Relative Density of Sand = 26% (Loose).

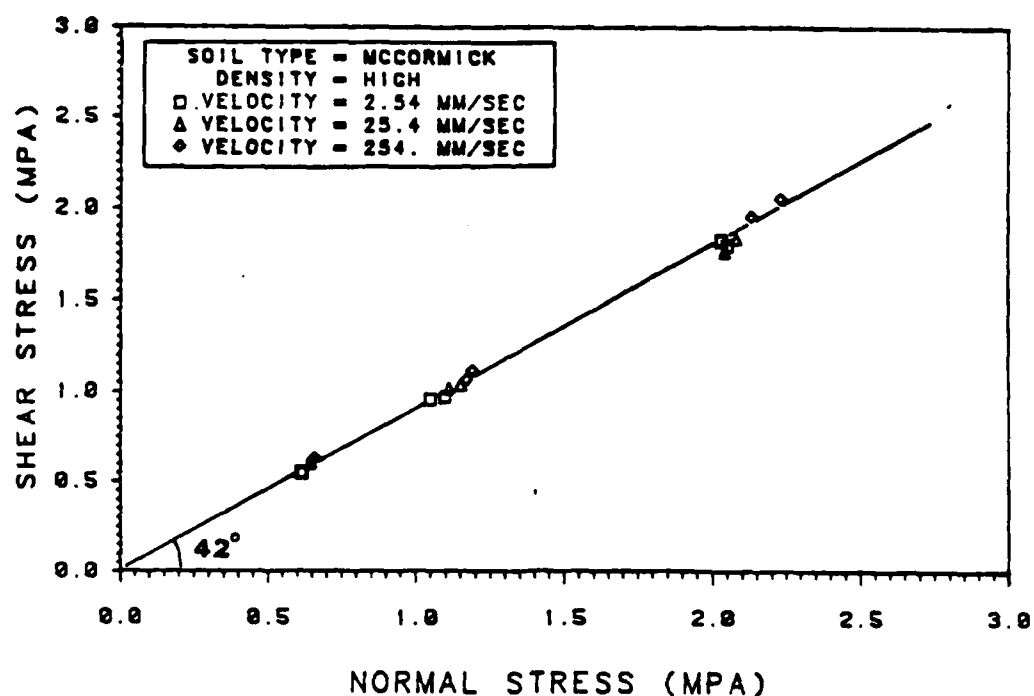


b. Mean Relative Density of Sand = 79% (Dense).

Figure 5.20 Mohr Envelopes for Yuma Sand/Concrete.



a. Mean Relative Density of Sand = 16% (Loose).



b. Mean Relative Density of Sand = 82% (Dense).

Figure 5.21 Mohr Envelopes for McCormick Sand/Concrete.

indicates that a greater strength was measured from the interface direct shear test than from the soil direct shear test. Theoretically the interface strength is limited to the strength of the soil mass adjacent to the interface. A value of f_ϕ greater than 1.00 should not be the result if the test is performed correctly.

Table 5.3 Friction angles and strength ratios from the dense sand tests.

Soiltype	ϕ (degrees)	δ (degrees)	f_ϕ
Yuma sand	43	43	1.00
McCormick sand	39	42	1.08

Two causes of the high strength ratio (f_ϕ) of 1.08 for the McCormick sand/concrete tests are suggested. First, this inaccuracy could result from the practice of comparing results obtained from two different shear devices. Because of the size and design difference of the soil direct shear device and the soil/concrete direct shear device, it could be expected that comparisons of results produced by these different devices could be slightly in error. This error could contribute to the total error in the McCormick sand/concrete result.

A second source of error is revealed by comparing sand densities at which the soil and interface tests were conducted. The Yuma sand tests for soil strength and

interface strength were conducted using the same sample densities of 1.60 g/cc (79% relative). However, due to human error, a sample density of 1.52 g/cc (76% relative) was used for the McCormick sand strength tests while an average sample density of 1.54 g/cc (82% relative) was used for the McCormick sand/concrete tests. This higher density would tend to increase the resulting friction angle. The comparison of results from two separate machines in which slightly different densities of sand samples were used appears to account for the error in the strength ratio for the McCormick sand/concrete.

5.2.2 Post-Failure Response

To determine the characteristics of post-failure softening, a method must be derived to quantify the amount of softening resulting from each experiment. This was accomplished by the method shown graphically in Figure 5.22. A stress ratio of shear stress divided by normal stress is calculated for two positions of the stress-displacement curve (shown in in Figure 3.1): A, the point of maximum shear stress (failure), and B, at 20 mm deflection (residual). The friction angle for both of these points is determined by taking the arctan of the stress ratio for that point. Finally, the difference between these two friction angles, i.e., the failure friction angle and the residual friction angle, is calculated to quantify the softening. Therefore, post-failure response will be described in terms

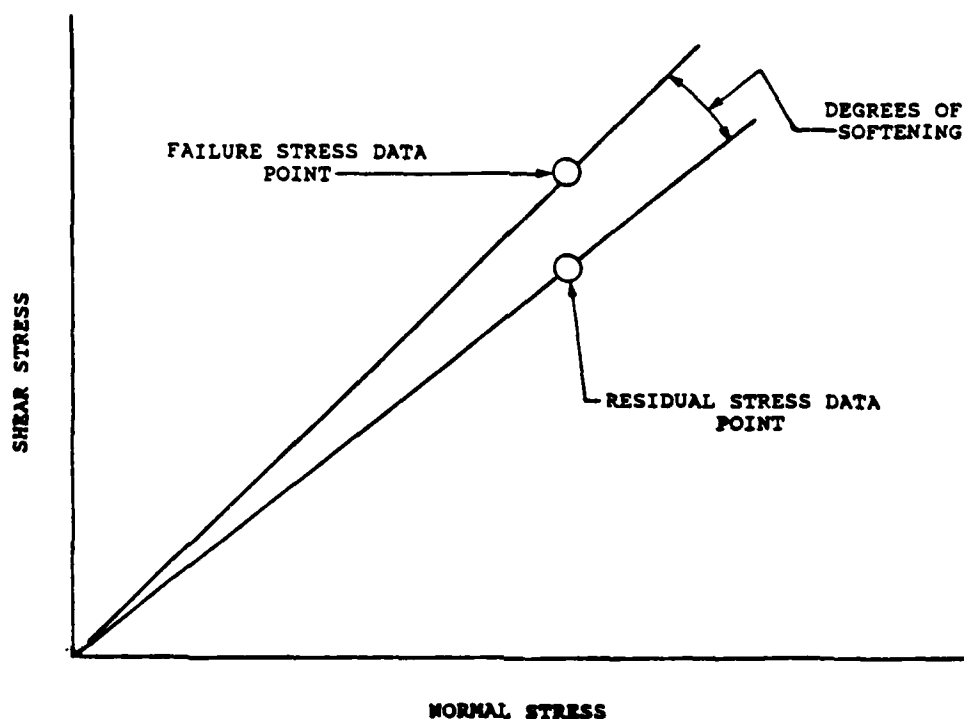


Figure 5.22 Method of Quantifying Post-Failure Response.

of degrees of softening.

Softening is plotted against density, normal stress, and velocity in Figures 5.23 through 5.28. It is noted by this author that many of the relationships between density, normal stress and velocity are not linear. However, to show general trends of dependence, a linear regression analysis is used. Because of the quantity, range and scatter of the data only general trends can be indicated.

From observation of these trends, it can be stated that softening increases with: increasing soil density, decreasing normal stress, and increasing velocity. Although

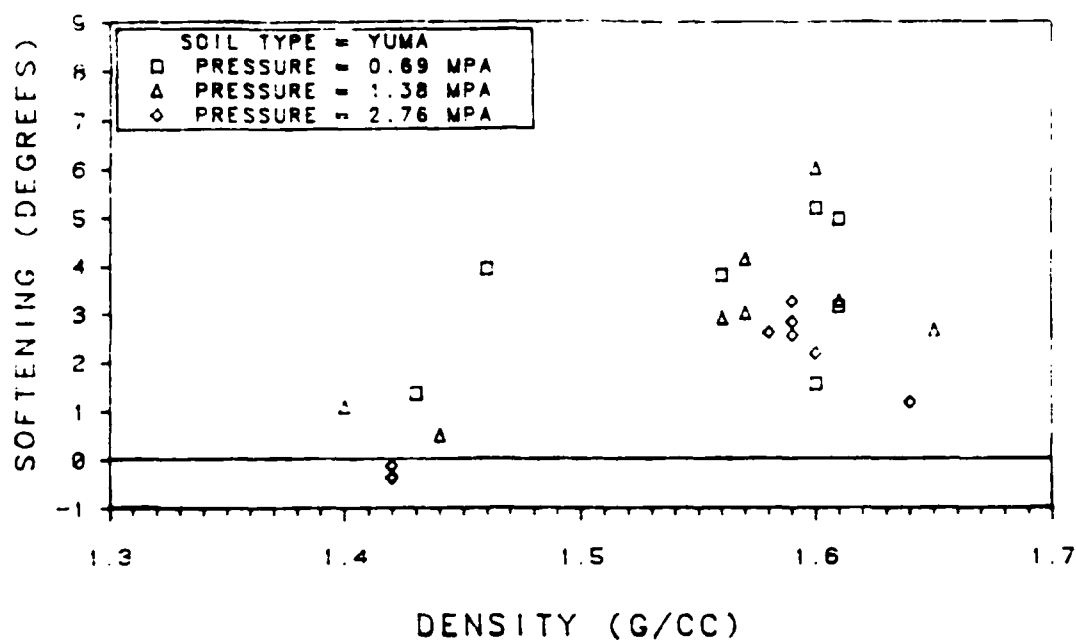


Figure 5.23 Softening vs. Density for Yuma Sand/Concrete (no linear regression).

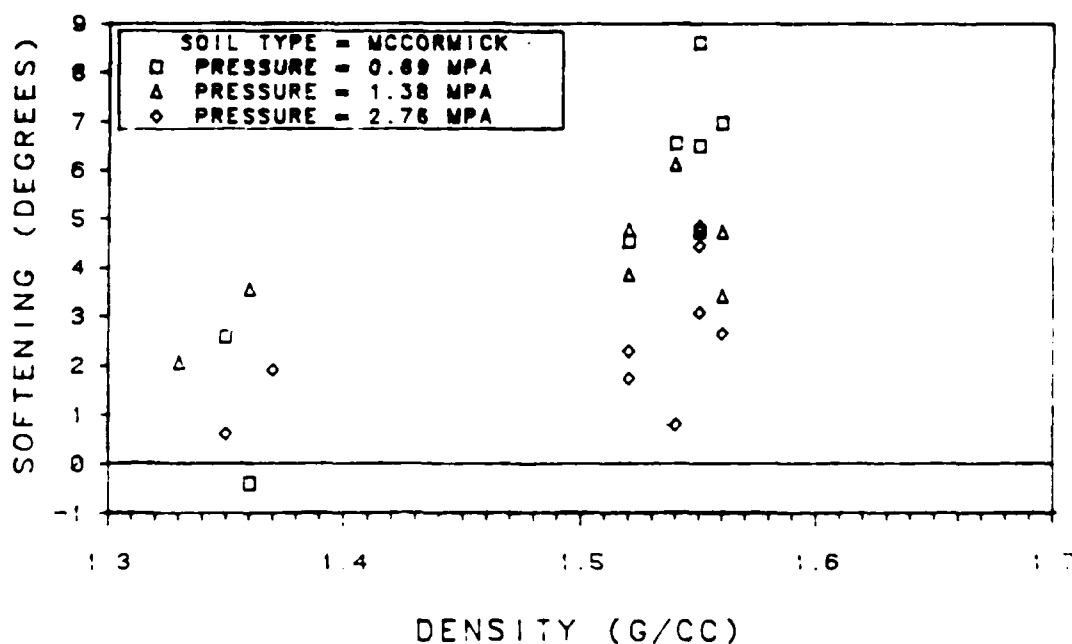


Figure 5.24 Softening vs. Density for McCormick Sand/Concrete (no linear regression).

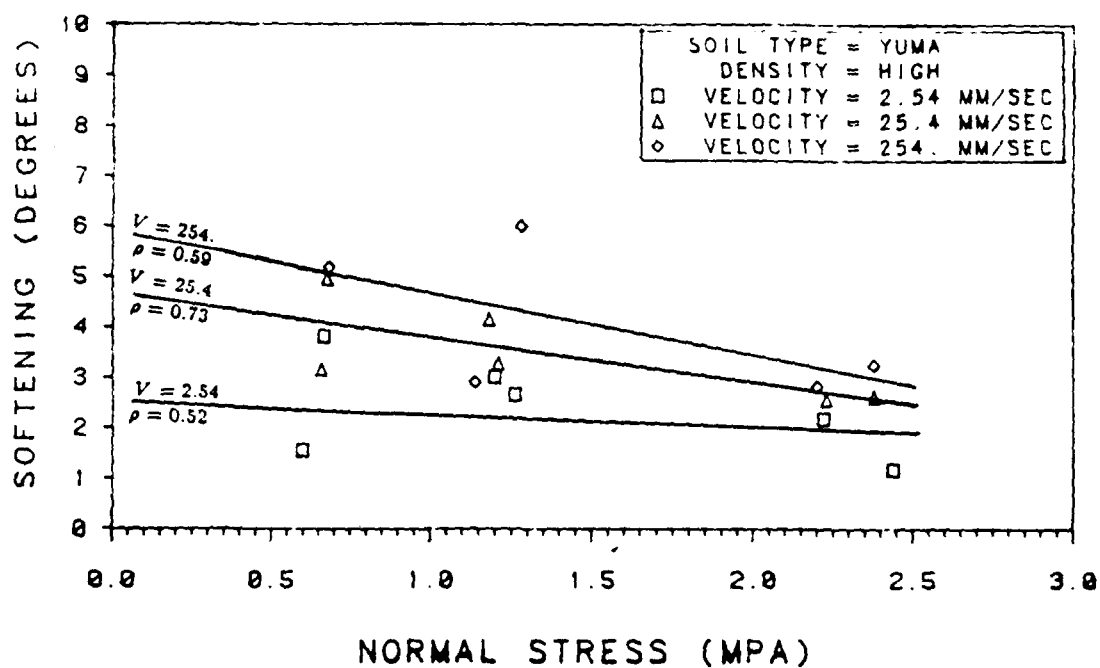


Figure 5.25 Softening vs. Normal Stress for Dense Yuma Sand/Concrete.

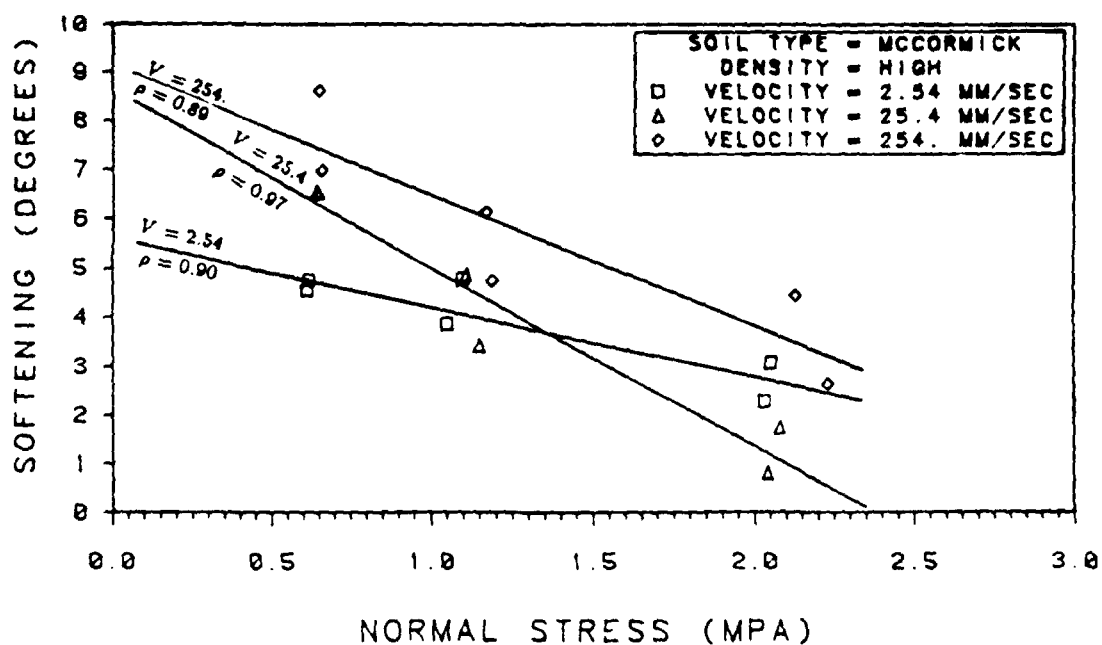


Figure 5.26 Softening vs. Normal Stress for Dense McCormick Sand/Concrete.

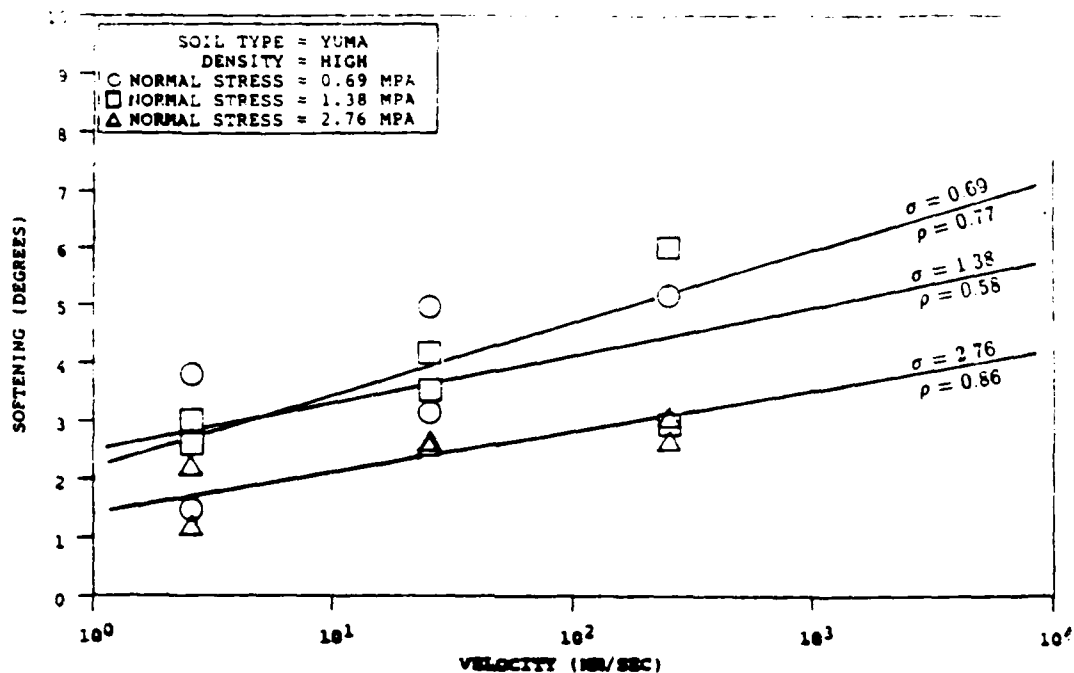


Figure 5.27 Softening vs. Velocity for Dense Yuma Sand/Concrete.

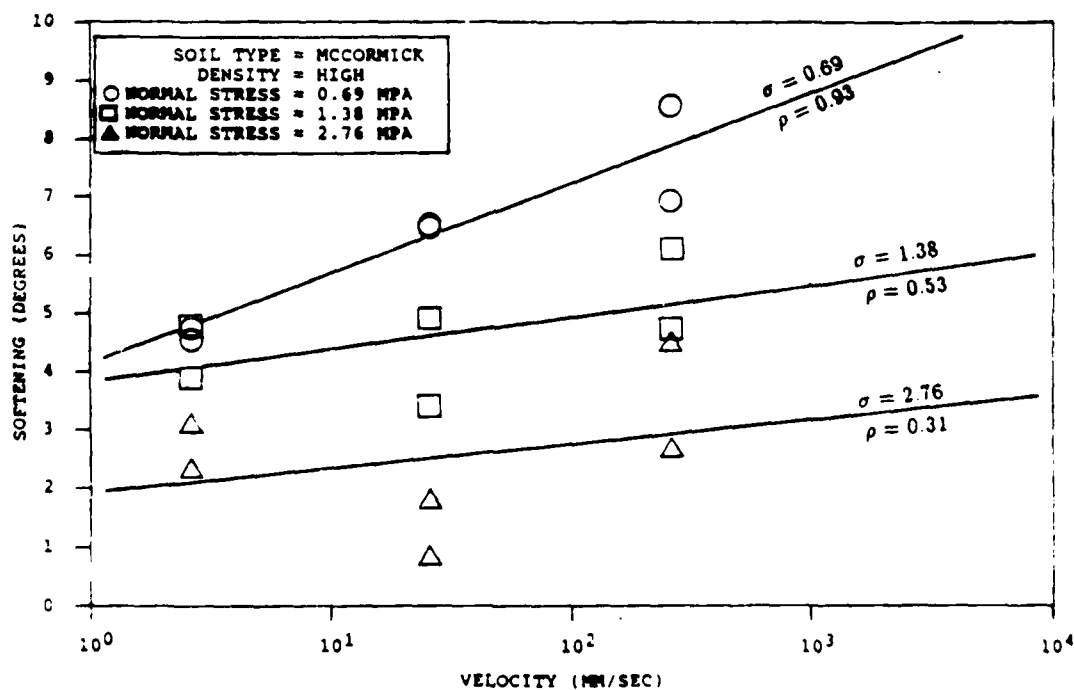


Figure 5.28 Softening vs. Velocity for Dense McCormick Sand/Concrete.

the trends of softening with density and normal stress are well documented, the increase in softening with increasing velocity is not.

One explanation for this trend could be that during the higher deformation rates, more post-peak sand particle /concrete asperity destruction occurs, thus producing a finer and more uniform distribution of soil and interface particles than for the lower velocity tests. Finer and more uniform soil particles will create a lower value of residual stress (22).

Another explanation is that this trend is the same trend that is observed for large volume, high velocity land slides. Friction coefficients calculated from observations of the slides reveal an apparent weakening of the soil strength during high velocity movement (12,15,18). An attempt to explain this behavior has been postulated by many researchers, the most popular theory being a phenomenon called "mechanical fluidization" (McSaveney (17), Erismann(11)). This theory suggests a reduction in shear friction transfer due to the unique particle kinetics that occur during high velocity shearing. A thorough explanation of this phenomenon is beyond the scope of this study.

The measured increase in softening with increasing velocity could also be due to experimental error. Differences in soil density and soil structure, especially at the interface, will produce a significant amount of

scatter in the data. However, this scatter would not explain the trend of rate dependent residual strength that was observed throughout the tests. No other discernable reasons for an experimental error have been perceived by this author. In short, no conclusive explanation will be given to justify the measured rate dependence of the residual strength.

5.3 Soil Deformation Measurement at the Interface

A recent paper by Chen and Schreyer (5) suggests that soil deformation near an interface behaves much like the velocity distribution of a moving fluid near a wall interface. This velocity distribution pattern is described by the boundary layer theory in fluid mechanics. Chen and Schreyer's explanation states that there is no relative slip between a soil and a structure during shear strain, but that a shear band is formed. The shear band is graphically depicted in Figure 5.29.

To verify Chen and Schreyer's explanation, a method was implemented to measure the shear deformation pattern of the soil in the shear box after the duration of the test. This was done by covering a 1.5 mm by 35 mm aluminum plate with blue chalk dye and then sliding the plate vertically downward into the soil sample. The location of insertion of the dyed plate, shown in Figure 5.30, was chosen to reduce the measured effects of the front constraining wall on shear strain. The plate was then pulled out, thus leaving a

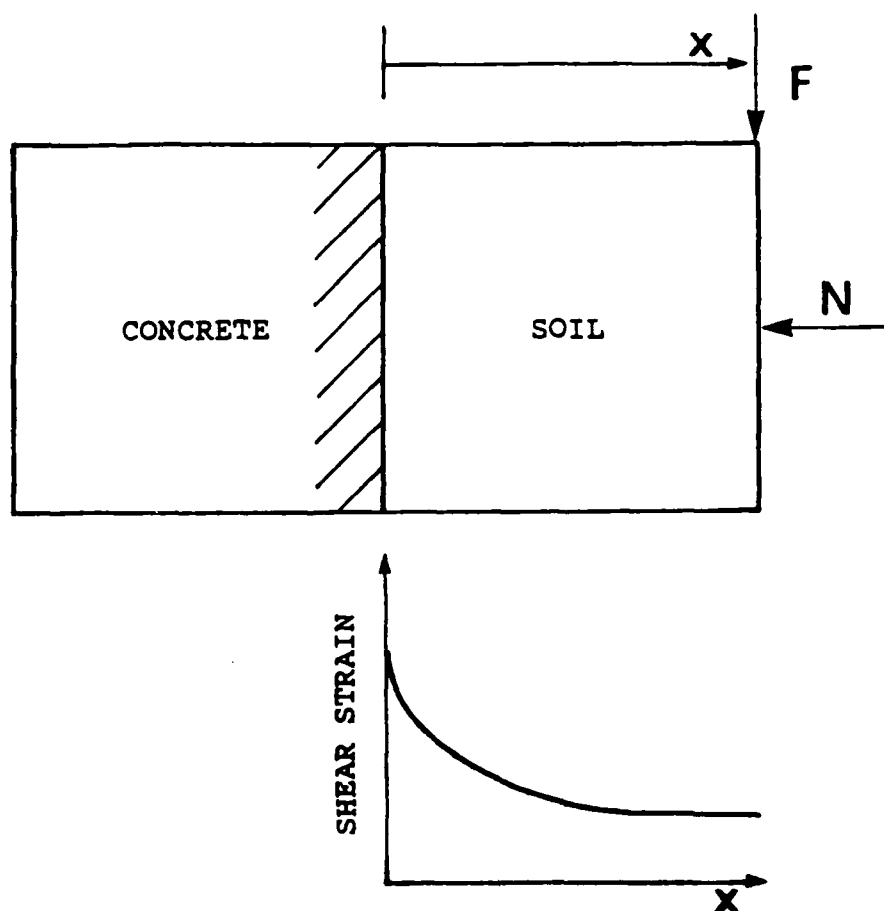


Figure 5.29 Interface Shear Band Deformation Theory (from Chen and Schreyer).

vertical line of soil particles stained with the blue dye.

After the shear test was conducted, the deformation pattern was measured by carefully scraping away the compacted and deformed soil sample and then measuring the coordinates of the exposed blue particles in reference to the stationary shear box. This procedure for deformation measurement was only performed once, and this test involved

a low density McCormick sand, a high normal stress, and a low velocity of deformation.

The deformation pattern measured is shown in Figure 5.30. This pattern indicates that, as Chen and Schreyer suggested, a shear band will develop when the interface is subjected to shear strain. Directly at the interface a 1.6 mm layer of fine sand particles and fine concrete particles were observed. This may be compared to the maximum soil particle diameter of 1.7 mm. This interface layer is created by soil particles becoming embedded into the relatively soft concrete surface during static normal load application. As shearing is begun, a combination of soil failure and surface concrete failure develops. The use of a different concrete specimen, and thus a fresh layer of soft concrete surface, could explain the strength ratio results that indicated soil failure was occurring at the interface.

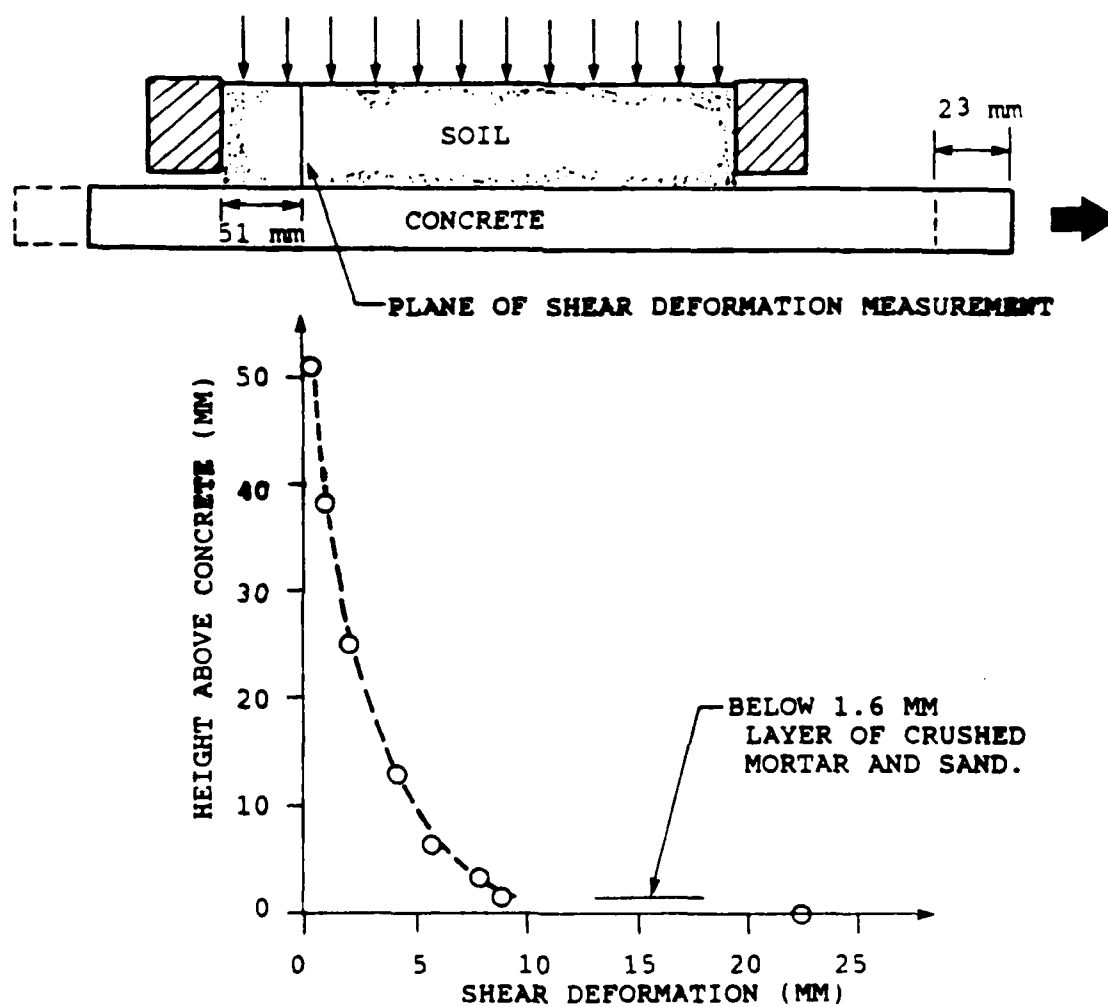


Figure 5.30 Measured Deformation Pattern.

CHAPTER 6

CONCLUSIONS AND RECOMMENDATIONS

6.1 Summary of Previous Literature

From previous literature it has been found that the strength ratios resulting from experiments performed on dry sand/rough concrete interfaces ranged between 0.75 and 1.0. Experiments performed by Huck (14) using a torsional shear ring device produced a strength ratio far below this range, approximately 0.5. It is unknown whether this lower value of the strength ratio is due to the use of the more accurate torsional ring device or to experimental error. In addition, the majority of the results from previous research indicated that there were slight to no rate dependent effects on the strength of dry sands and sand/concrete interfaces.

6.2 Conclusions

The strength of a sand/concrete interface is not rate dependent within the shearing velocity range of 2.54 mm/second to 254. mm/seconds. A slight decrease in strength was observed with a decrease in sand density.

The strength ratio f_{ϕ} produced by dry sands/rough concrete interfaces is much closer to 1.0 than predicted by previous research. It is predicted that under high normal pressures the soft layer on the outside surface of a concrete will significantly effect the interface strength.

The failure criterion can be represented by a single failure mode. This is in contrast to the separate failure modes of soil failure and interface failure suggested by Huck (14). A comparison of results from this research to results found by Huck is shown in Figure 6.1.

While strength of the interface is independent of the shearing velocity, the post-peak behavior is rate dependent. Post failure softening can be qualitatively explained by the following trends:

- Softening increases with increasing density
- Softening decreases with increasing normal stress
- Softening increases with increasing shearing velocity.

The most predominant of these trends is the dependance on normal stress. By extrapolation of the test data, it is concluded that under high values of normal stress (> 10 MPa) softening will change the friction angle less than 1 degree and that the dependence of the residual strength on shearing velocity becomes insignificant.

Soil deformation near the interface creates a shear band as suggested by Chen and Schreyer (5).

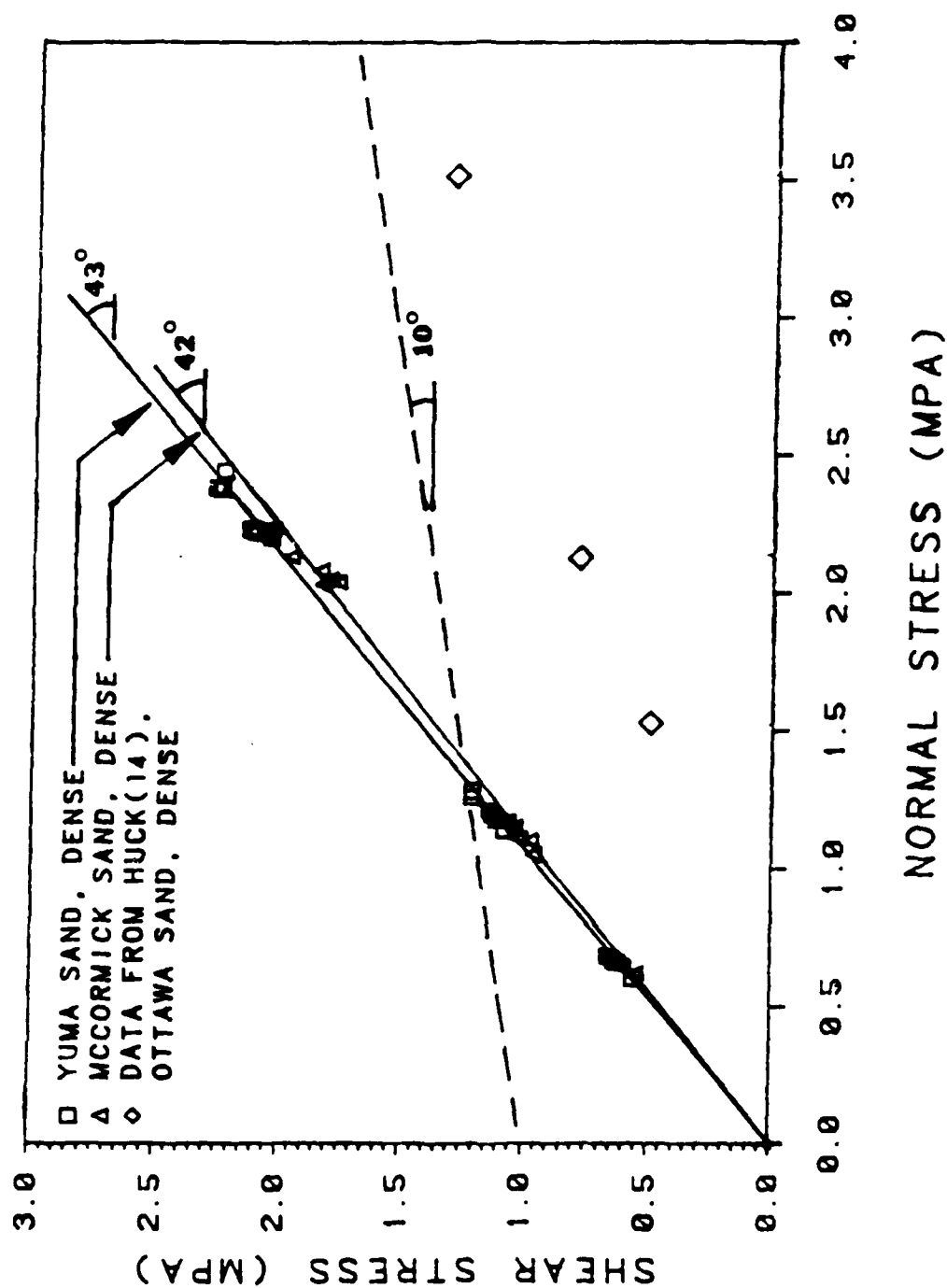


Figure 6.1 Comparison of Observed Mohr Envelopes from This Research and from Hück.

6.3 Recommendations

1. Failure criterion for a sand/concrete interface should be modelled as being 0.9 to 1.0 times the friction angle of the soil. This recommendation is made based on the results from this experimental program as well as the results from previous experimental programs. It is anticipated that under large ranges of normal stress (greater than 5 MPa) the Mohr envelope will have to be modified to account for the slight curvature in the Mohr envelope of dense sands. This can be accomplished, as shown in Figure 6.2, by conducting triaxial tests on the soil using the full range of confining stresses anticipated. This will result in a curved Mohr envelope. To estimate the interface strength it is suggested that the resulting failure shear stress values be modified by the formula:

$$\tau_i = \sigma_s \cdot \tan \left[(f_\phi) \cdot \tan^{-1}(\tau_s/\sigma_s) \right] \quad (6.1)$$

where (σ_s, τ_s) is a failure point from a triaxial test, (σ_s, τ_i) is the estimated failure point for the weaker interface, and f_ϕ is the interface strength ratio. Plotting of these new data values produces the failure curve for the sand/concrete interface. To model this nonlinear curve using the SAMSON2 code, the bi-linear envelope shown in Figure 6.2 is suggested.

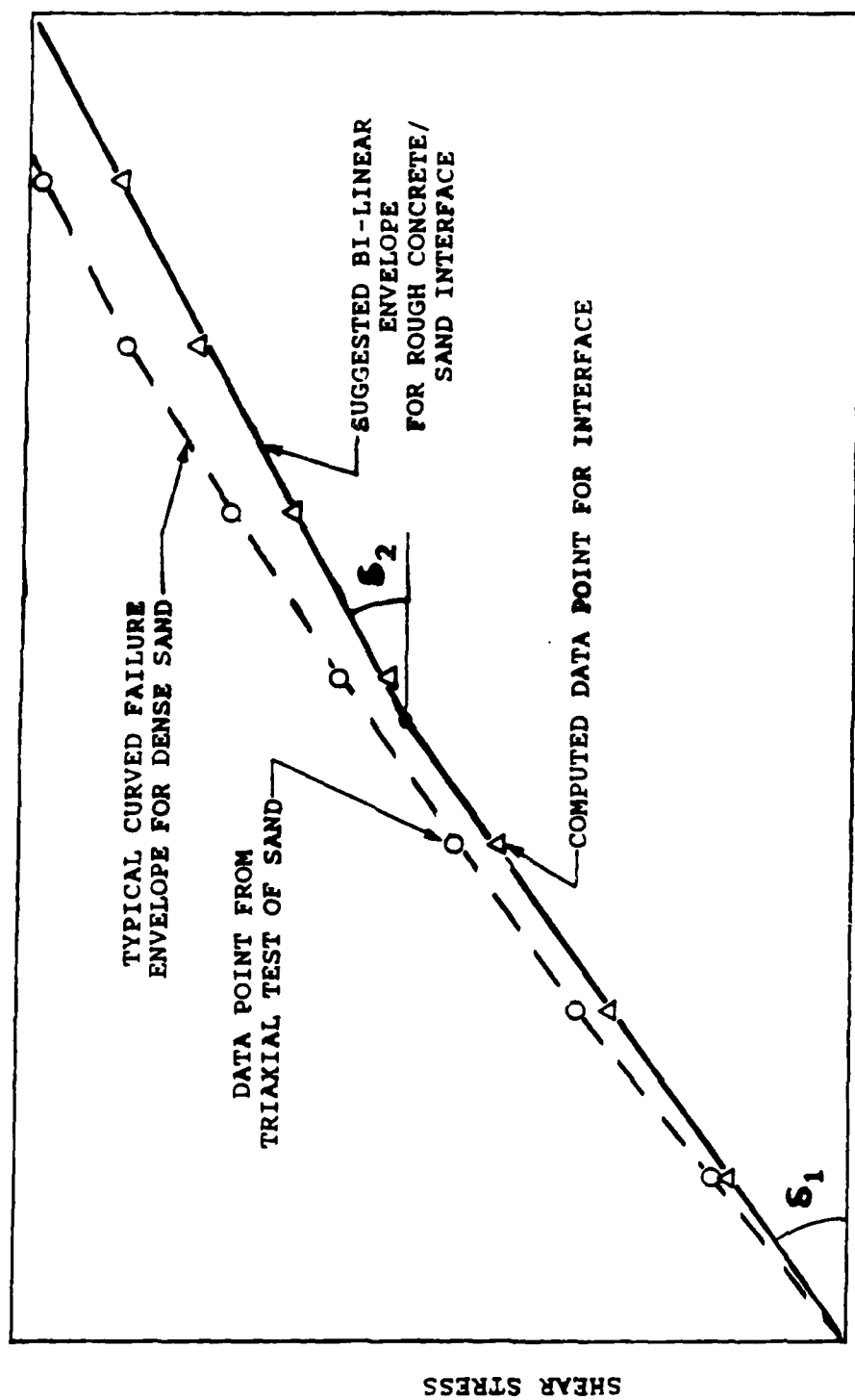


Figure 6.2 Recommended Method for Determining the Mohr Envelope of a Dry Sand/Rough Concrete Interface.

2. It is recommended that post-failure response be modelled using a perfectly-plastic model. Although this type of modelling technique may not be sufficiently accurate in simulating the shear response during low magnitudes of interface normal stress, it becomes more accurate as the normal stress increases. This model is also very time efficient and easy to program.
3. To model interface behavior using the slideline technique currently in use at the AFWL, it is recommended that interface nodes be bonded together until interface failure occurs and that the post-failure frictional transfer across the slideline be simulated by the perfectly-plastic model. It is also suggested that a sensitivity study be performed on the parameters used in the SAMSON2 code to model the non-linear pre-failure response of the interface. This non-linear behavior is governed by a Drucker-Prager failure surface and a non-associated flow rule for the soil elements adjacent to the interface.
4. Future experimental programs should use the torsional shear ring device. The use of the direct shear device introduces a number of uncertainties and inaccuracies (inhomogeneous shear strain and axial deformation distribution, effect of shear on sidewalls, gap size effects, etc). It is also recommended that soil

friction angles and interface friction angles be determined using the same torsional ring device. This will eliminate inaccuracies produced by comparison of separate testing devices and methods.

REFERENCES

1. Bishop, A.W., "The Strength of Soils as Engineering Materials," Milestones in Soil Mechanics, pp 131-171.
2. Bowles, J.E., Engineering Properties of Soils and Their Measurement, 2nd ed., McGraw-Hill, New York, 1978.
3. Bridgwater, J., "Stress-Velocity Relationships for Particulate Solids," ASME Paper No. 72 MH-21, New York American Society of Mechanical Engineers, 1972.
4. Brummond, W.F., and Leonards, G.A., "Experimental Study of Static and Dynamic Friction Between Sand and Typical Construction Materials," ASTM J. Testing and Evaluation, Vol. 1, No. 2, pp 162-165, 1973.
5. Chen, Z., and Schreyer, H.L., A Constitutive Model for Simulating Soil-Concrete Interfaces, AFWL-TR-XX-XX, Air Force Weapons Laboratory, Kirtland Air Force Base, New Mexico, 1985.
6. Clough, G.W., and Duncan, J.M., "Finite Element Analysis of Retaining Wall Behavior," J. Soil Mech. Found. Div., ASCE, Vol. 97, No. SM12, pp 1657-1673, 1971.
7. Desai, C.S., and Holloway, D.M., "Load-Deformation Analysis of Deep Pile Foundations," Proc. Symp. Appl. Finite Elem. Meth. Geotech. Engrg., Vicksburg, Mississippi, 1972.
8. Desai, C.S., "Finite Element Method for Analysis and Design of Piles," Misc. Paper S-76-21, U.S. Army Engr. Waterways Exp. Station, Vicksburg, Mississippi, 1976.
9. Deutschman, A.D., et al., Machine Design: Theory and Practice, Macmillan Publishing Co., Inc., New York, 1975.
10. Drumm, E.C., and Desai, C.S., Testing and Constitutive Modelling for Interface Behavior in Dynamic Soil-Structure Interaction, Report to the National Science Foundation, 1983.
11. Dunn, I.S., Anderson, L.R., and Kiefer, F.W., Fundamentals of Geotechnical Analysis, John Wiley and Sons, New York, 1980.
12. Erismann, T.H., "Mechanisms of Large Landslides," Rock Mechanics, Vol. 12, pp 15-46, 1979.

AD-A193 595

BEHAVIOR OF SAND/CONCRETE INTERFACES UNDER DYNAMIC
LOADS(U) WASHINGTON STATE UNIV PULLMAN

2/2

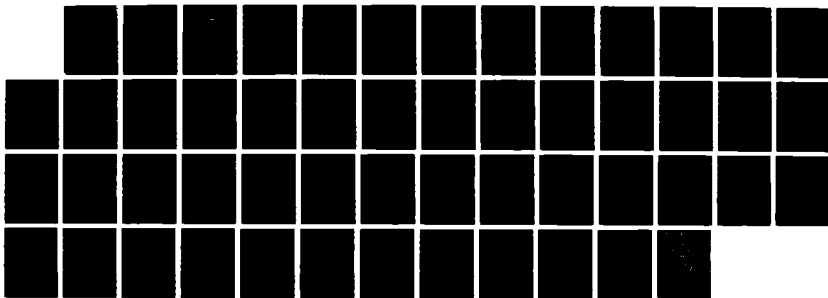
R L BIGELIS ET AL. APR 88 AFNL-TR-86-104

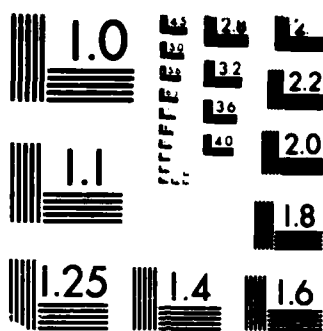
UNCLASSIFIED

F29681-85-K-0050

F/G 20/11

NL





MICROCOPY RESOLUTION TEST CHART
 NATIONAL BUREAU OF STANDARDS-1963-A

13. Healy, K. A., The Dependence of Dilation in Sand on Rate of Shear Strain, PhD thesis, Massachusetts Institute of Technology, 1963.
14. Huck, P.J., et al., Dynamic Response of Soil/Concrete Interfaces at High Pressure, AFWL-TR-73-264, Air Force Weapons Laboratory, Kirtland Air Force Base, New Mexico, April 1974.
15. Hungr, O., and Morgenstern, N. R., "High Velocity Ring Shear Tests on Sand," Geotechnique, Vol 34, No. 3, 1984, pp 415-421.
16. Ito, T., and Fujimoto, K., "Strain Rate Effects on Stress-Strain Relationships of Sand," Proceedings of the 30th Japan National Conference for Applied Mechanics, Vol. 30, University of Tokyo Press, 1980, pp 17-24.
17. Kulhawy, F.H., and Peterson, M.S., "Behavior of Sand Concrete Interfaces," Proc. 6th Pan American Conf. on Soil Mech. and Found. Engrg., Vol. 2, pp 225-236, 1979.
18. McSaveney, M.J., "Sherman Glacier Rock Avalanche, Alaska," Rockslides and Avalanches, (Voight, B., ed.), Vol. 1, Elsevier Scientific Publishing Company, Amsterdam, pp 197-258, 1978.
19. Novosad, J., "Studies on Granular Materials II", Collection Czech. Chem. Commun., Vol. 29, pg 2697, 1969.
20. Potyondy, J.G., "Skin Friction Between Various Soils and Construction Materials," Geotechnique, Vol. 11, No. 4, pp 339-353, 1961.
21. Scarlett, B. and Todd, A.C., "The Critical Porosity of Free Flowing Solids," J. Engng. Ind., Ser. A, Vol. 91, Part I, pp 478-488.
22. Sowers, G.F., Introductory Soil Mechanics and Foundations: Geotechnical Engineering, 4th ed., Macmillan Publishing Co., 1979.
23. Vesic, A.S., and Clough, G.W., "Behavior of Granular Materials Under High Stress," J. Soil Mech. Found. Div., ASCE, Vol. 90, No. SM8, pp 661-688, 1968.

24. Whitman, R., and Healy, K., "Shear Strength of Sands During Rapid Loadings", J. of Soil Mech. Found. Div., ASCE, Vol 88, No. SM2, 1962, pp 99-132.
25. Windham, J.E., Shear Friction Test Support Program: Mechanical Property Recommendations for Yuma Clayey Sand Backfill at a Dry Density of 115 PCF, U.S. Army Waterways Experiment Station, Vicksburg, Mississippi, 1985.

APPENDIX

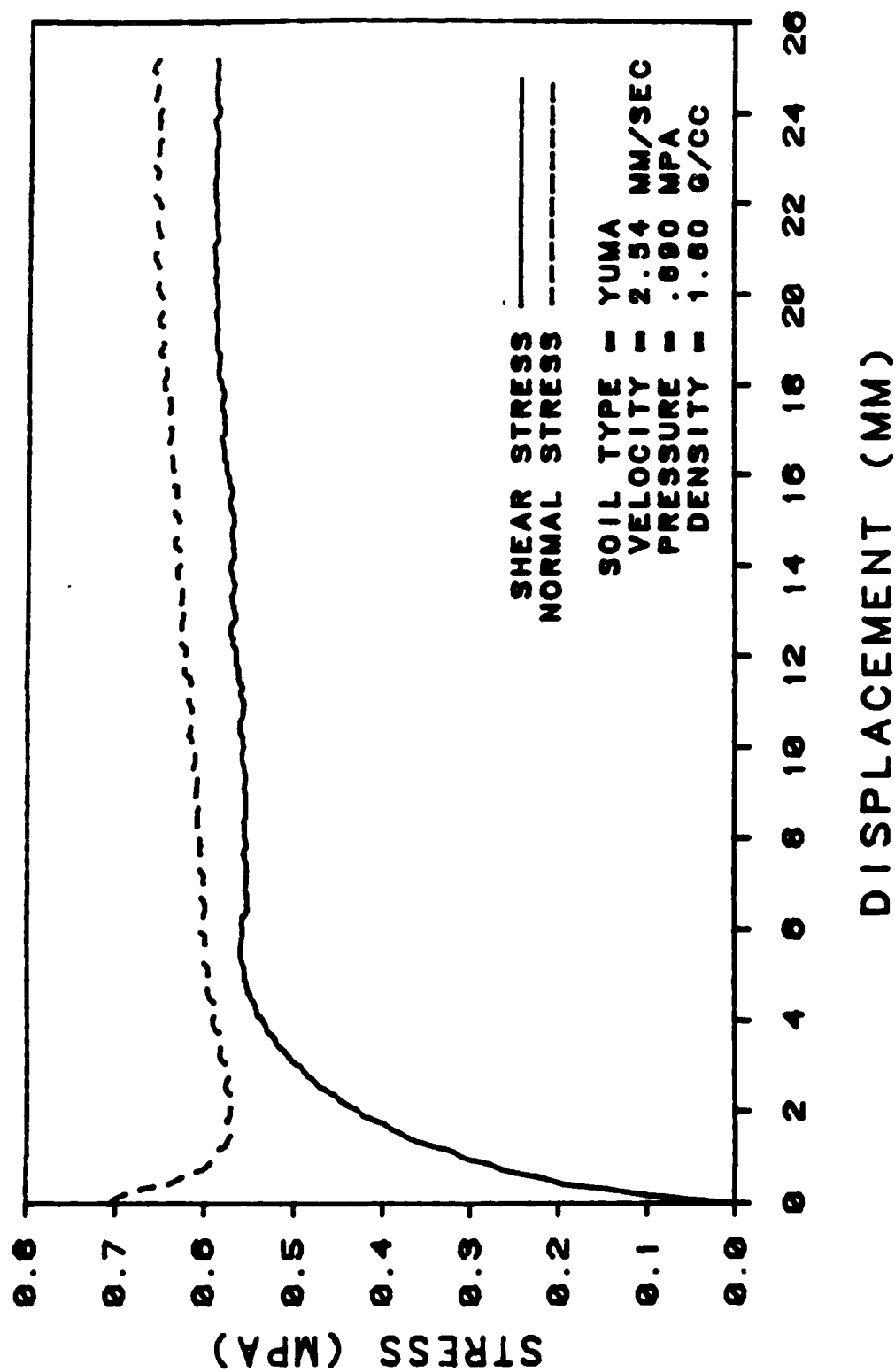


Figure A.1 Yuma Sand/Concrete, $V=2.54$ mm/s, $P=0.69$ MPa, 1st Repetition.

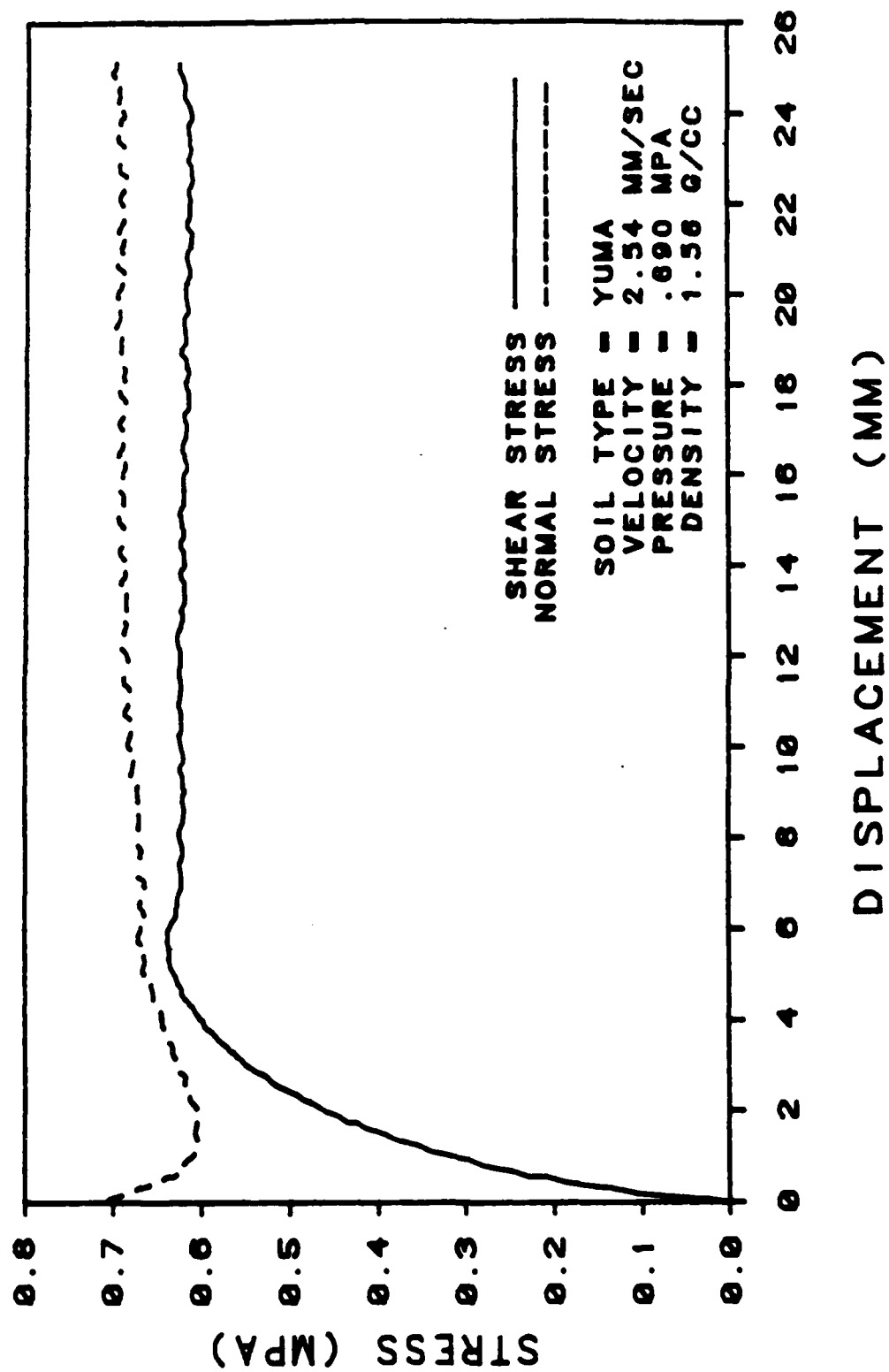


Figure A.2 Yuma Sand/Concrete, $V=2.54$ mm/s, $P=0.69$ MPa, 2nd Repetition.

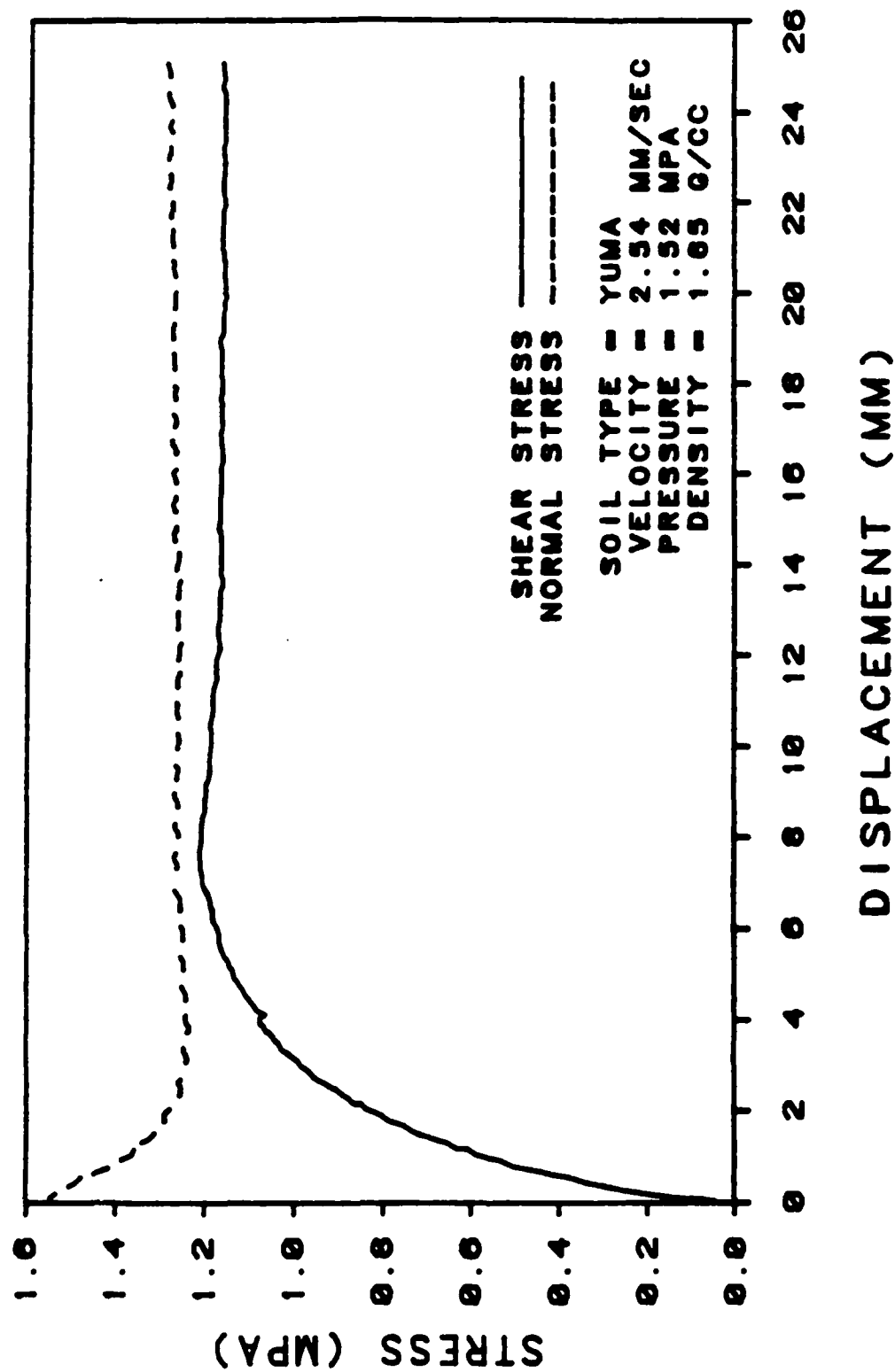


Figure A.3 Yuma Sand/Concrete, V=2.54 mm/s, P=1.38 MPa, 1st Repetition.

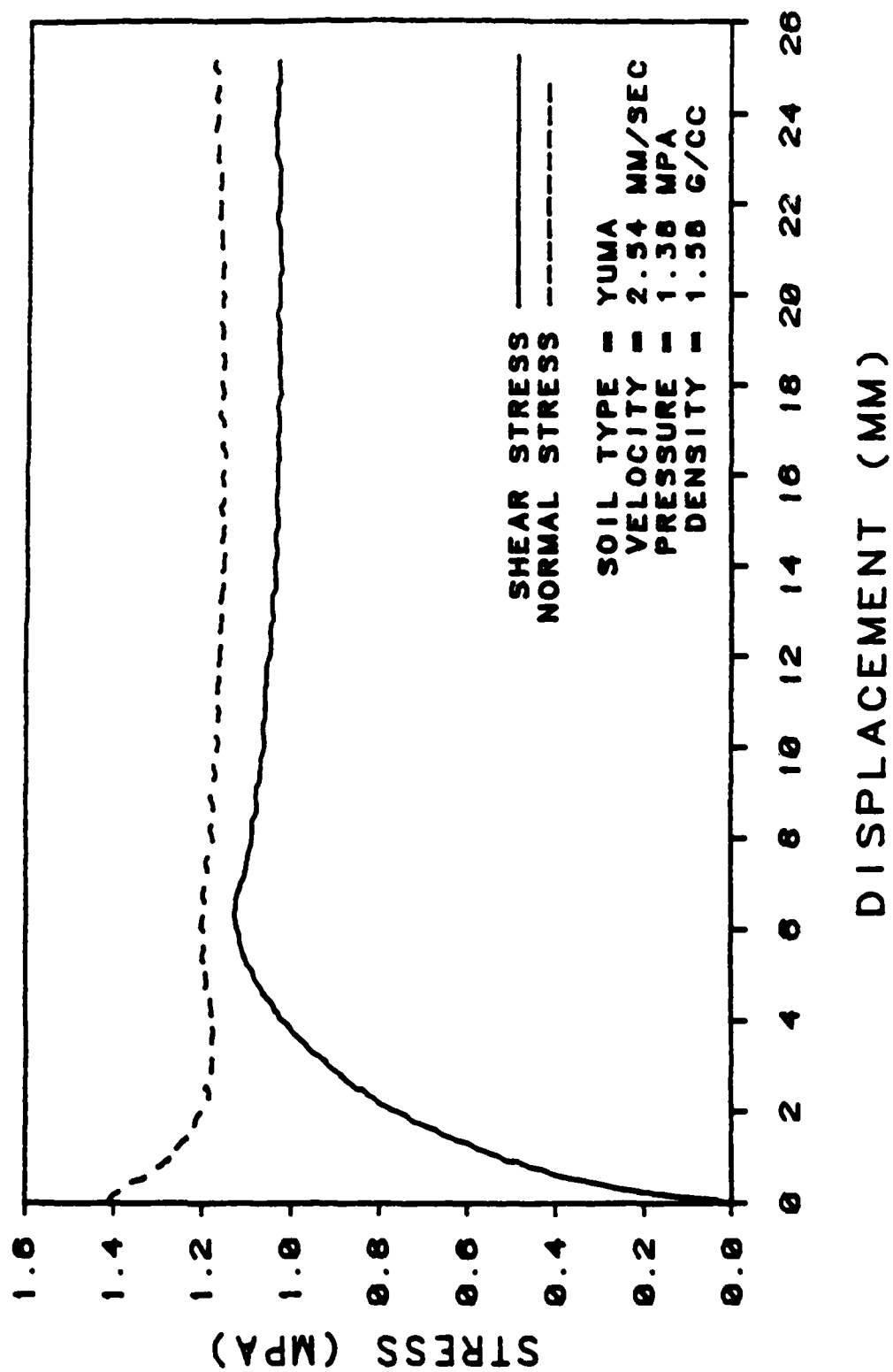


Figure A.4 Yuma Sand/Concrete, $V=2.54$ mm/s, $P=1.38$ MPa, 2nd Repetition.

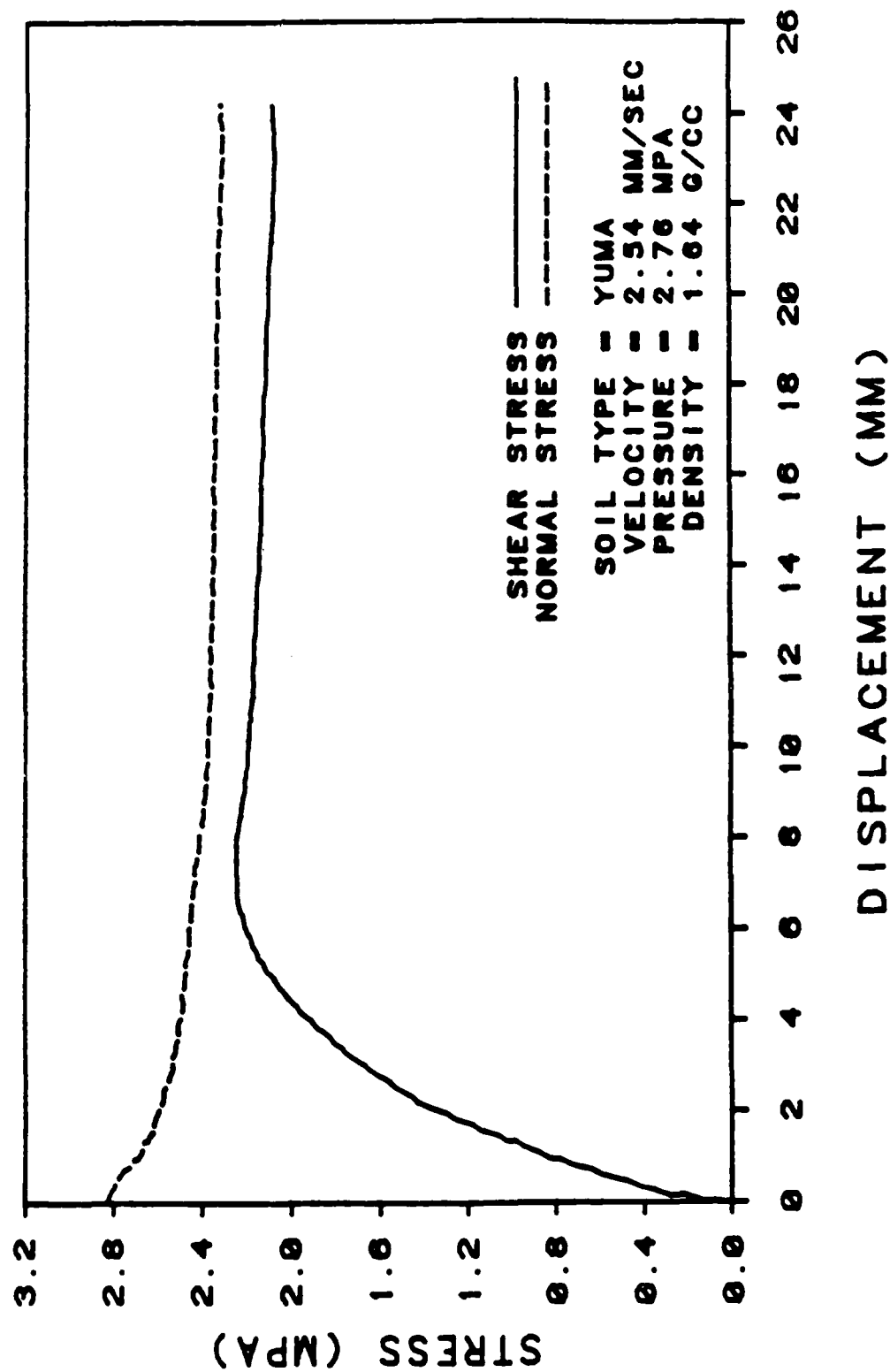


Figure A.5 Yuma Sand/Concrete, V=2.54 mm/s, P=2.76 MPa, 1st Repetition.

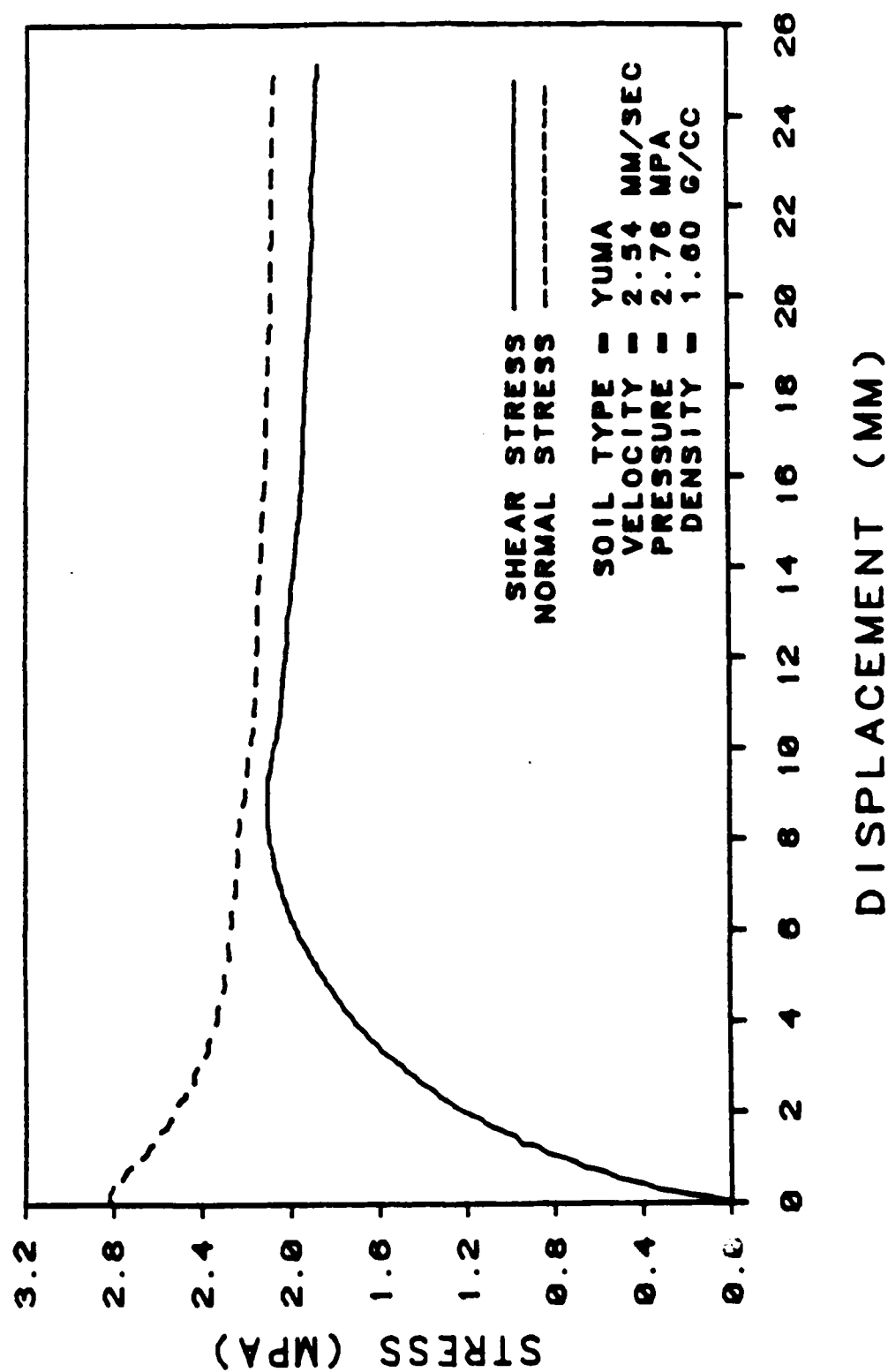


Figure A.6 Yuma Sand/Concrete, $V=2.54$ mm/s, $P=2.76$ MPa, 2nd Repetition.

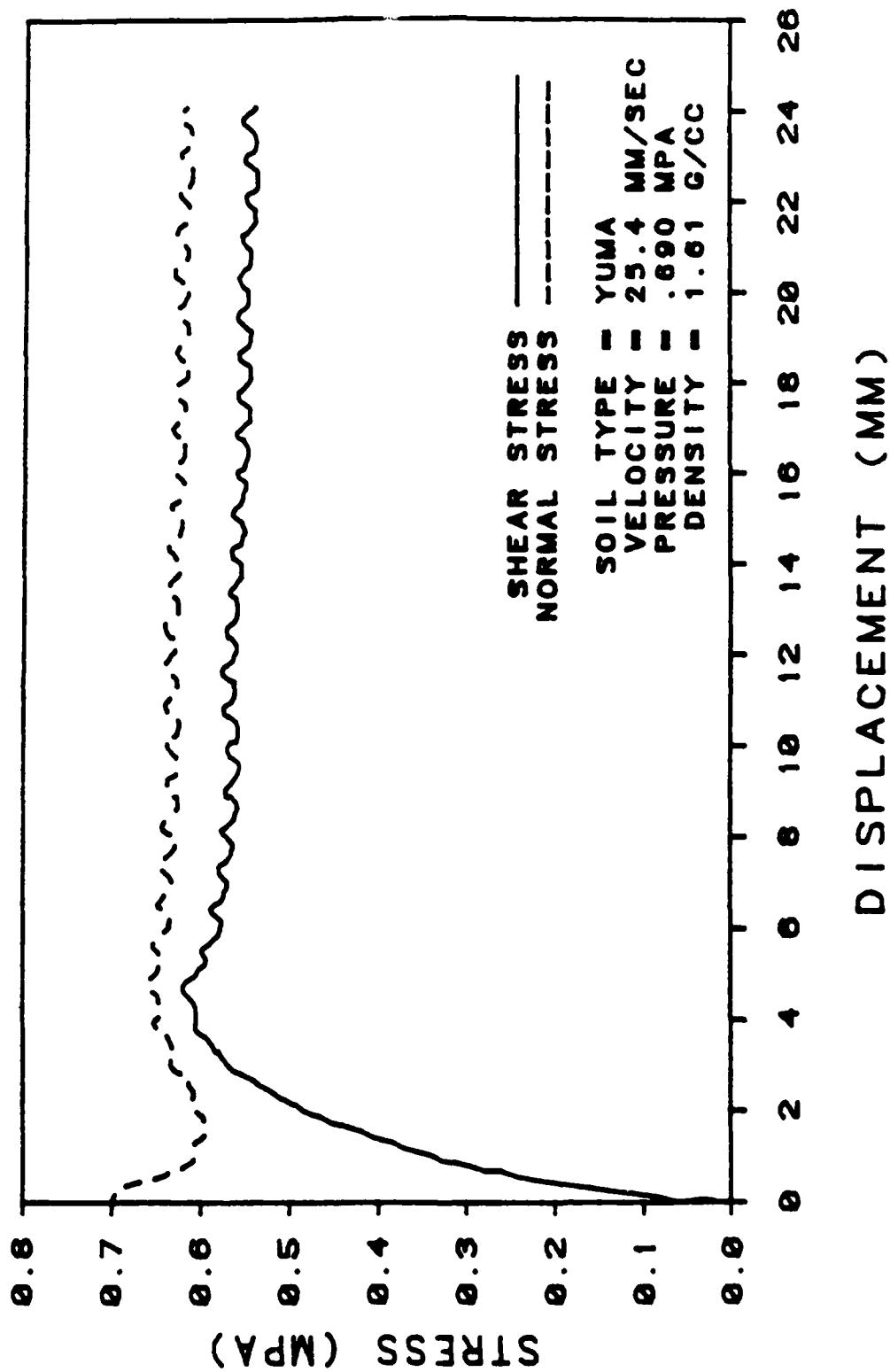


Figure A.7 Yuma Sand/Concrete, V=25.4 mm/s, P=0.69 MPa, 1st Repetition.

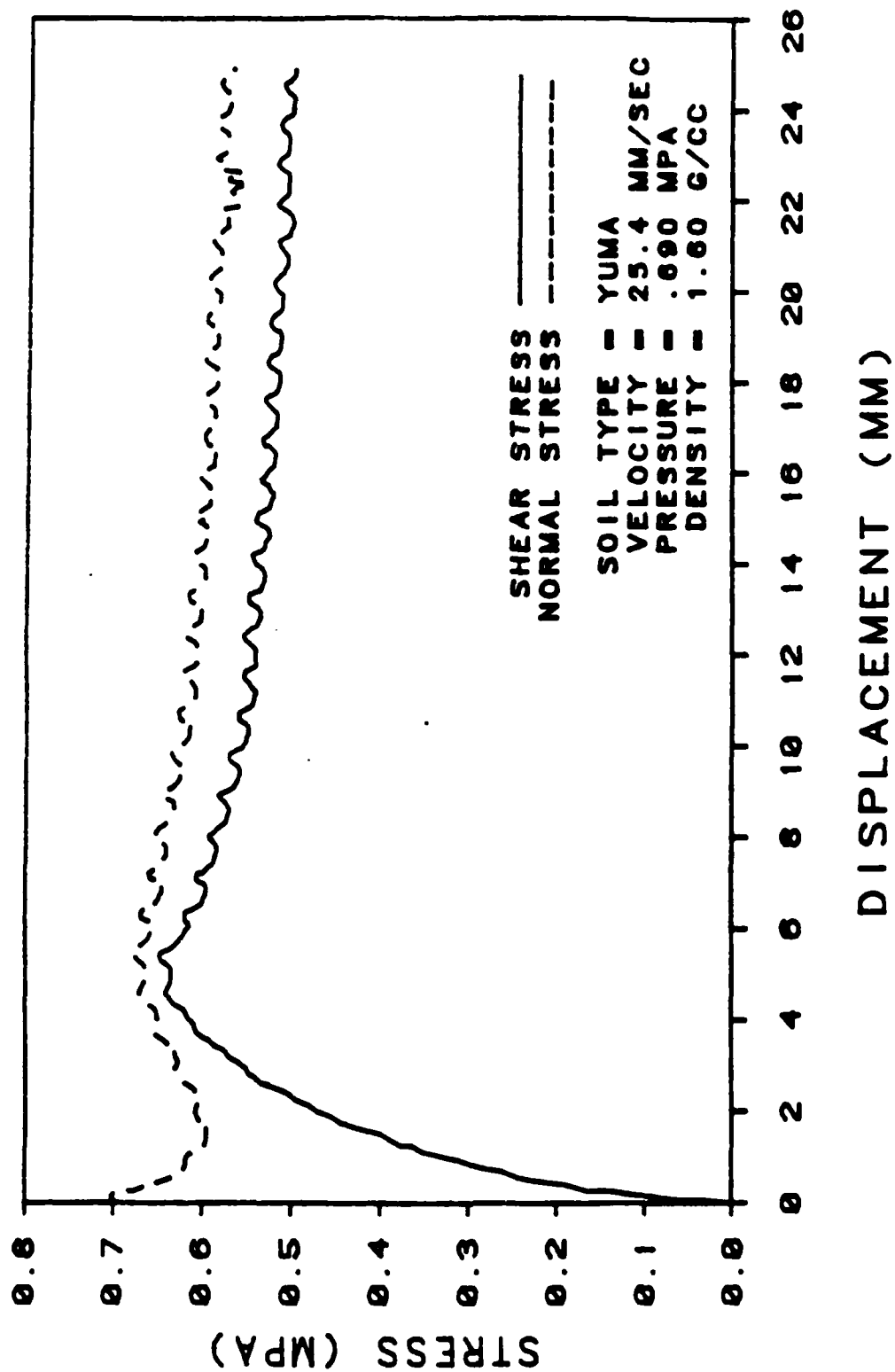


Figure A.8 Yuma Sand/Concrete, $V=25.4$ mm/s, $P=0.69$ MPa, 2nd Repetition.

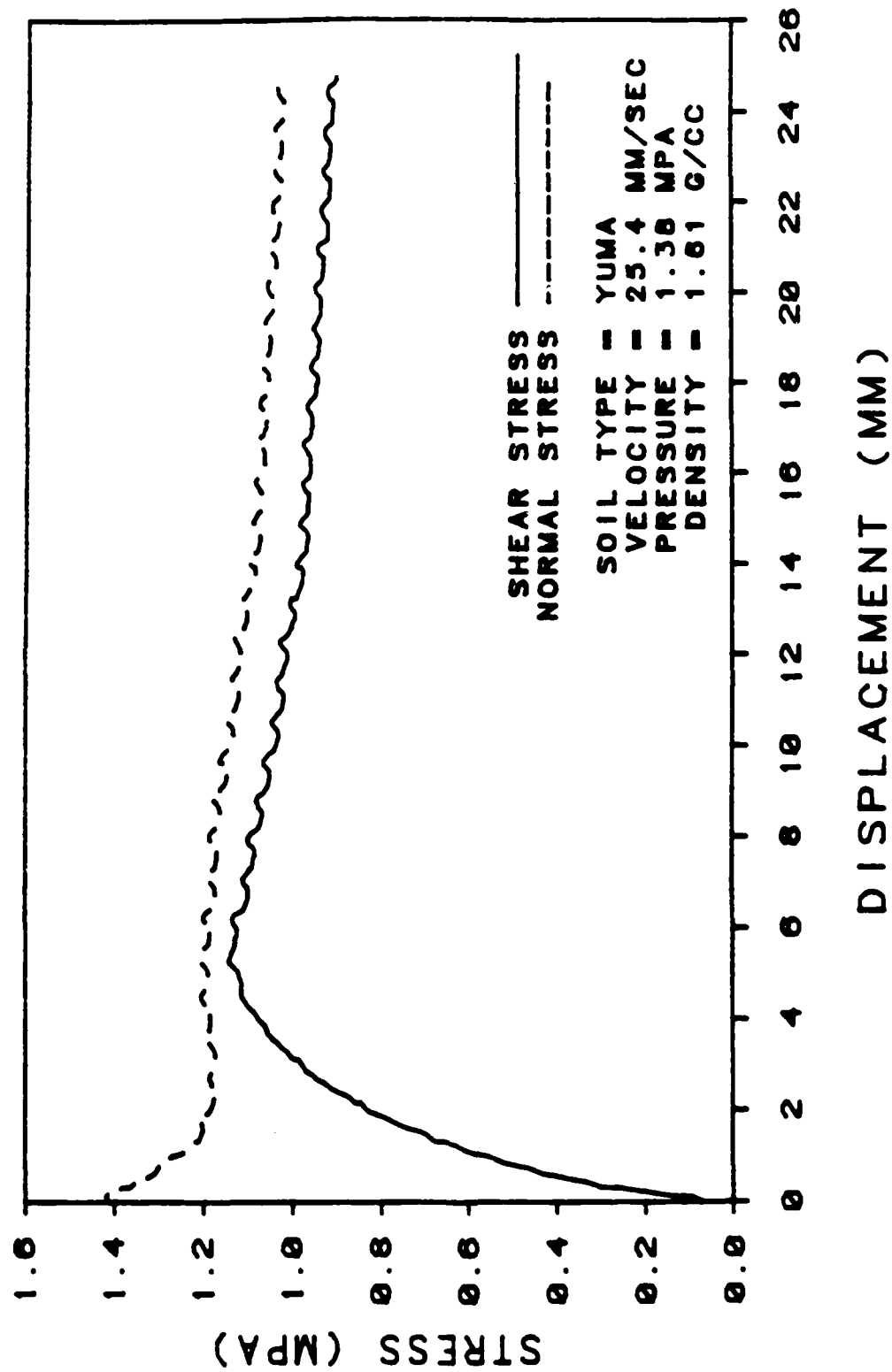


Figure A.9 Yuma Sand/Concrete, $V=25.4$ mm/s, $P=1.38$ MPa, 1st Repetition.

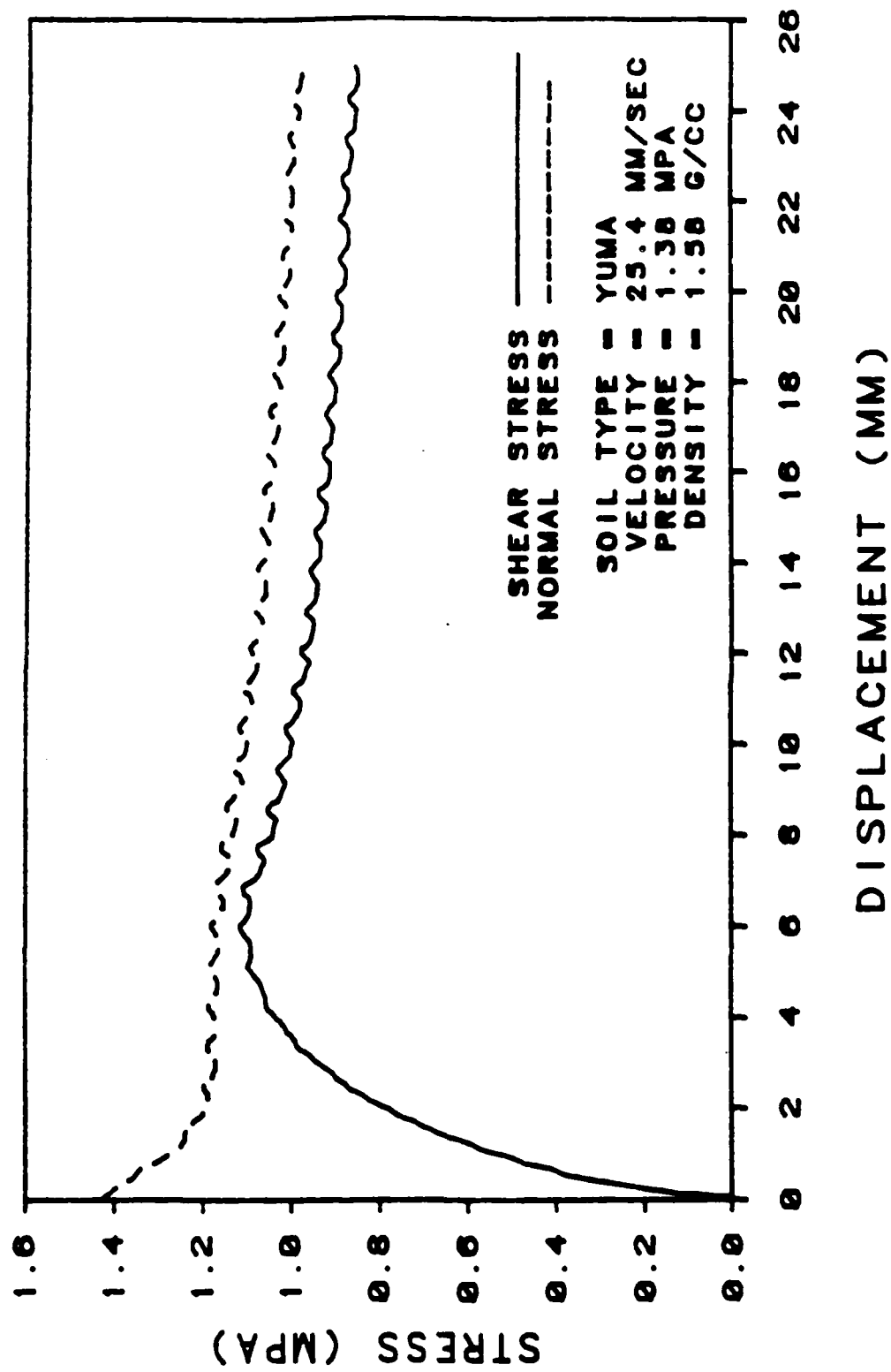


Figure A.10 Yuma Sand/Concrete, $V=25.4$ mm/s, $P=1.38$ MPa, 2nd Repetition.

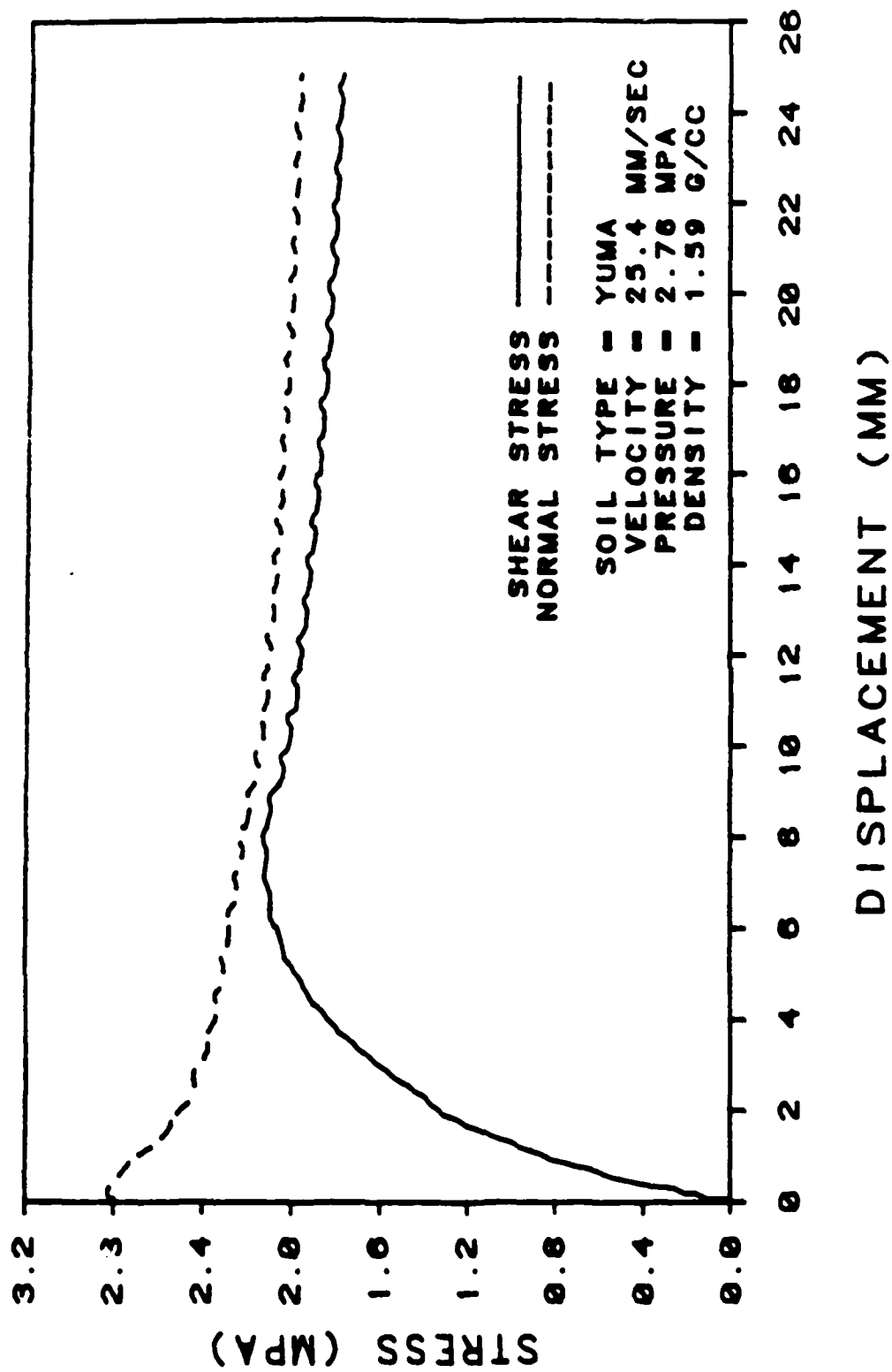


Figure A.11 Yuma Sand/Concrete, $V=25.4$ mm/s, $P=2.76$ MPa, 1st Repetition.

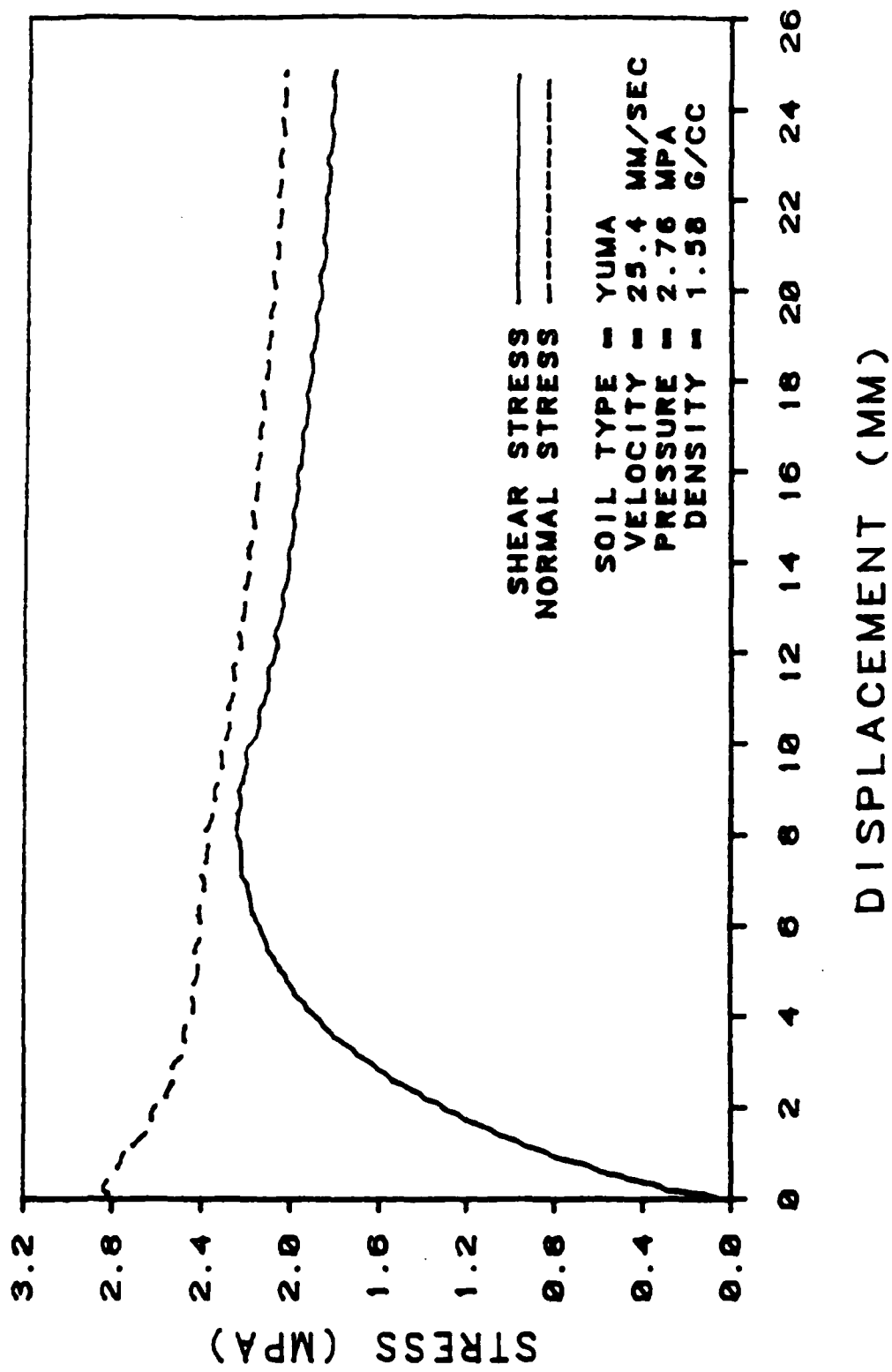


Figure A.12 Yuma Sand/Concrete, V=25.4 mm/s, P=2.76 MPa, 2nd Repetition.

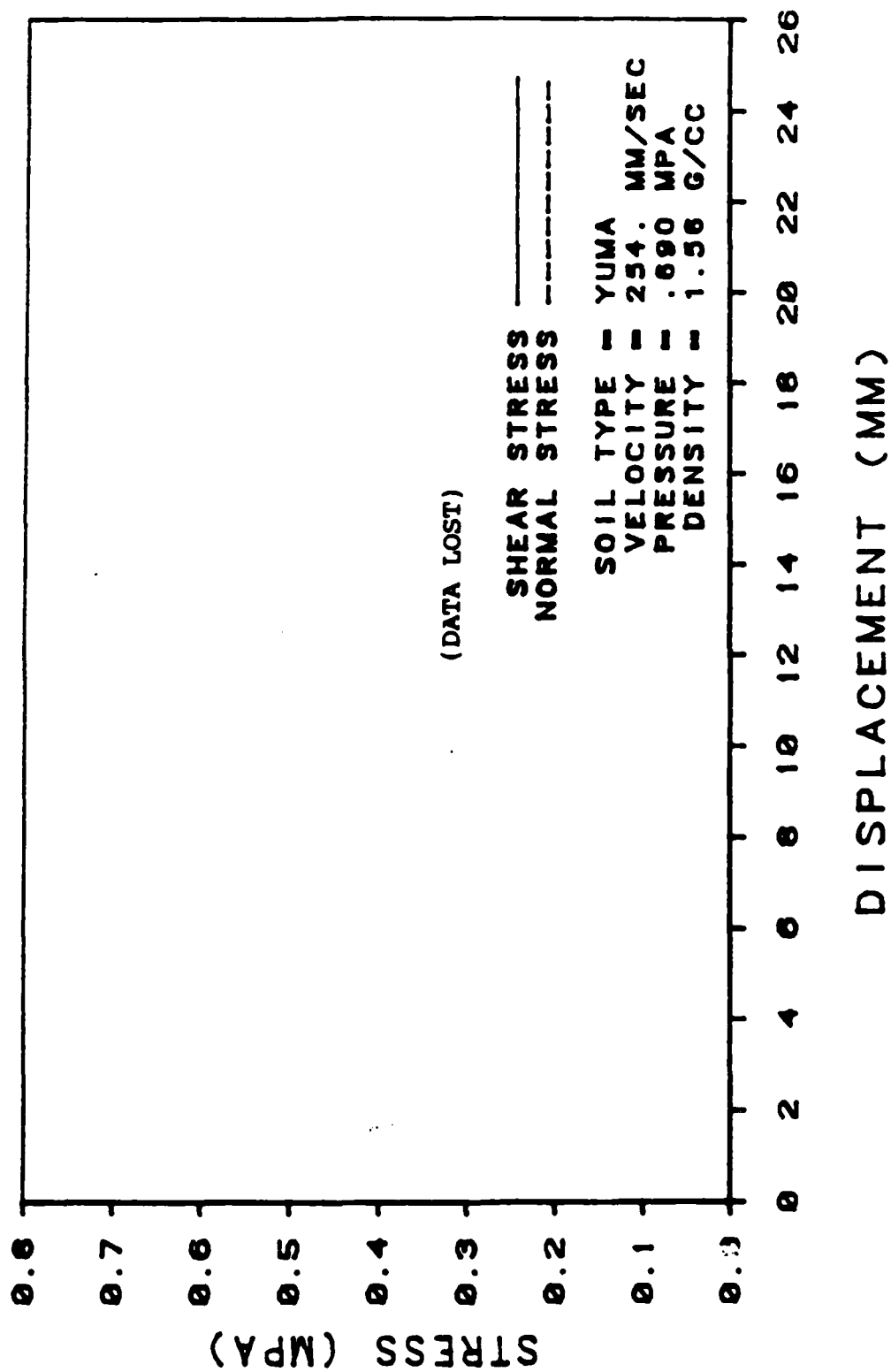


Figure A.13 Yuma Sand/Concrete, $v=254$. mm/s, $p=0.69$ MPa, 1st Repetition.

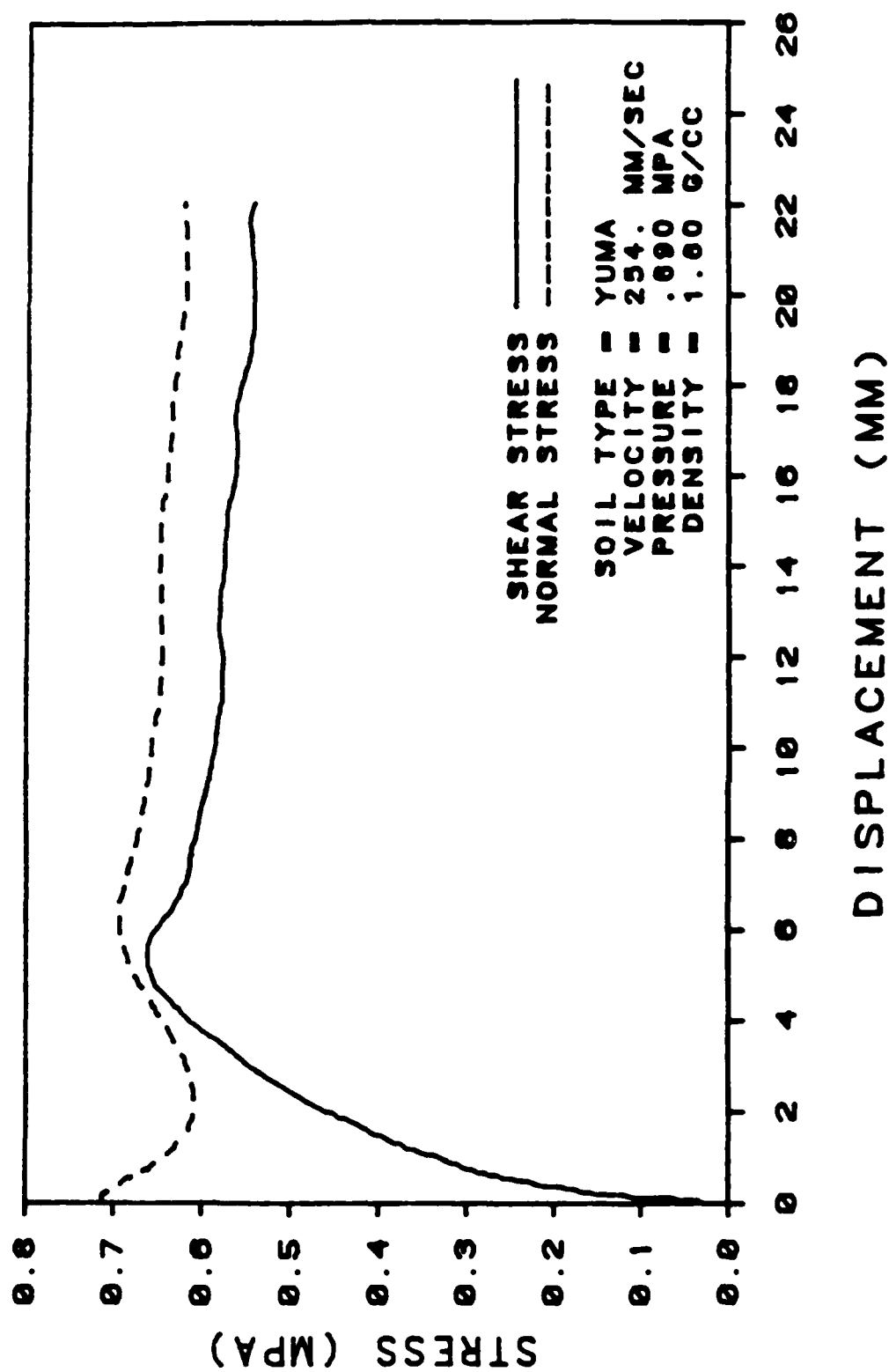


Figure A.14 Yuma Sand/Concrete, $V=254$. mm/s, $P=0.69$ MPa, 2nd Repetition.

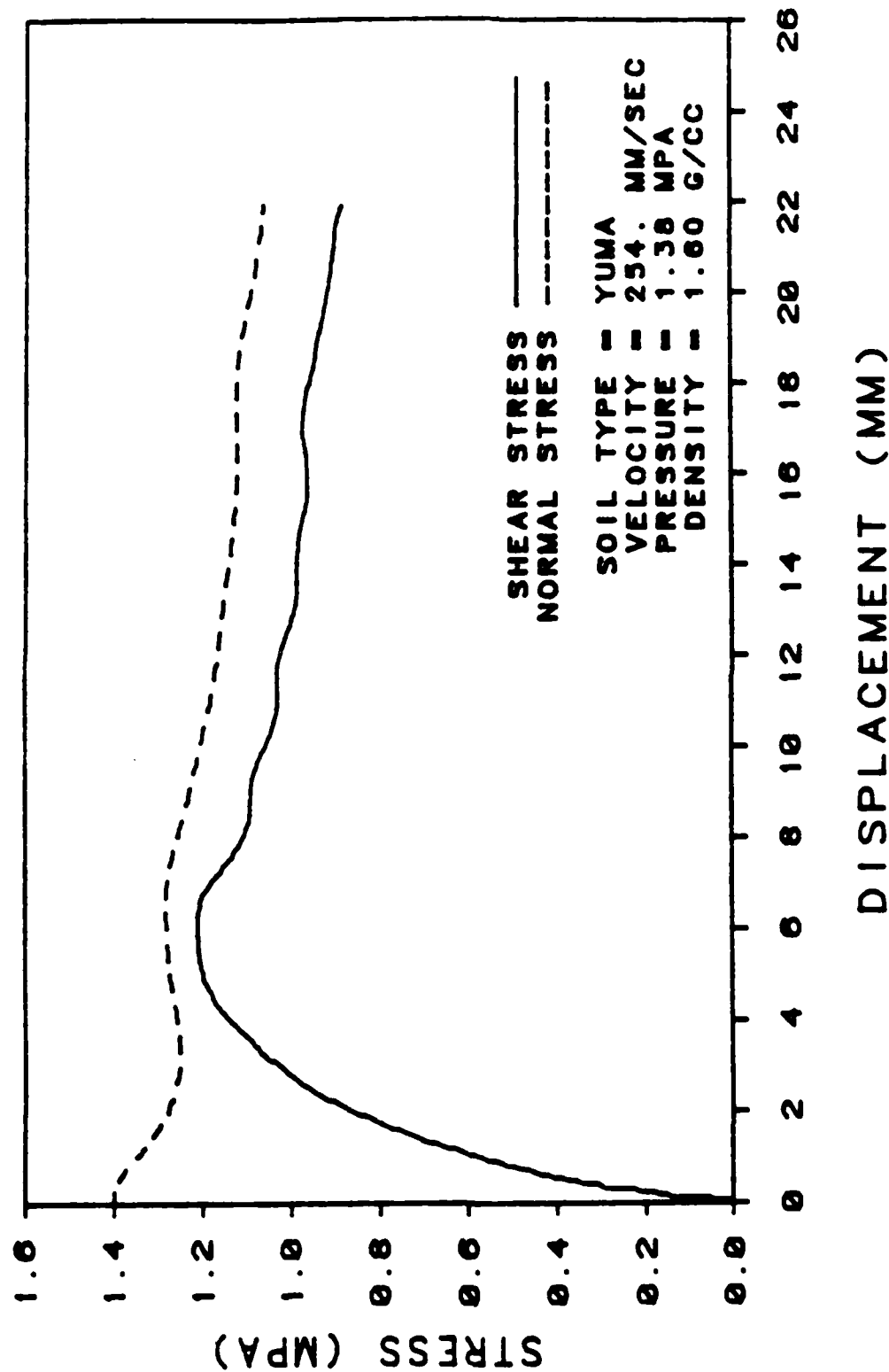


Figure A.15 Yuma Sand/Concrete, V=254. mm/s, P=1.38 MPa, 1st Repetition.

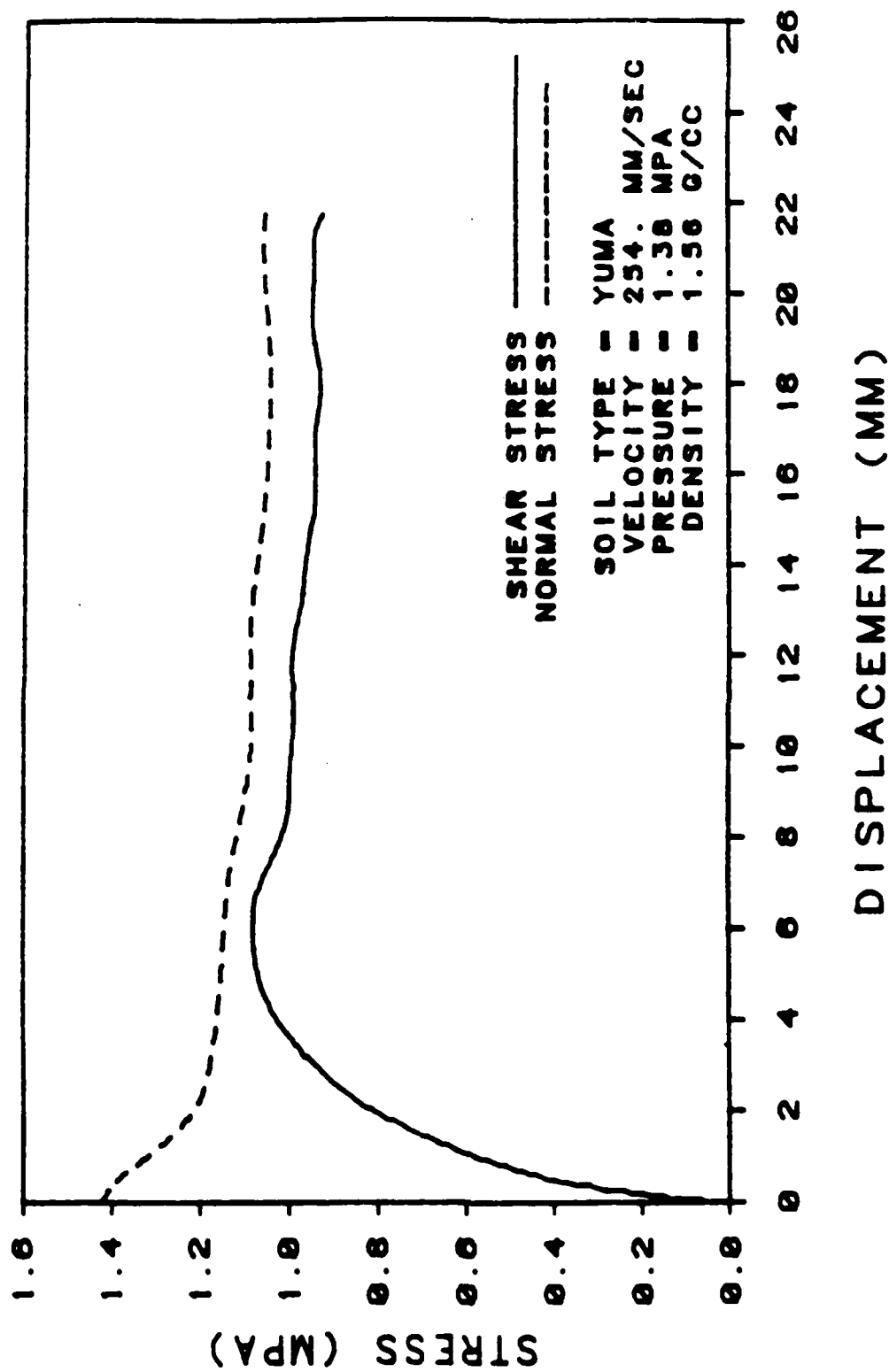


Figure A.16 Yuma Sand/Concrete, $V=254. \text{ mm/s}$, $P=1.38 \text{ MPa}$, 2nd Repetition.

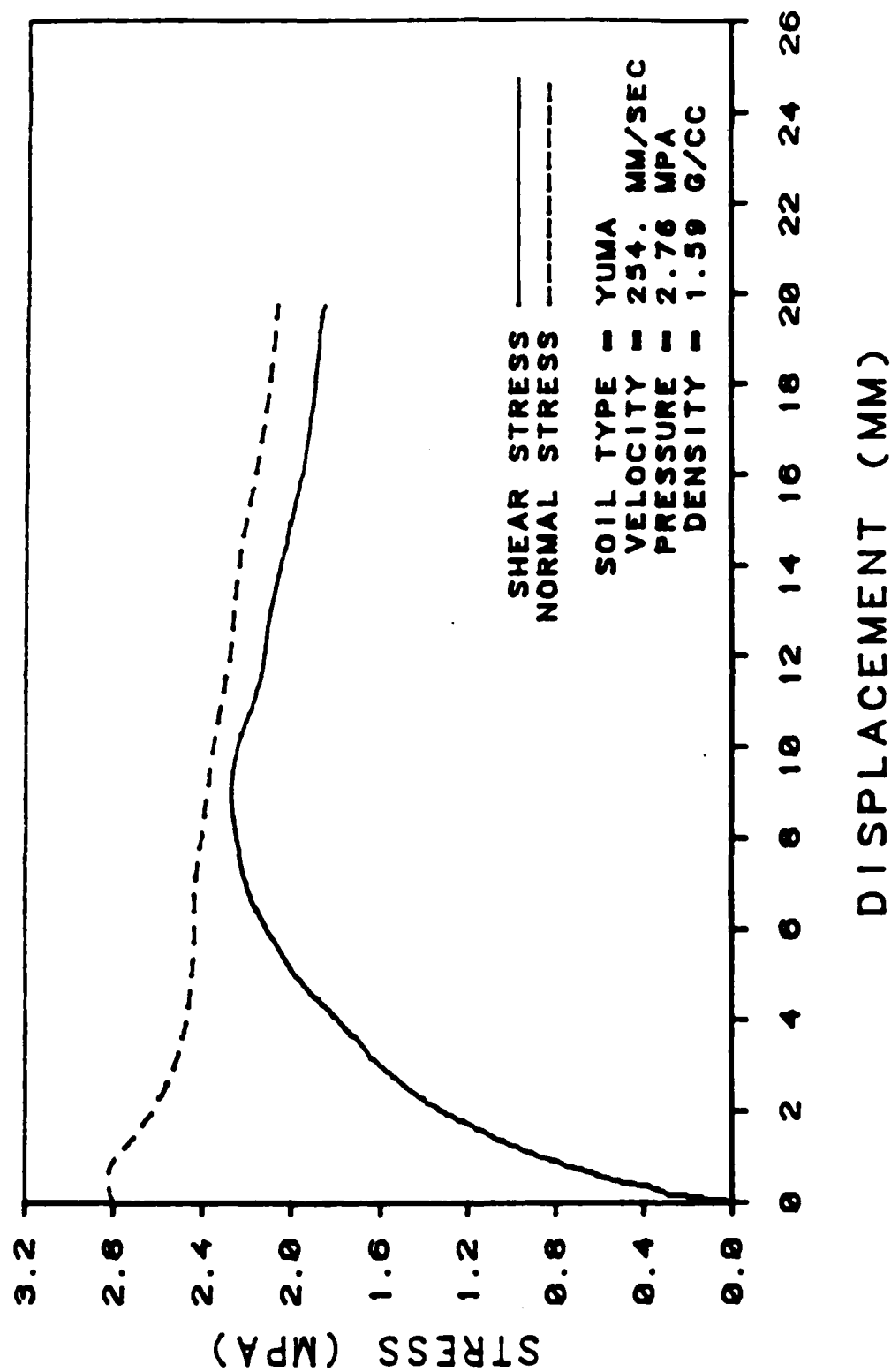


Figure A.17 Yuma Sand/Concrete, V=254. mm/s, P=2.76 MPa, 1st Repetition.

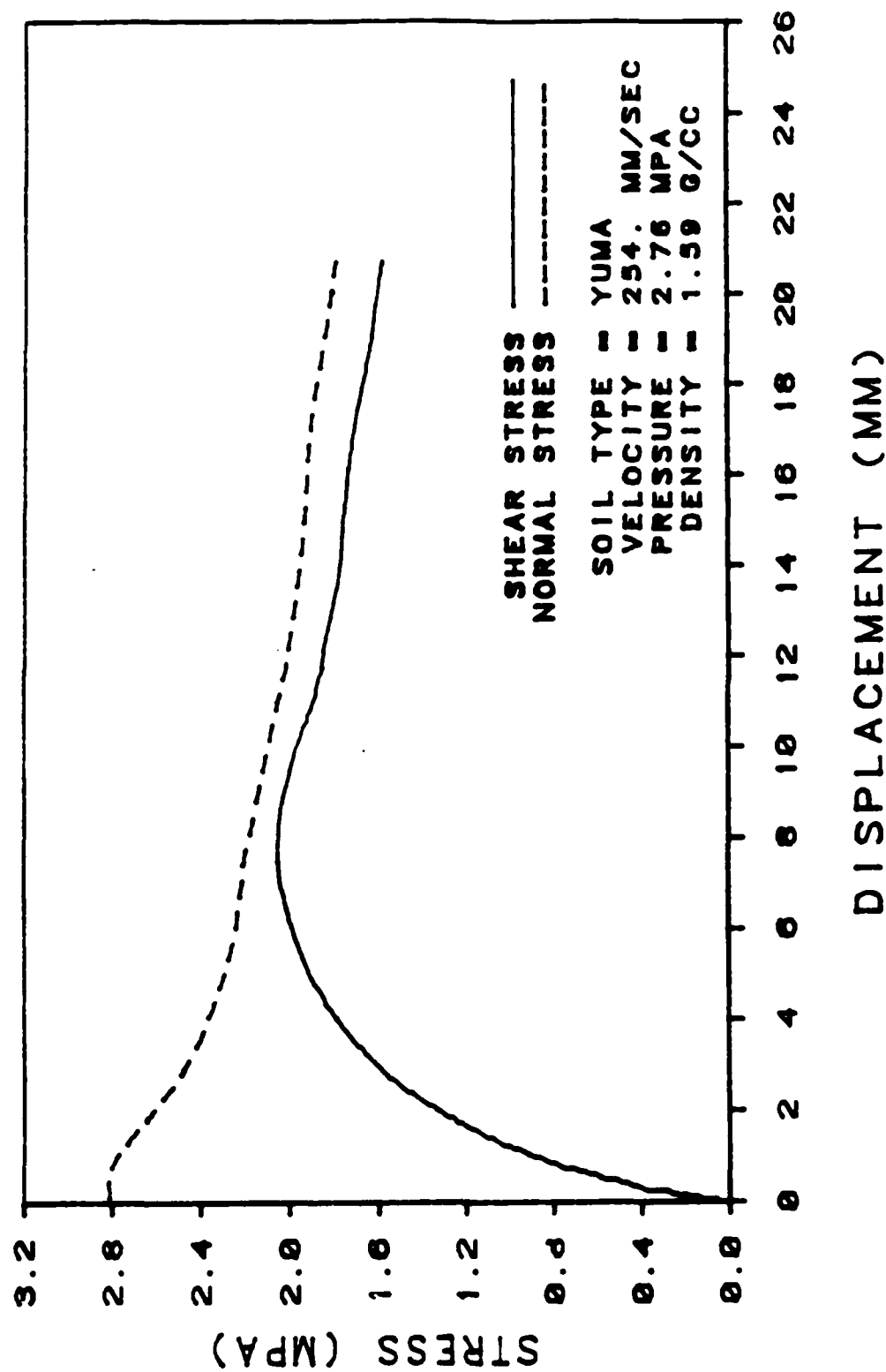


Figure A.18 Yuma Sand/Concrete, V=254. mm/s, P=2.76 MPa, 2nd Repetition.

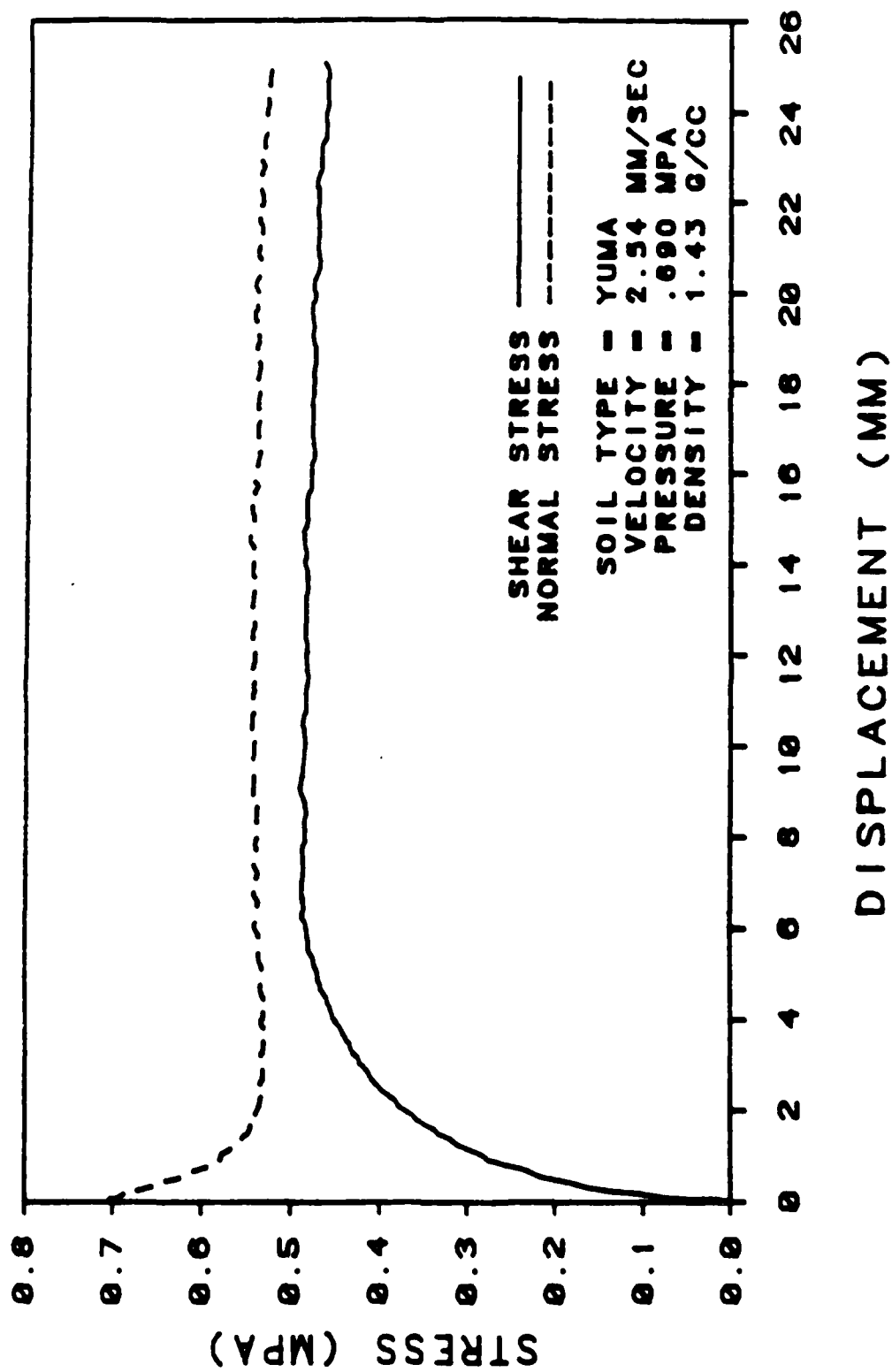


Figure A.19 Loose Yuma Sand/Concrete, $V=2.54$ mm/s, $P=0.69$ MPa.

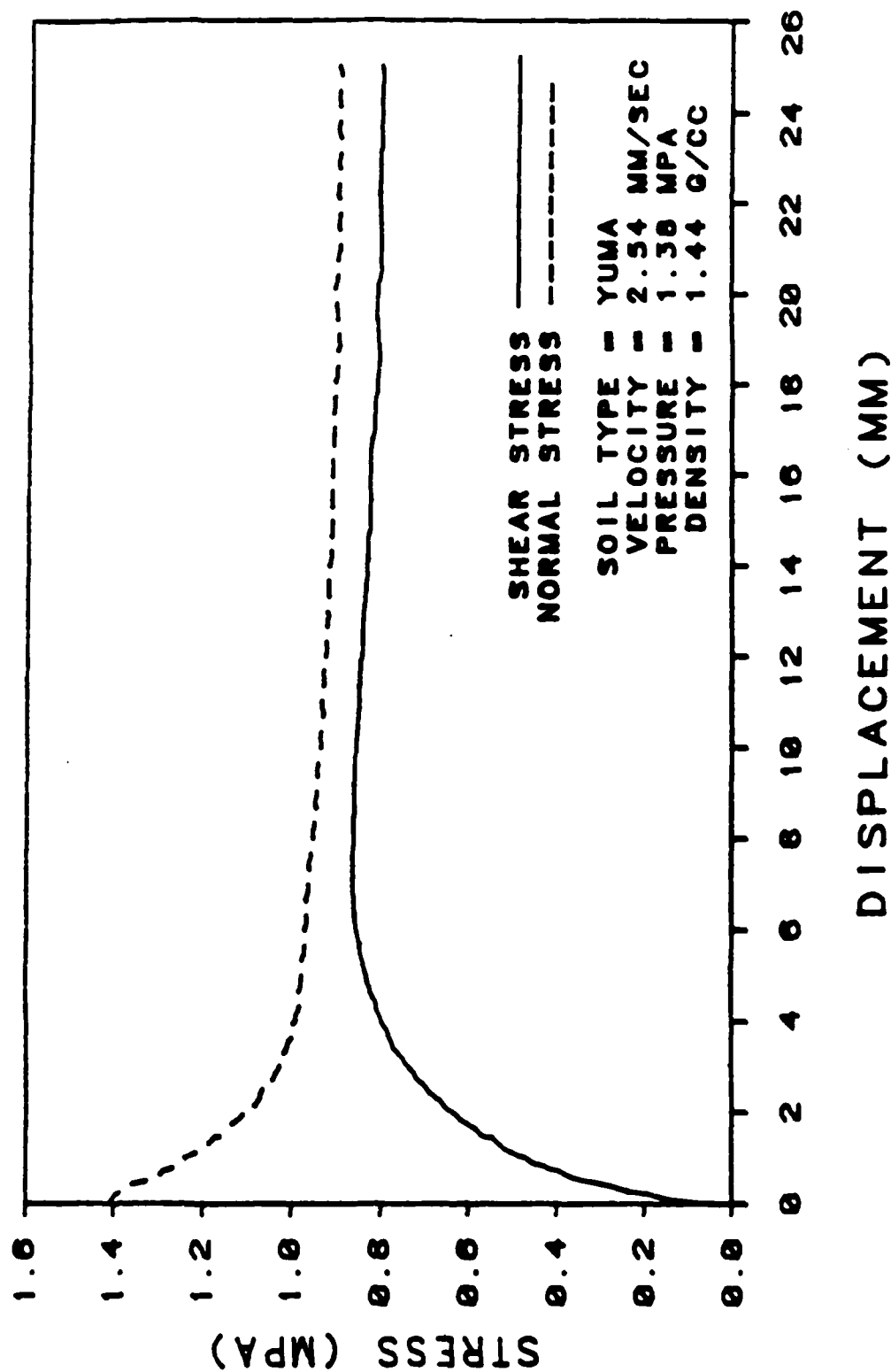


Figure A.20 Loose Yuma Sand/Concrete, $V=2.54$ mm/s, $P=1.38$ MPa.

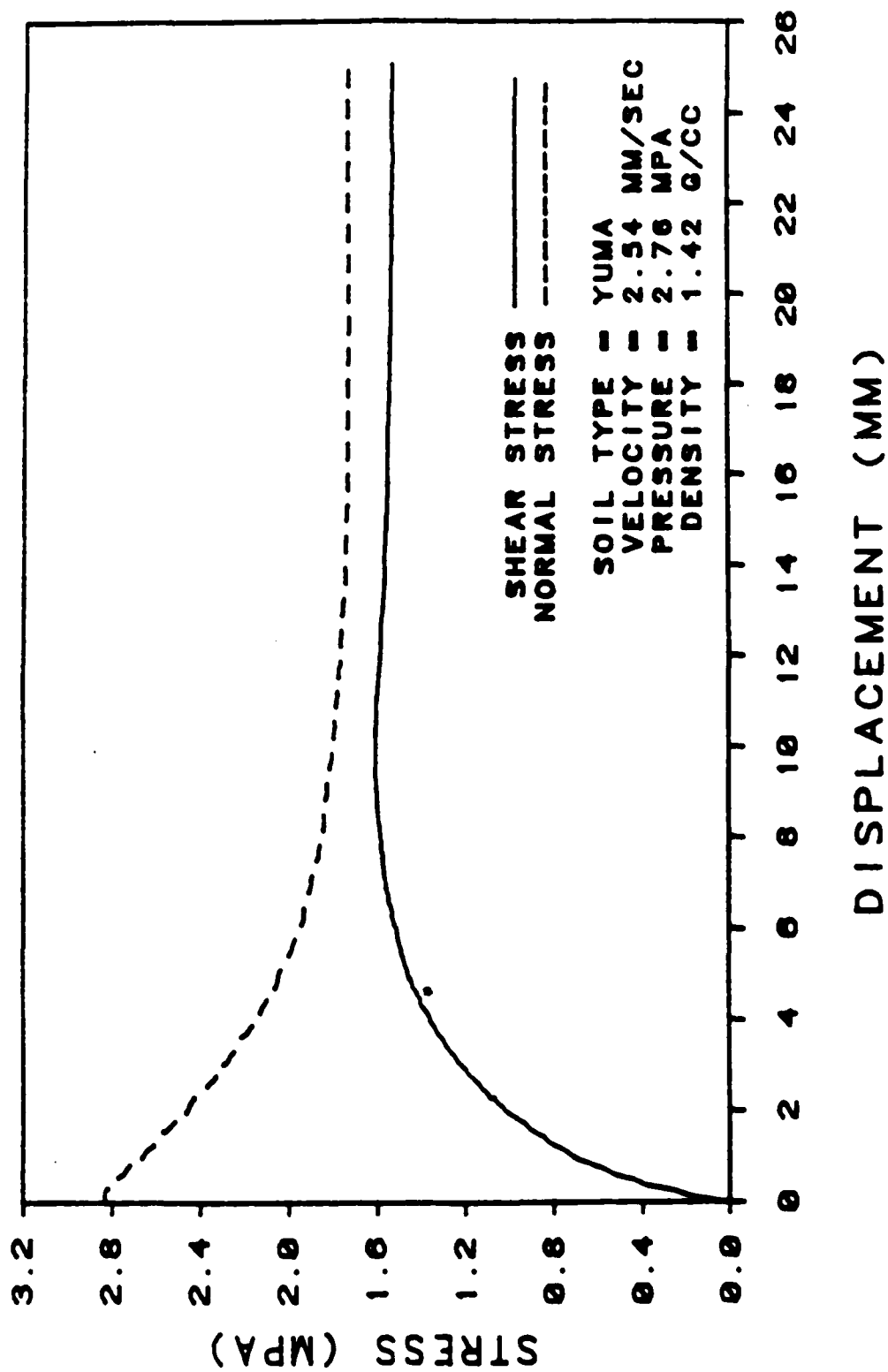


Figure A.21 Loose Yuma Sand/Concrete, $V=2.54$ mm/s, $P=2.76$ MPa.

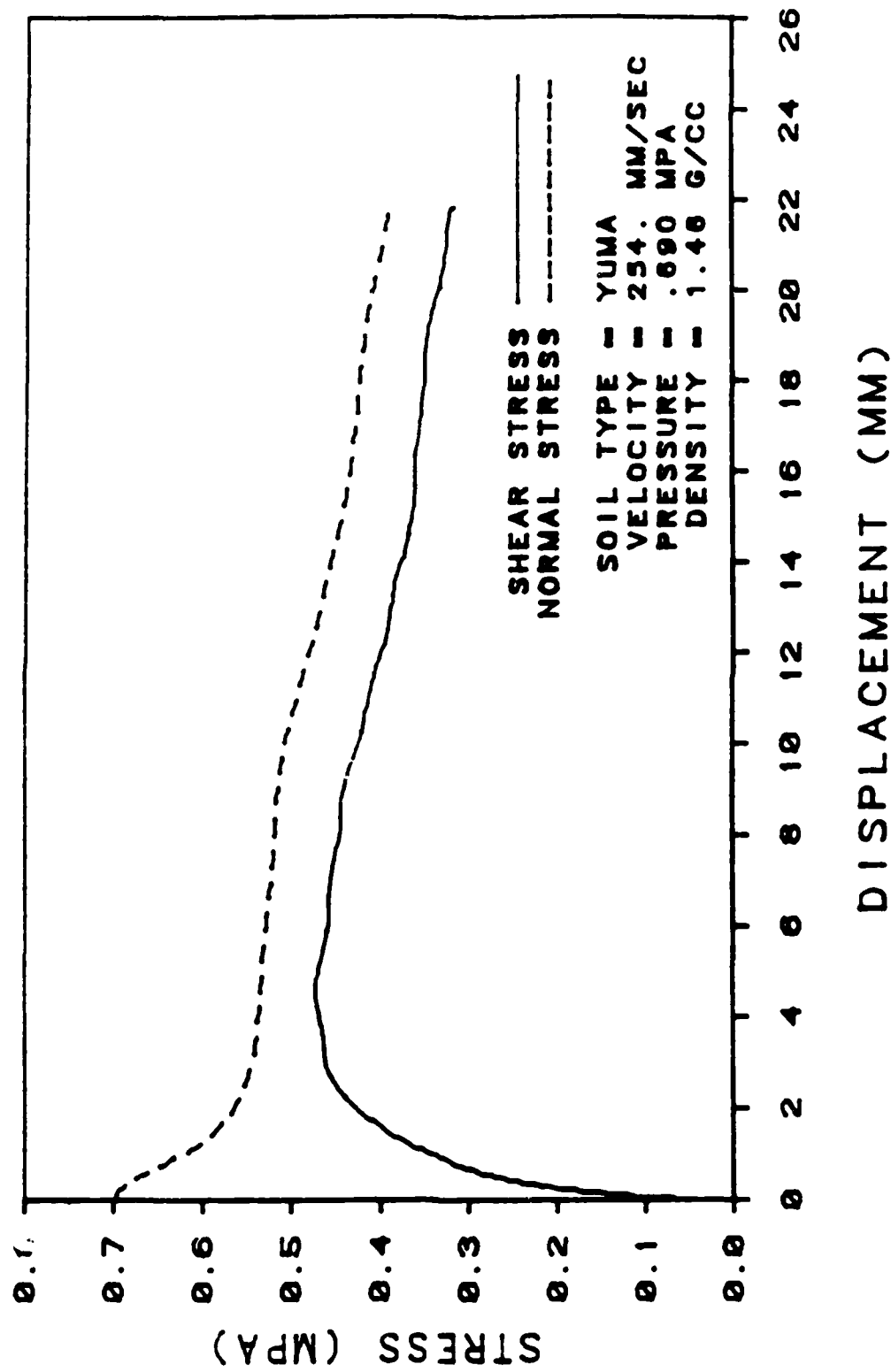


Figure A.22 Loose Yuma Sand/Concrete, V=254. mm/s, P=0.69 MPa.

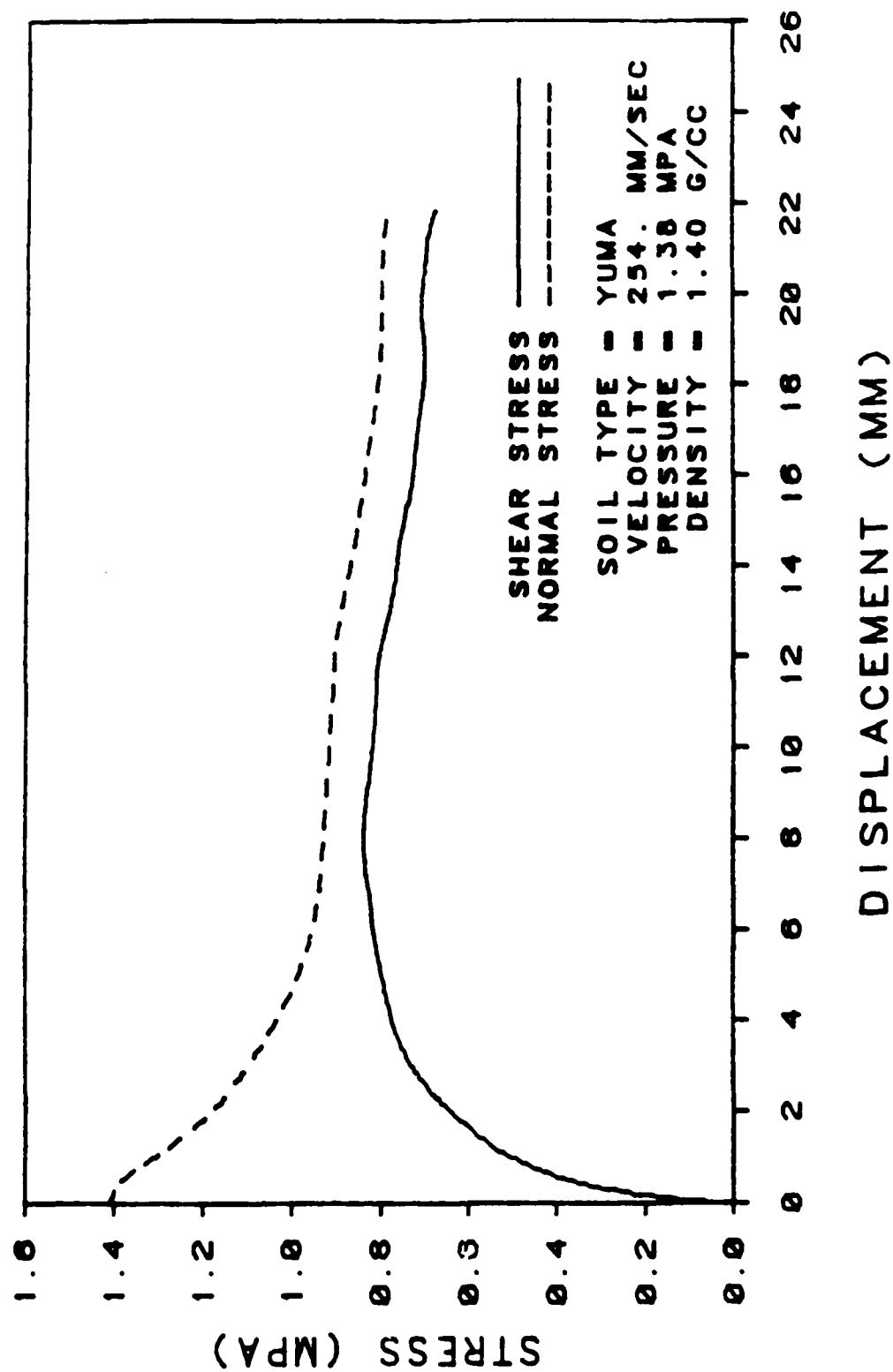


Figure A.23 Loose Yuma Sand/Concrete, $V=254$. mm/s, $P=1.38$ MPa.

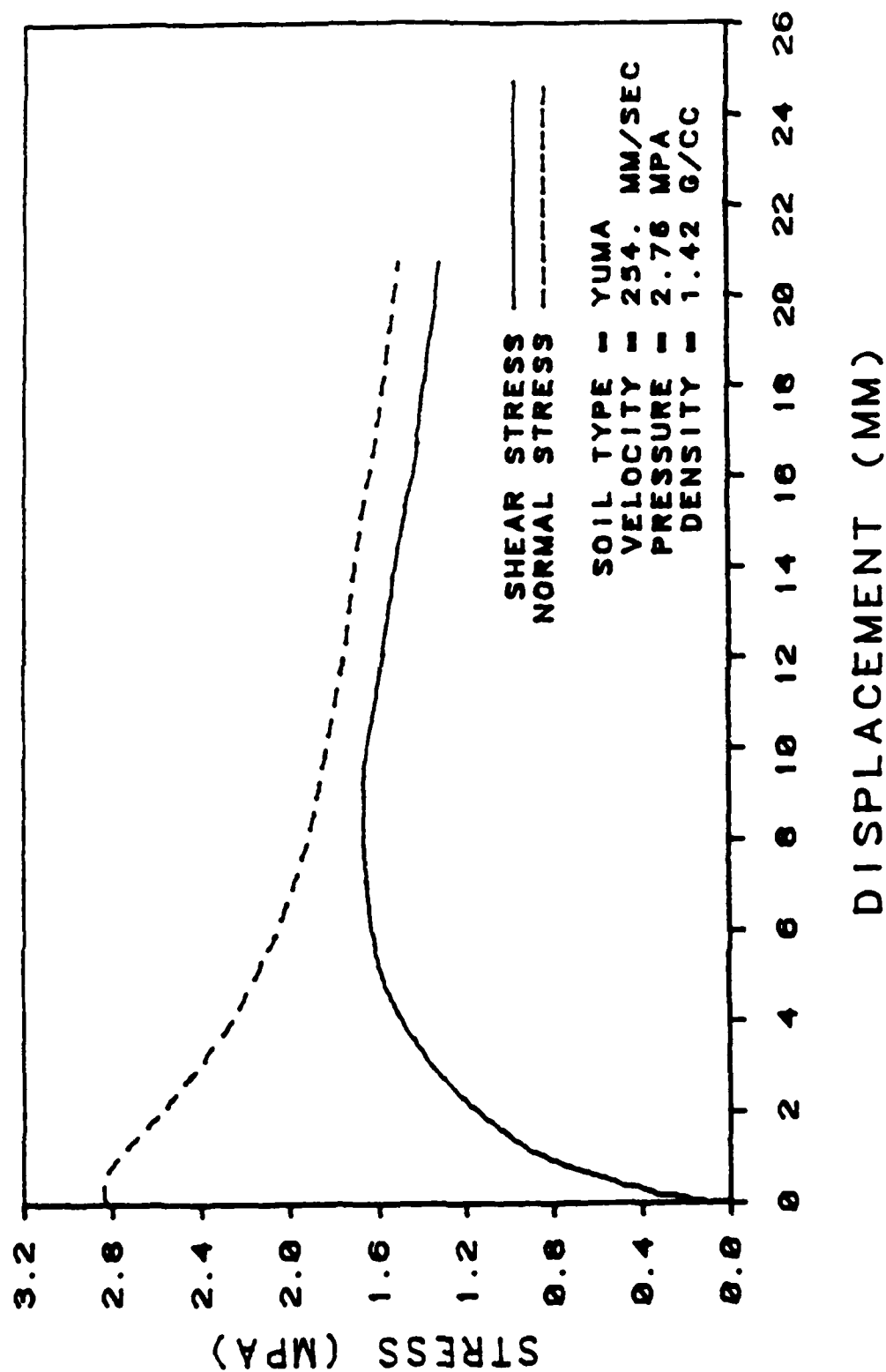


Figure A.24 Loose Yuma Sand/Concrete, $v=254$. mm/s, $P=2.76$ MPa.

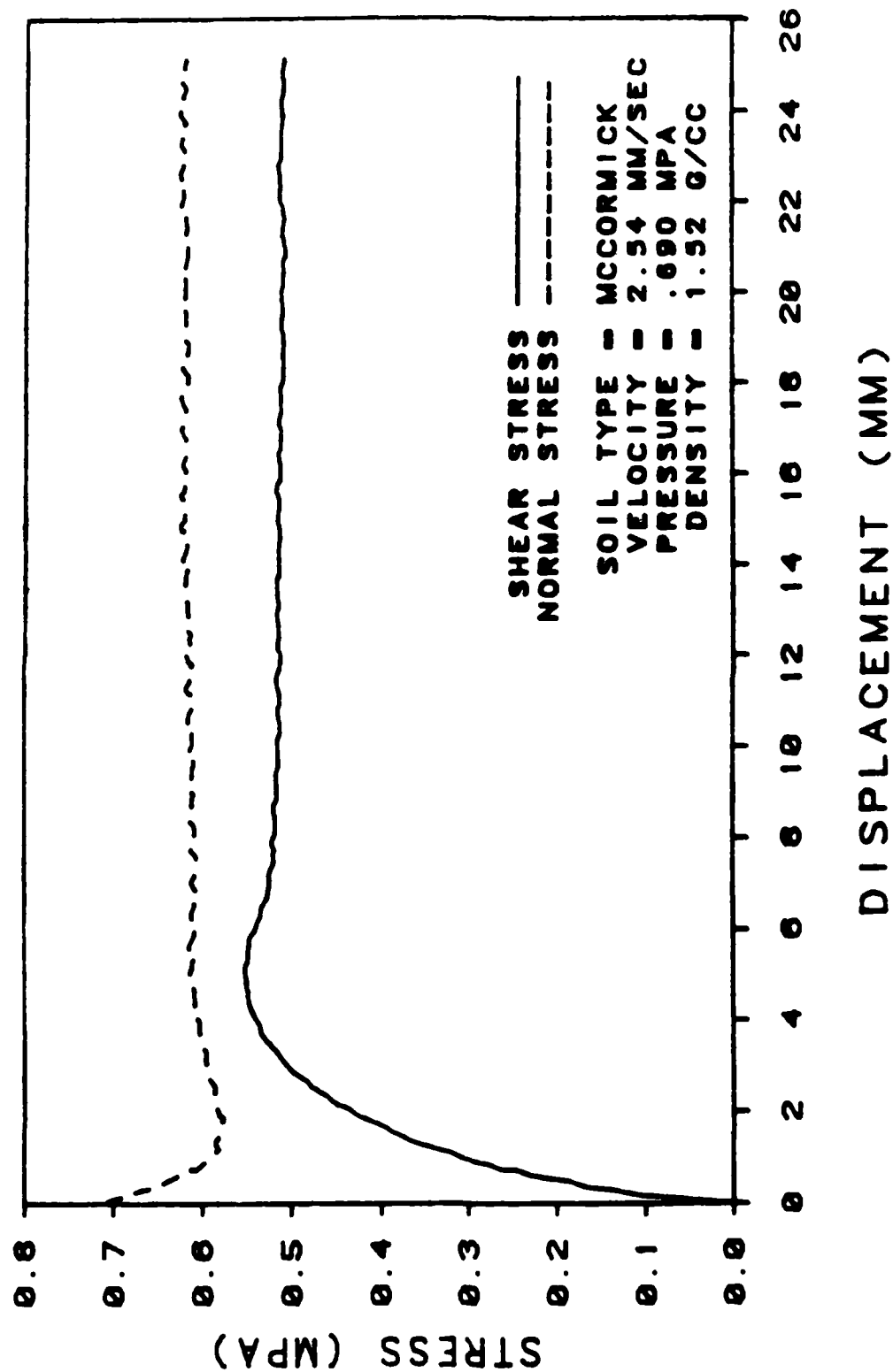


Figure A.25 McCormick Sand/Concrete, $V=2.54$ mm/s, $P=0.69$ MPa, 1st Repetition.

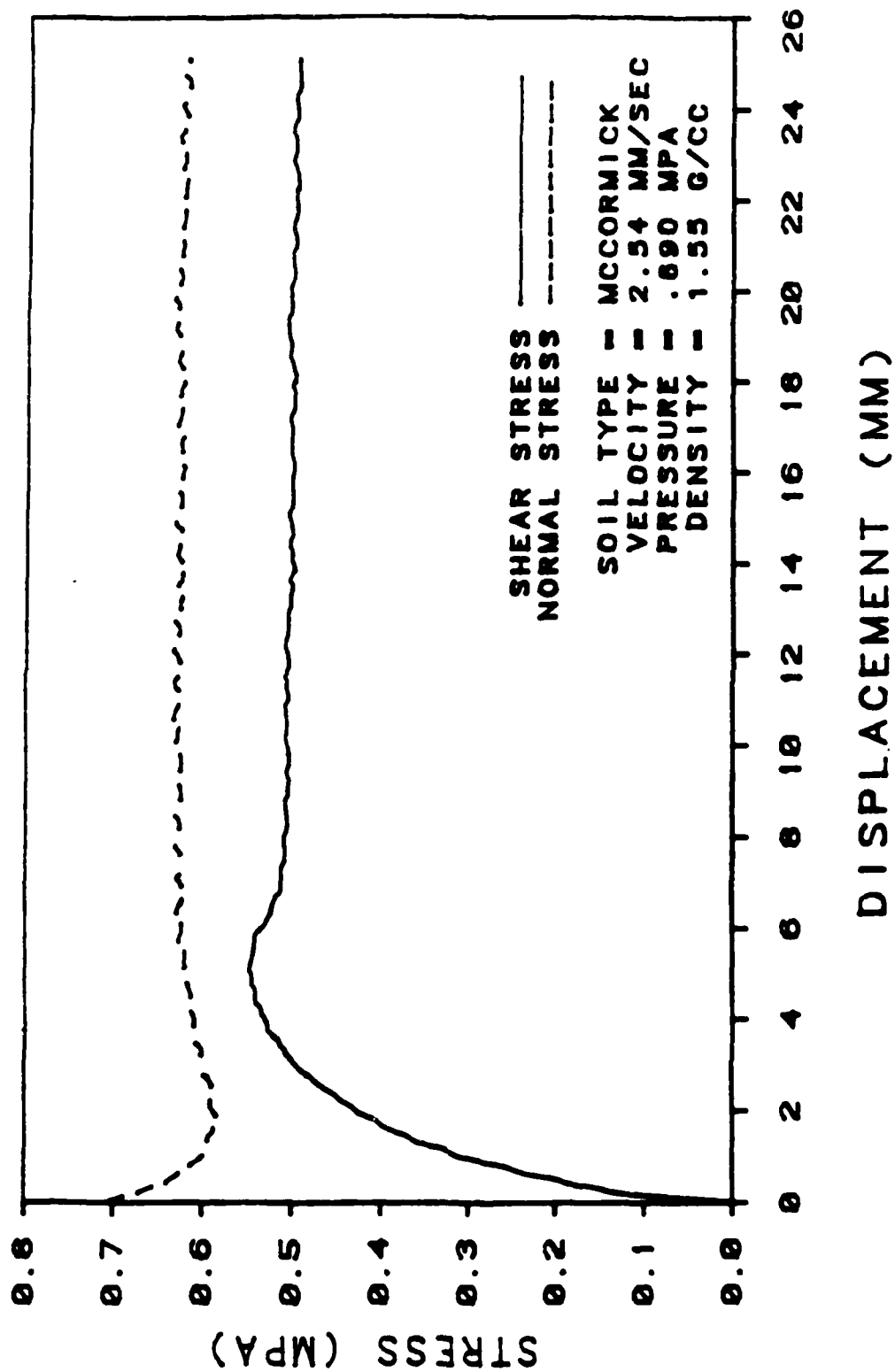


Figure A.26 McCormick Sand/Concrete, $V=2.54$ mm/s, $P=0.69$ MPa, 2nd Repetition.

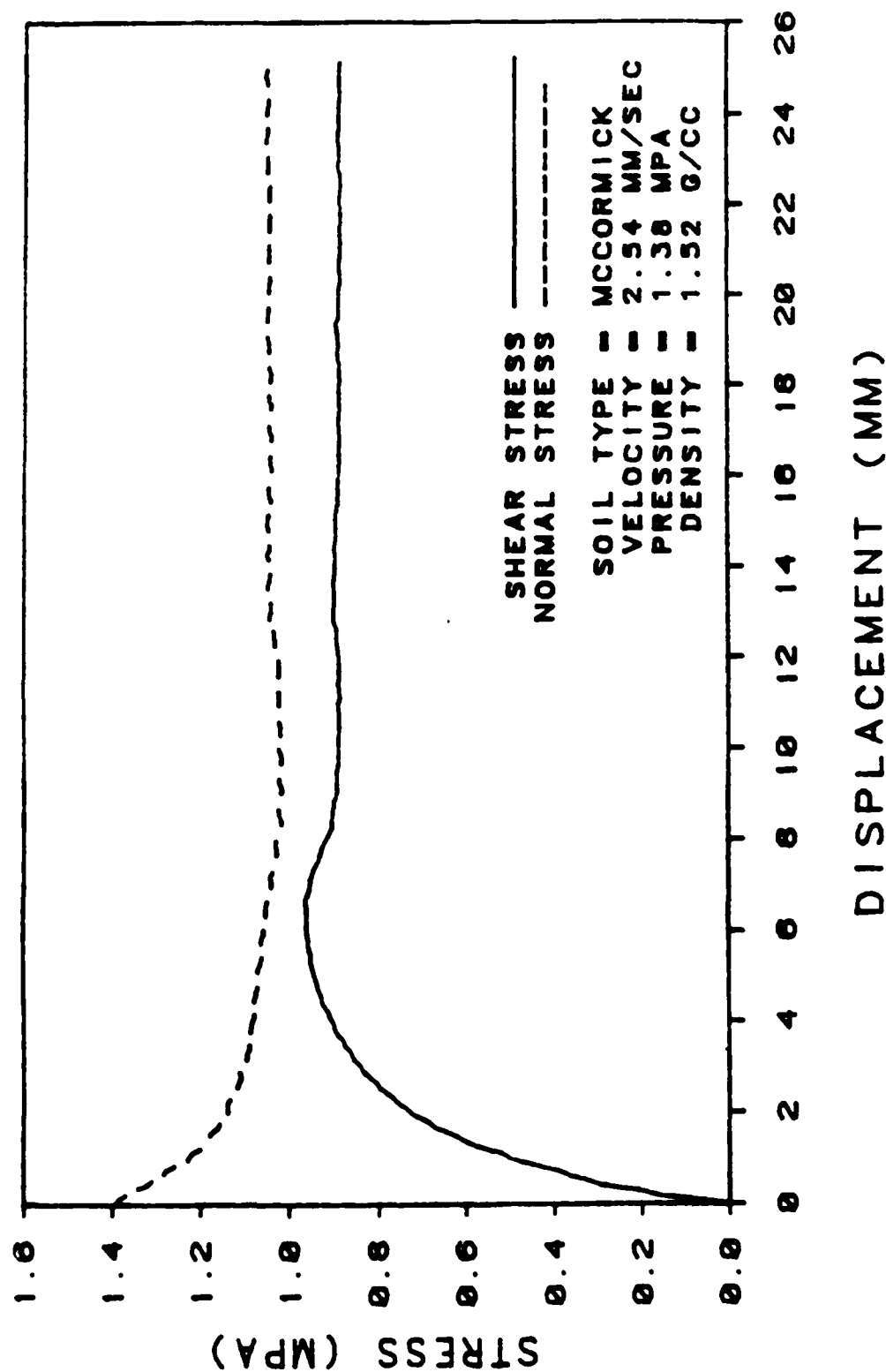


Figure A.27 McCormick Sand/Concrete, V=2.54 mm/s, P=1.38 MPa, 1st Repetition.

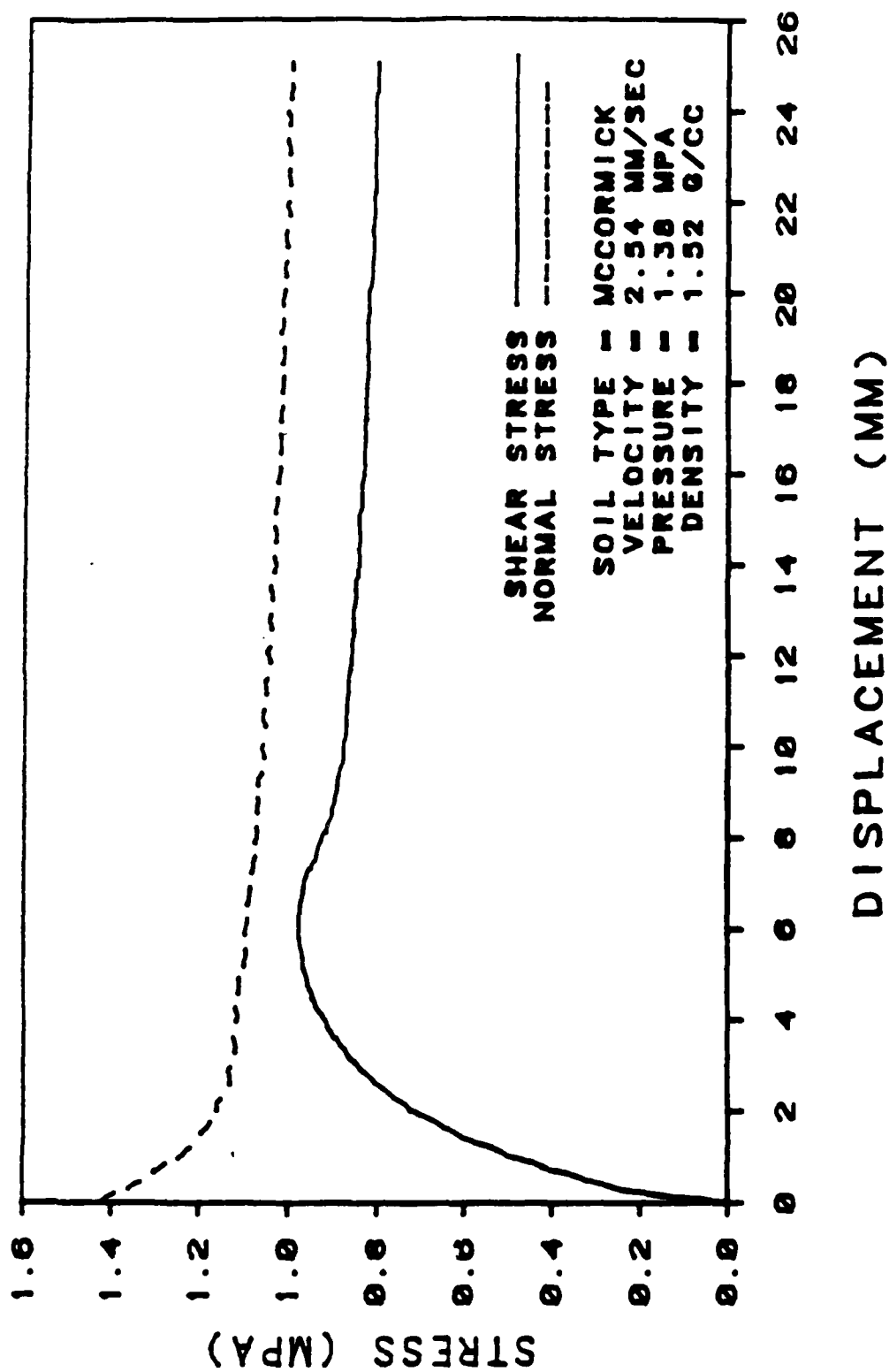


Figure A.28 McCormick Sand/Concrete, $V=2.54$ mm/s, $P=1.38$ MPa, 2nd Repetition.

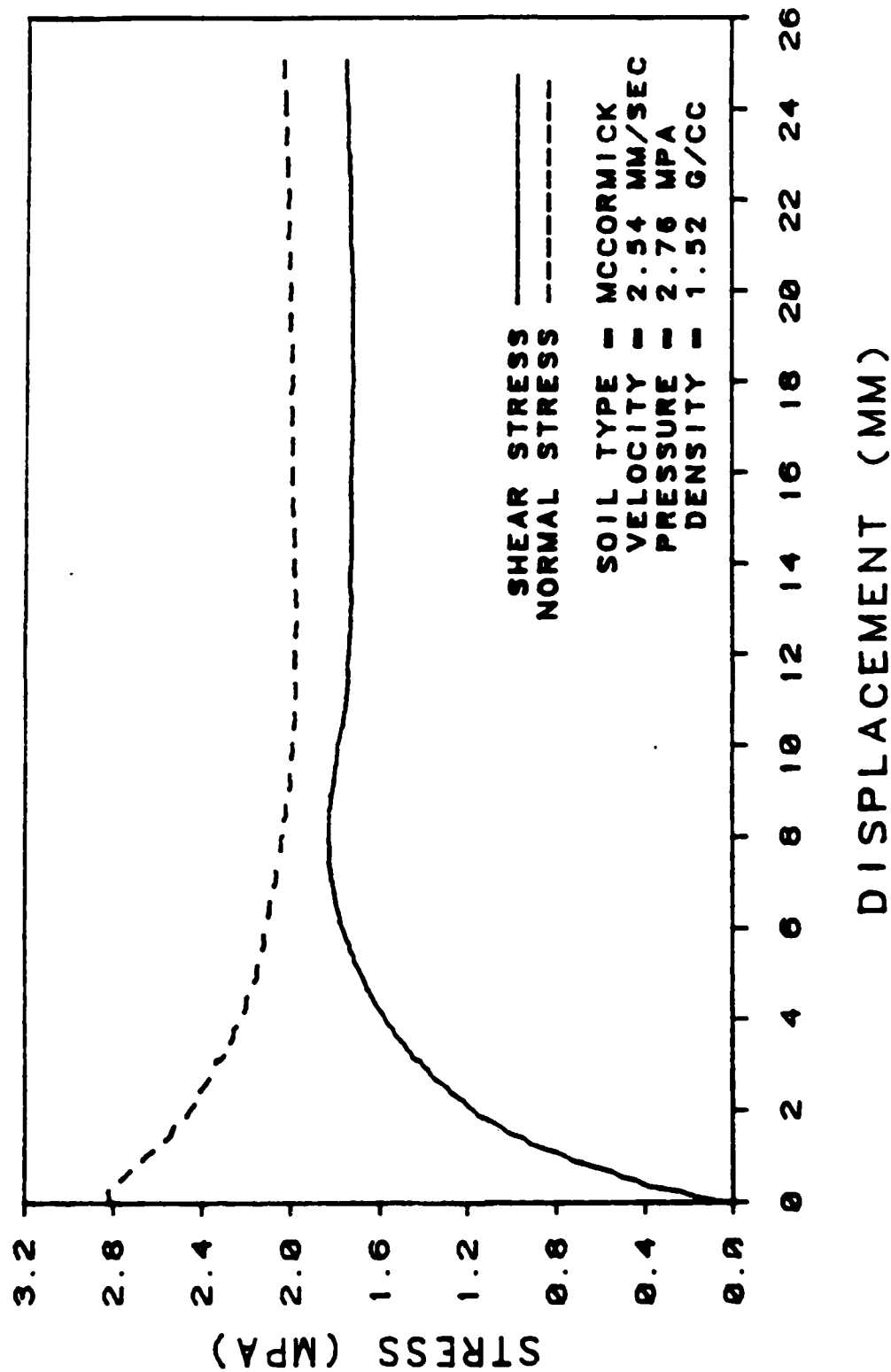


Figure A.29 McCormick Sand/Concrete, $V=2.54$ mm/s, $P=2.76$ MPa, 1st Repetition.

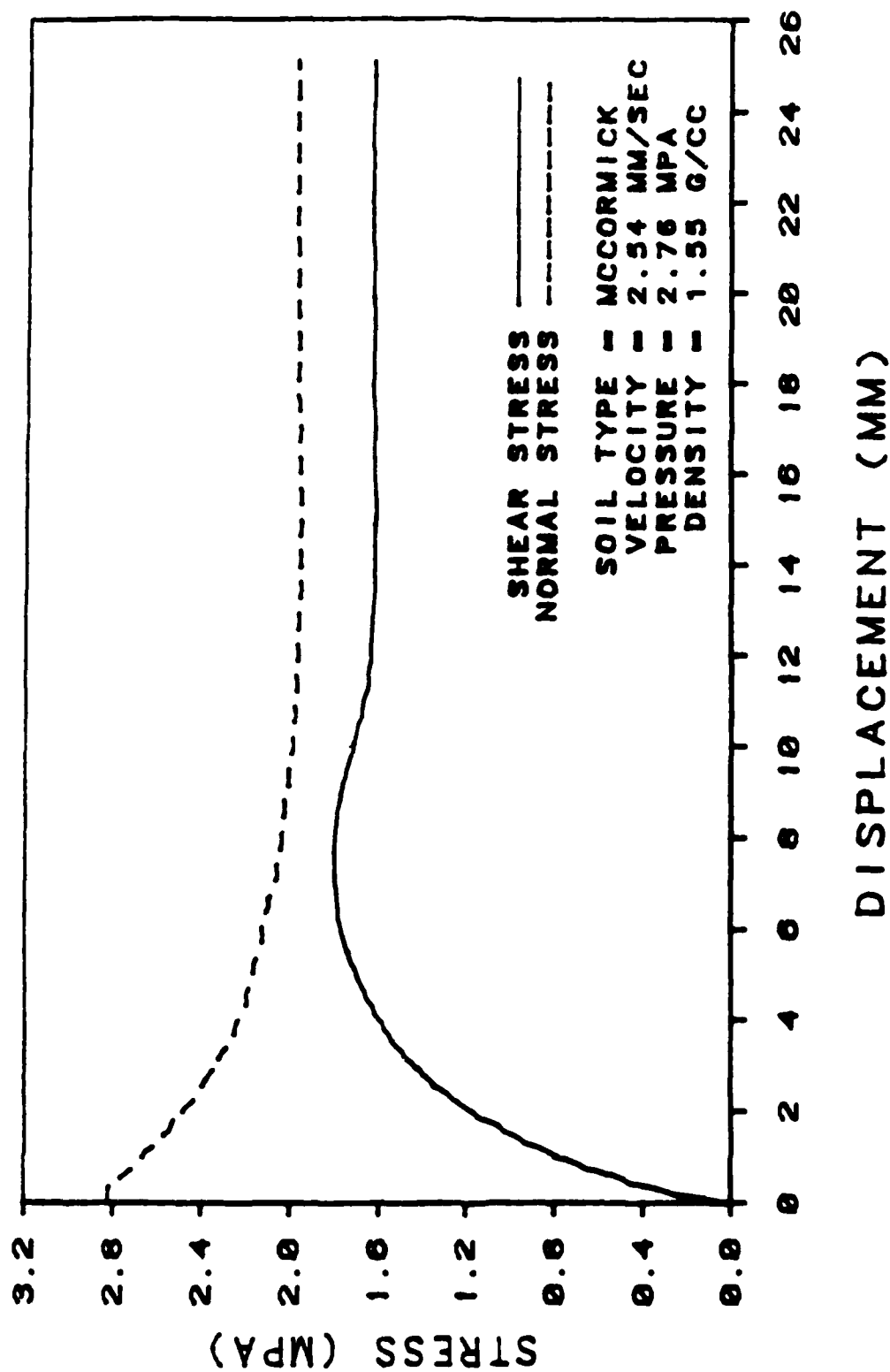


Figure A.30 McCormick Sand/Concrete, $V=2.54$ mm/s, $P=2.76$ MPa, 2nd Repetition.

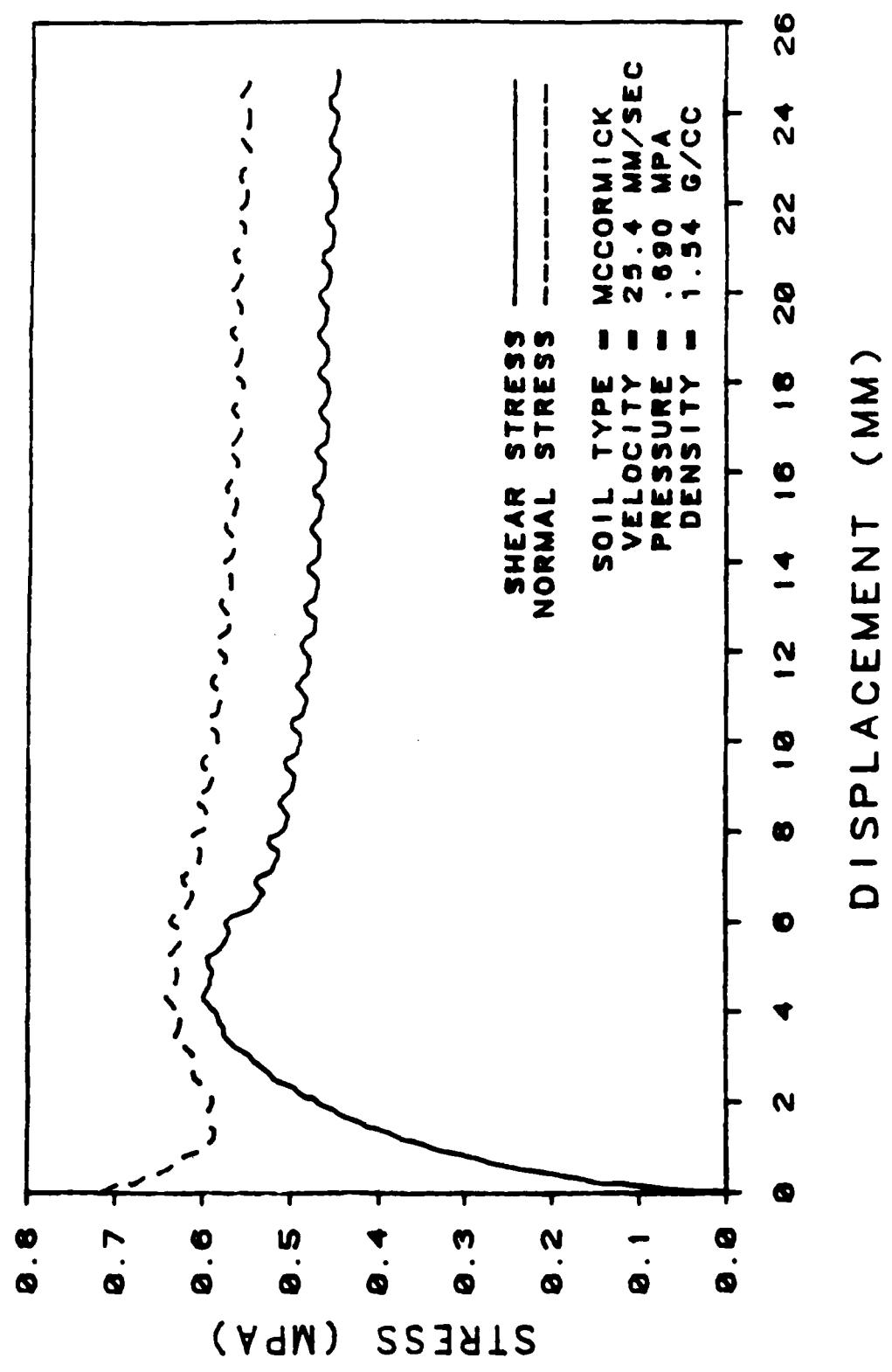


Figure A.31 McCormick Sand/Concrete, V=25.4 mm/s, P=0.69 MPa, 1st Repetition.

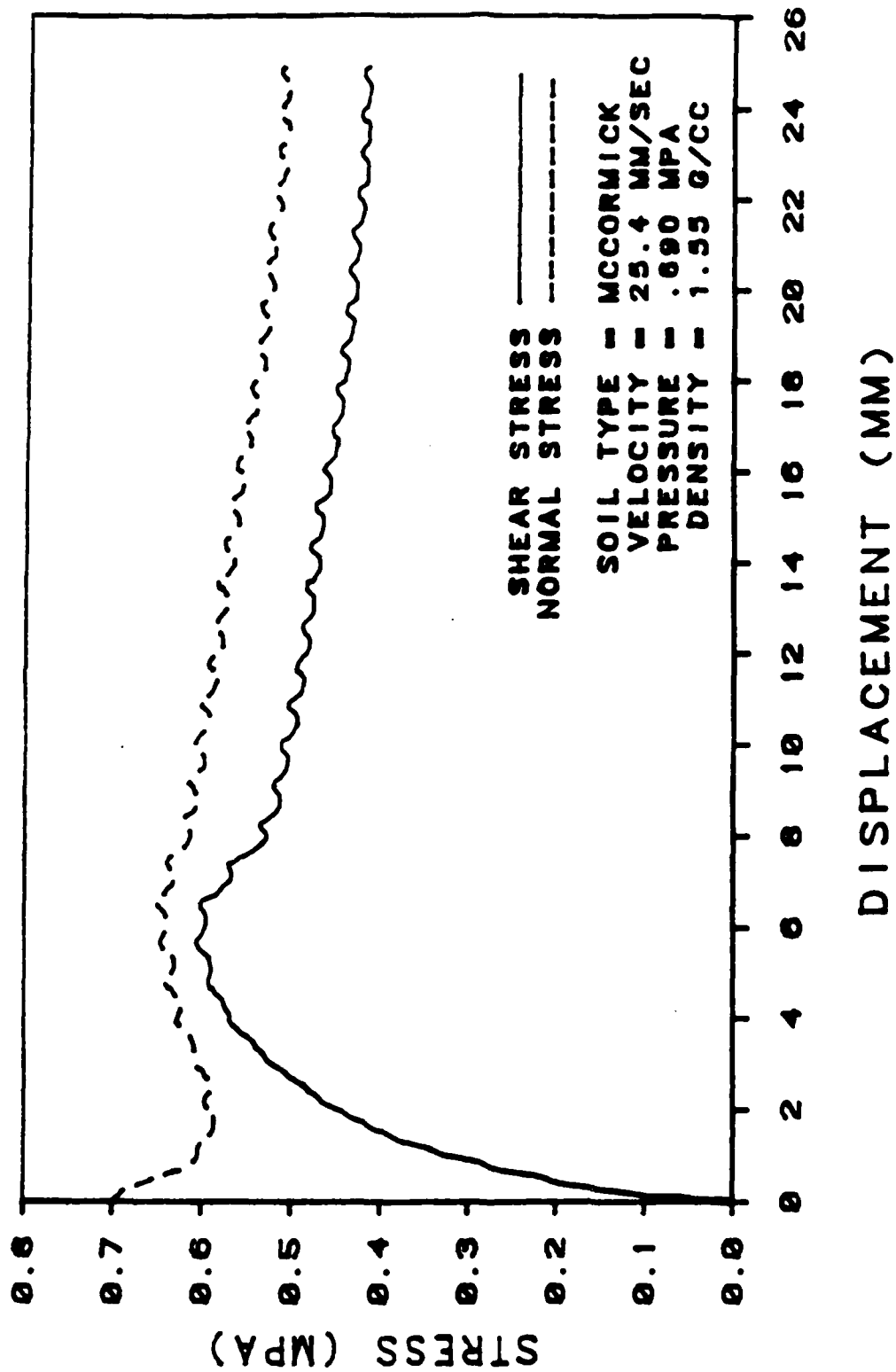


Figure A.32 McCormick Sand/Concrete, $V=25.4$ mm/s, $P=0.69$ MPa, 2nd Repetition.

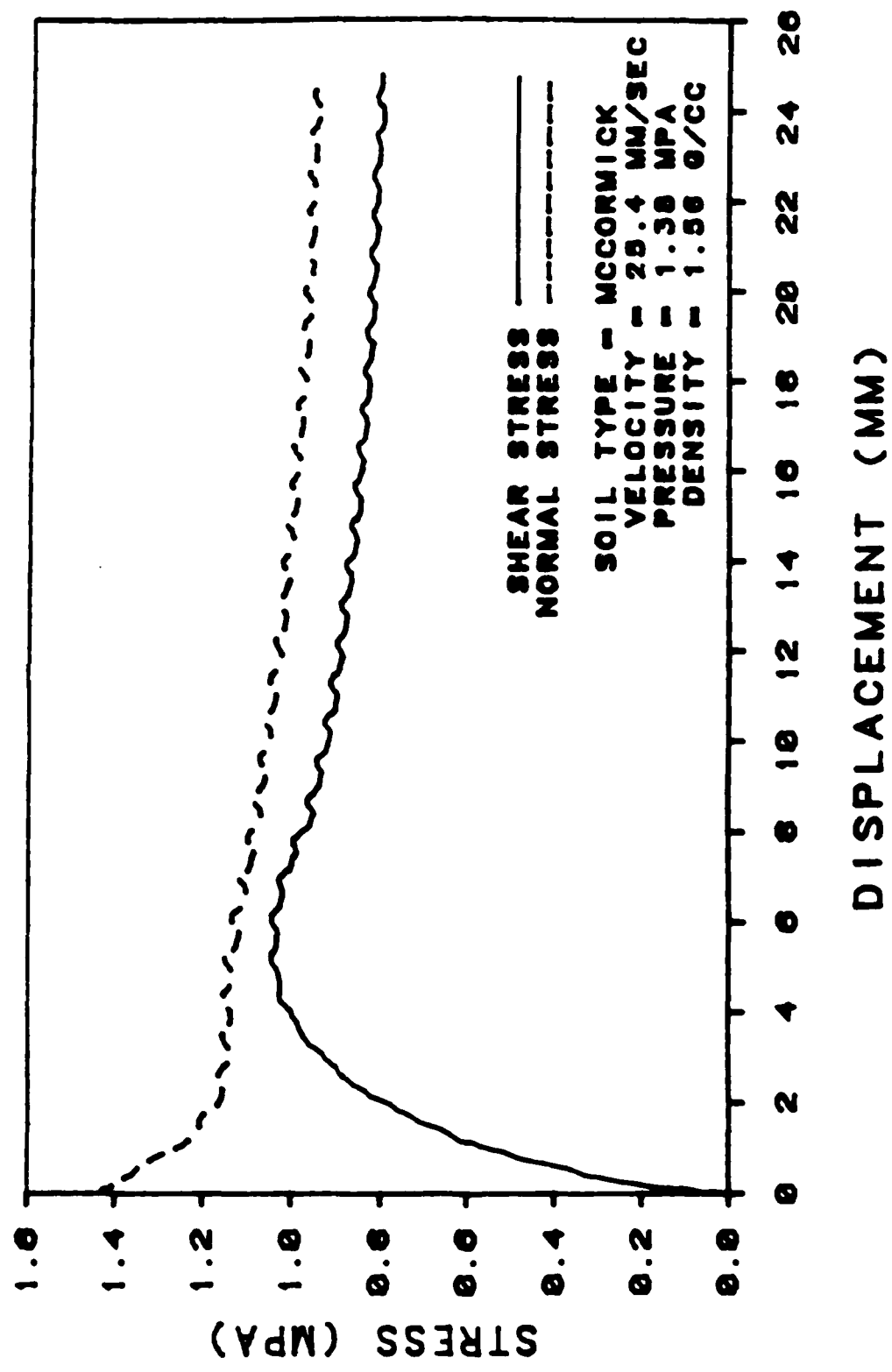


Figure A.33 McCormick Sand/Concrete, V=25.4 mm/s, P=1.38 MPa, 1st Repetition.

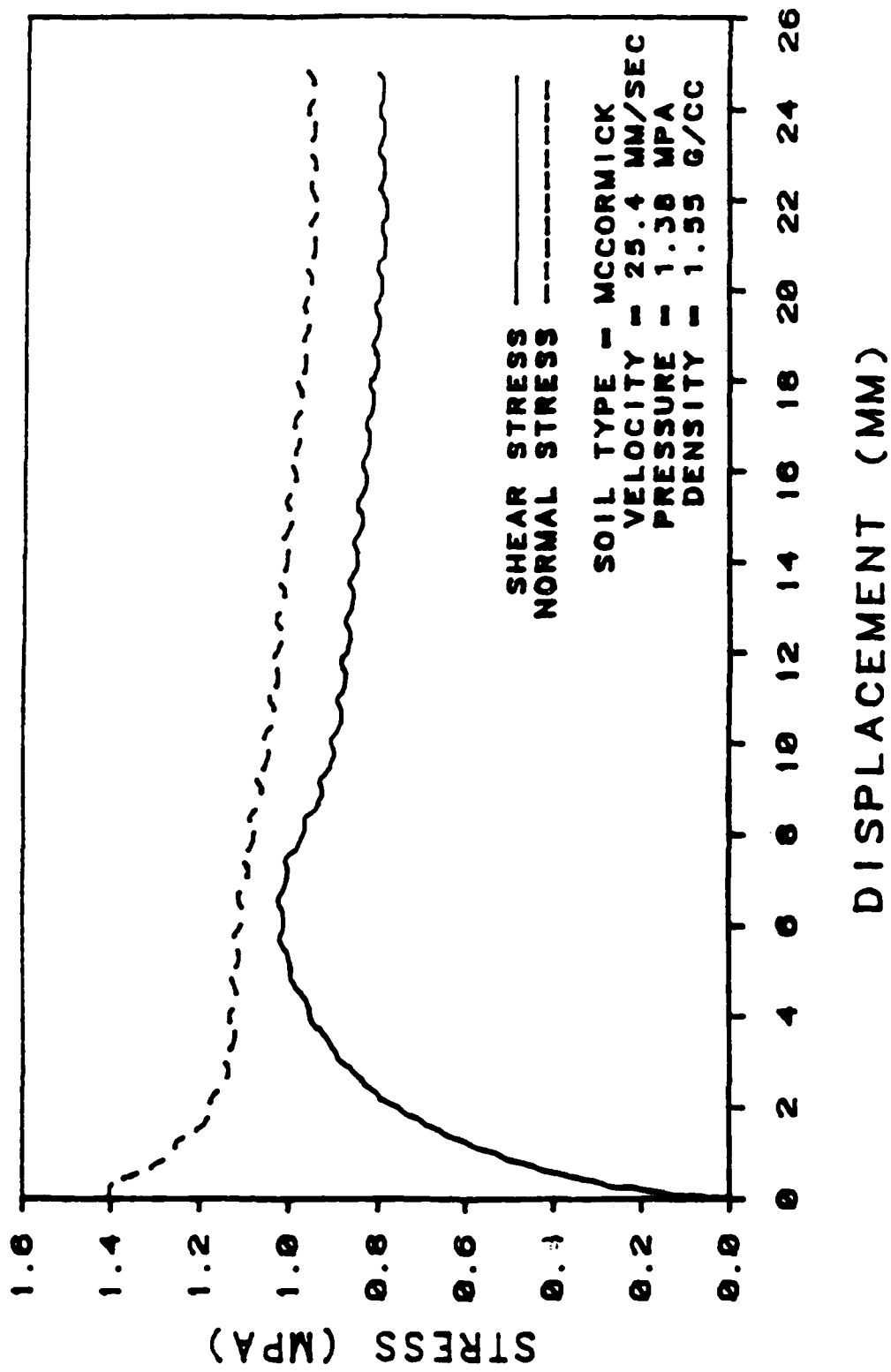


Figure A.34 McCormick Sand/Concrete, $v=25.4$ mm/s, $P=1.38$ MPa, 2nd Repetition.

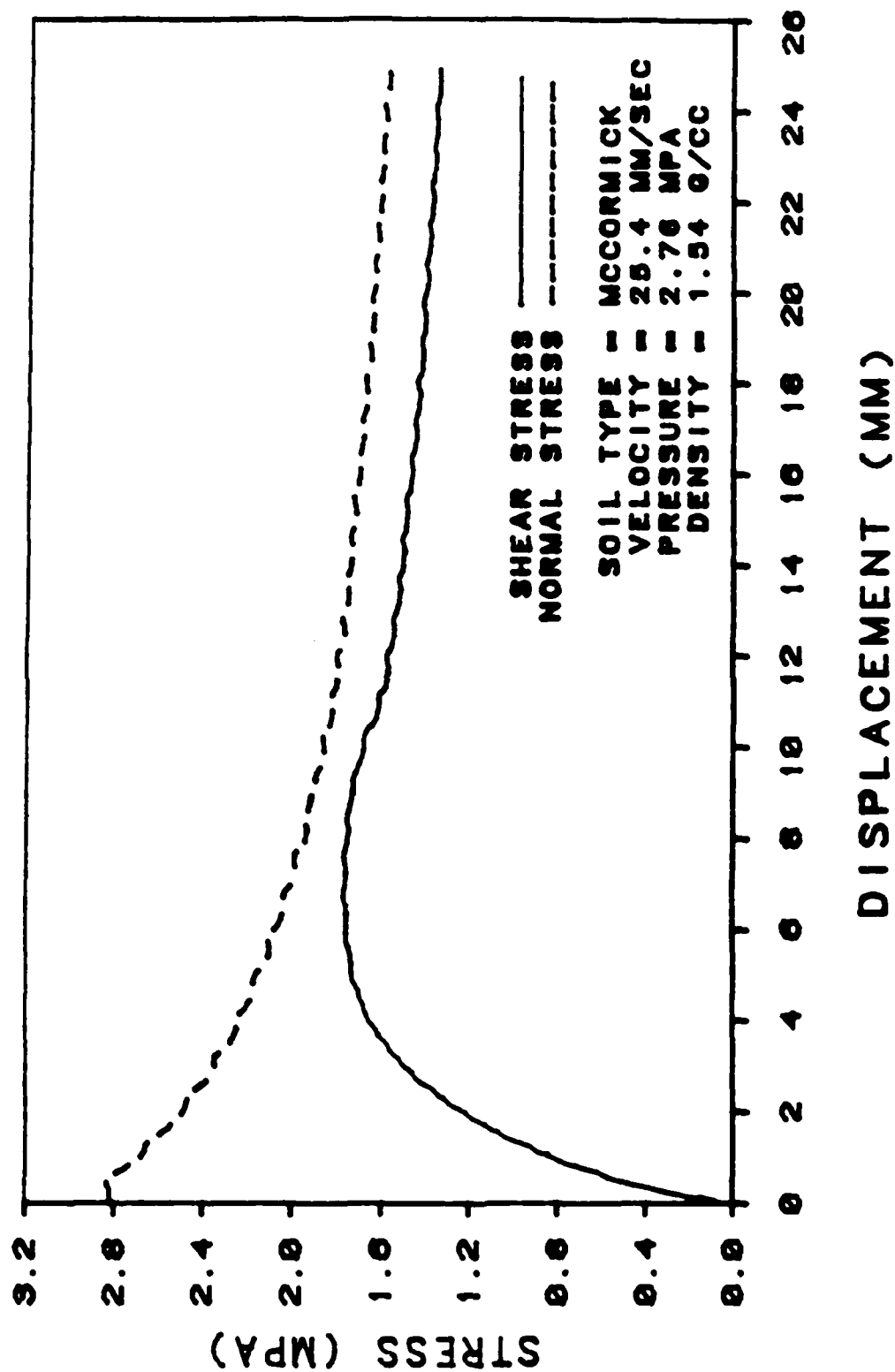


Figure A.35 McCormick Sand/Concrete, $V=25.4$ mm/s, $P=2.76$ MPa, 1st Repetition.

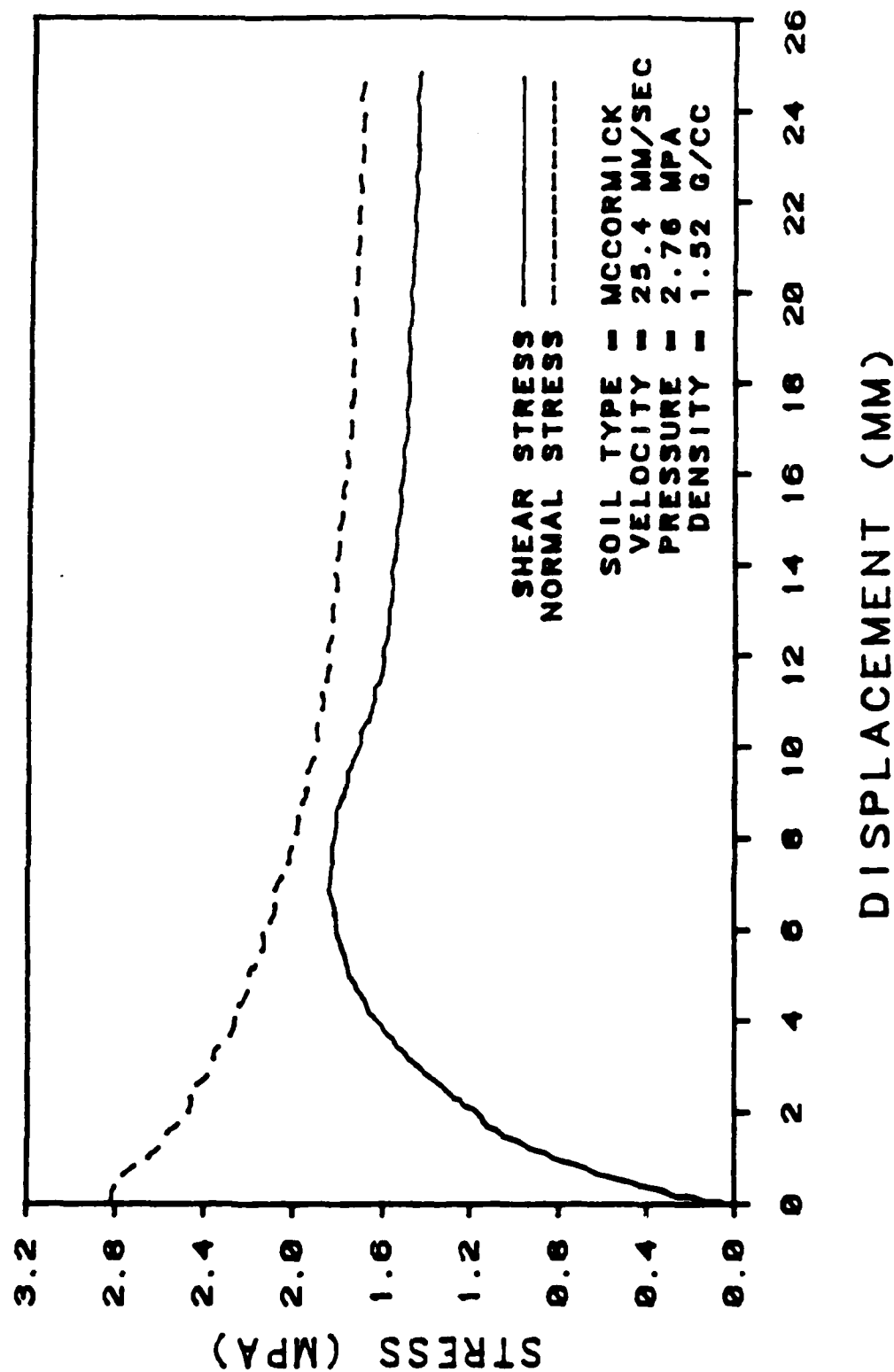


Figure A.36 McCormick Sand/Concrete, $V=25.4$ mm/s, $P=2.76$ MPa, 2nd Repetition.

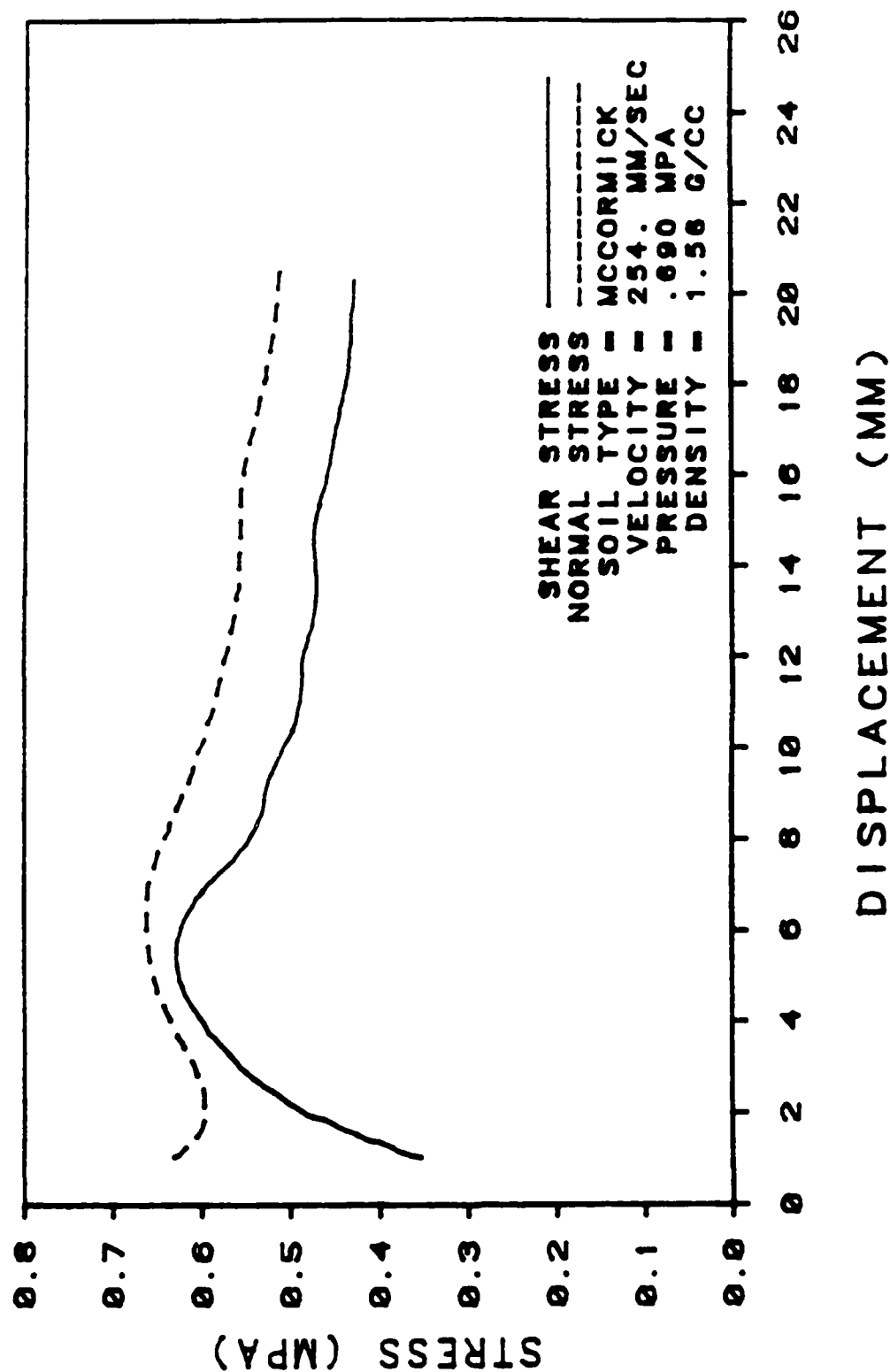


Figure A.37 McCormick Sand/Concrete, $V=254$. mm/s, $P=0.69$ MPa, 1st Repetition.

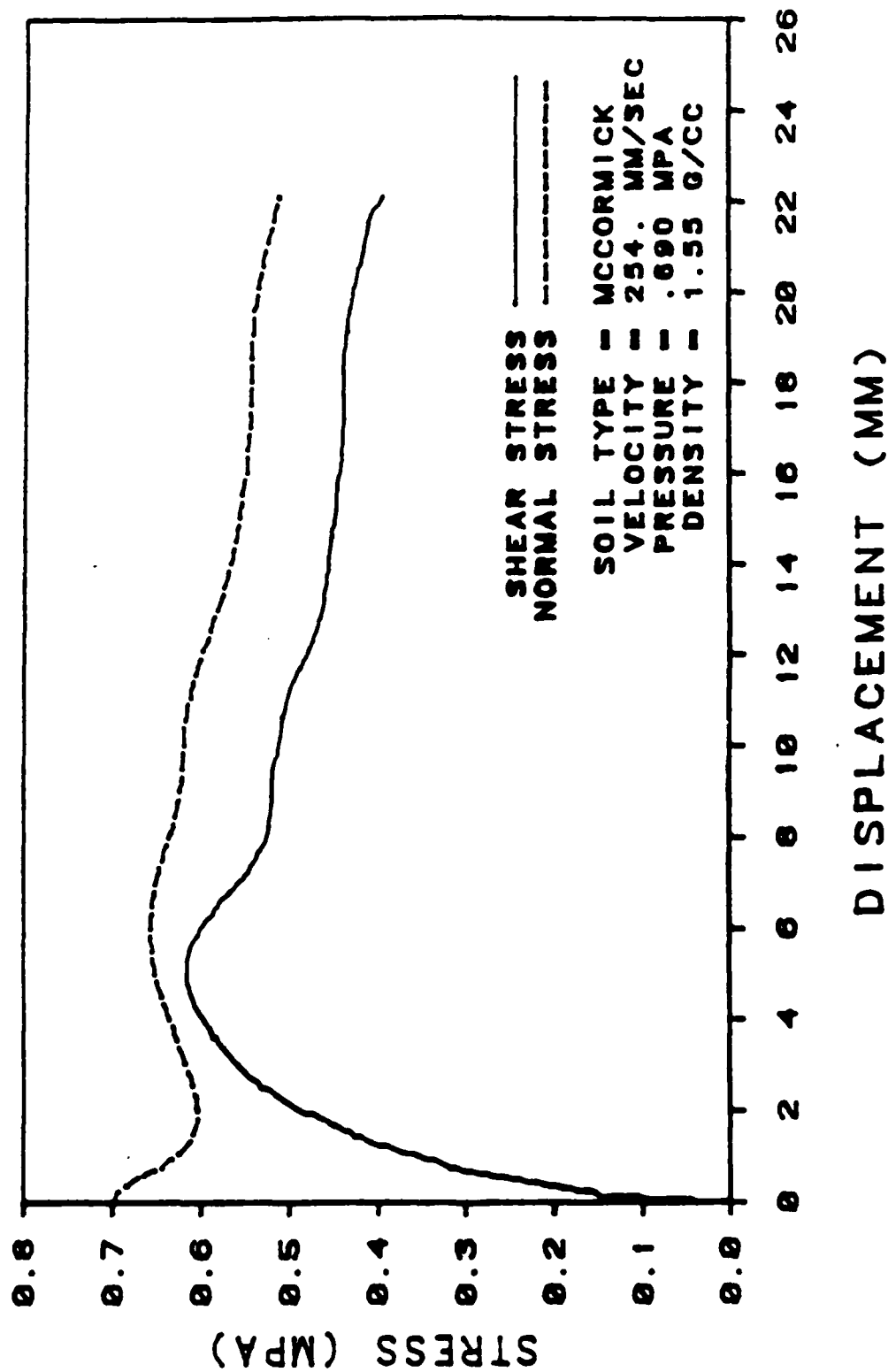


Figure A.38 McCormick Sand/Concrete, V=254. mm/s, P=0.69 MPa, 2nd Repetition.

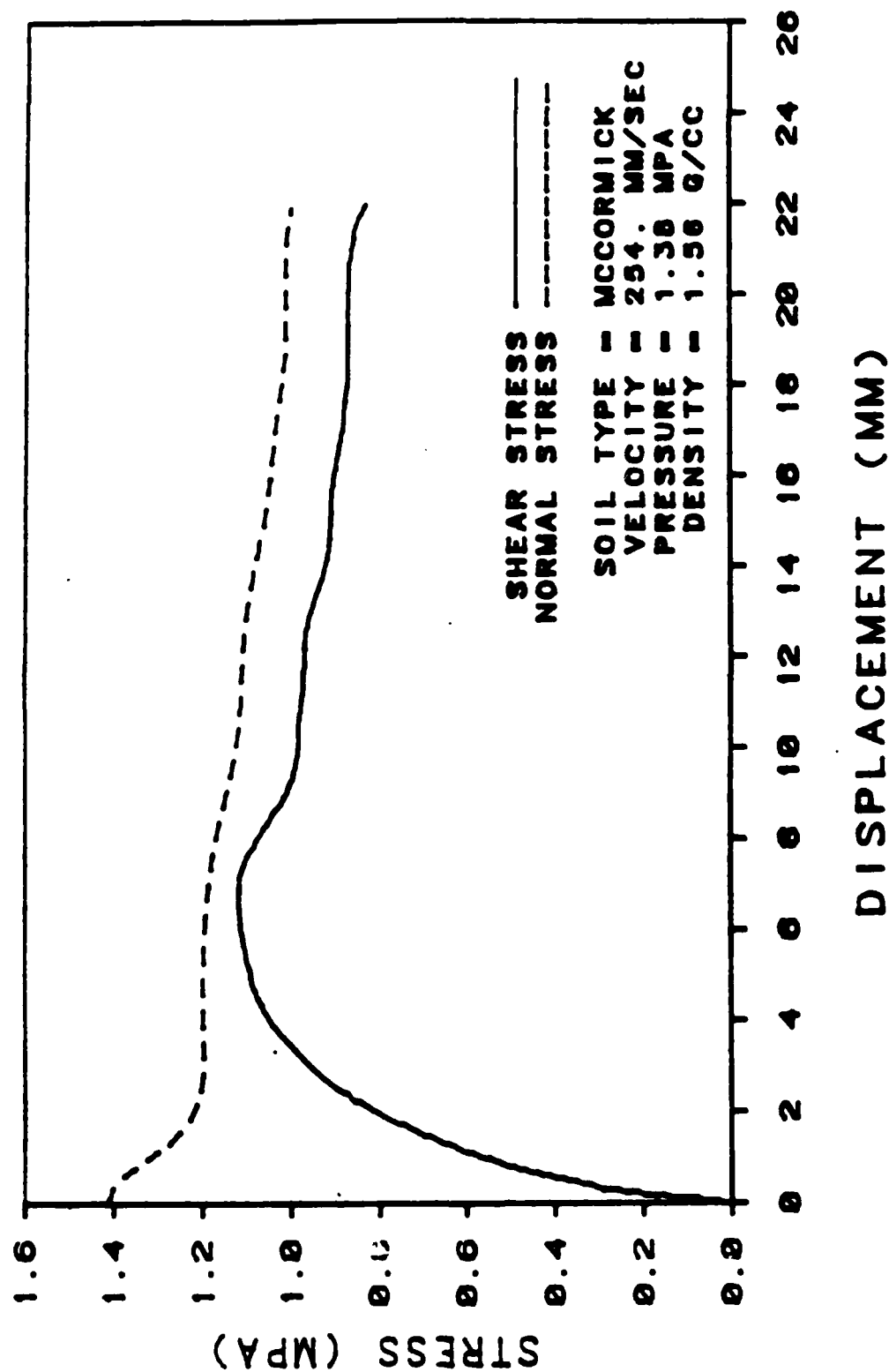


Figure A.39 McCormick Sand/Concrete, $V=254$ mm/s, $P=1.38$ MPa, 1st Repetition.

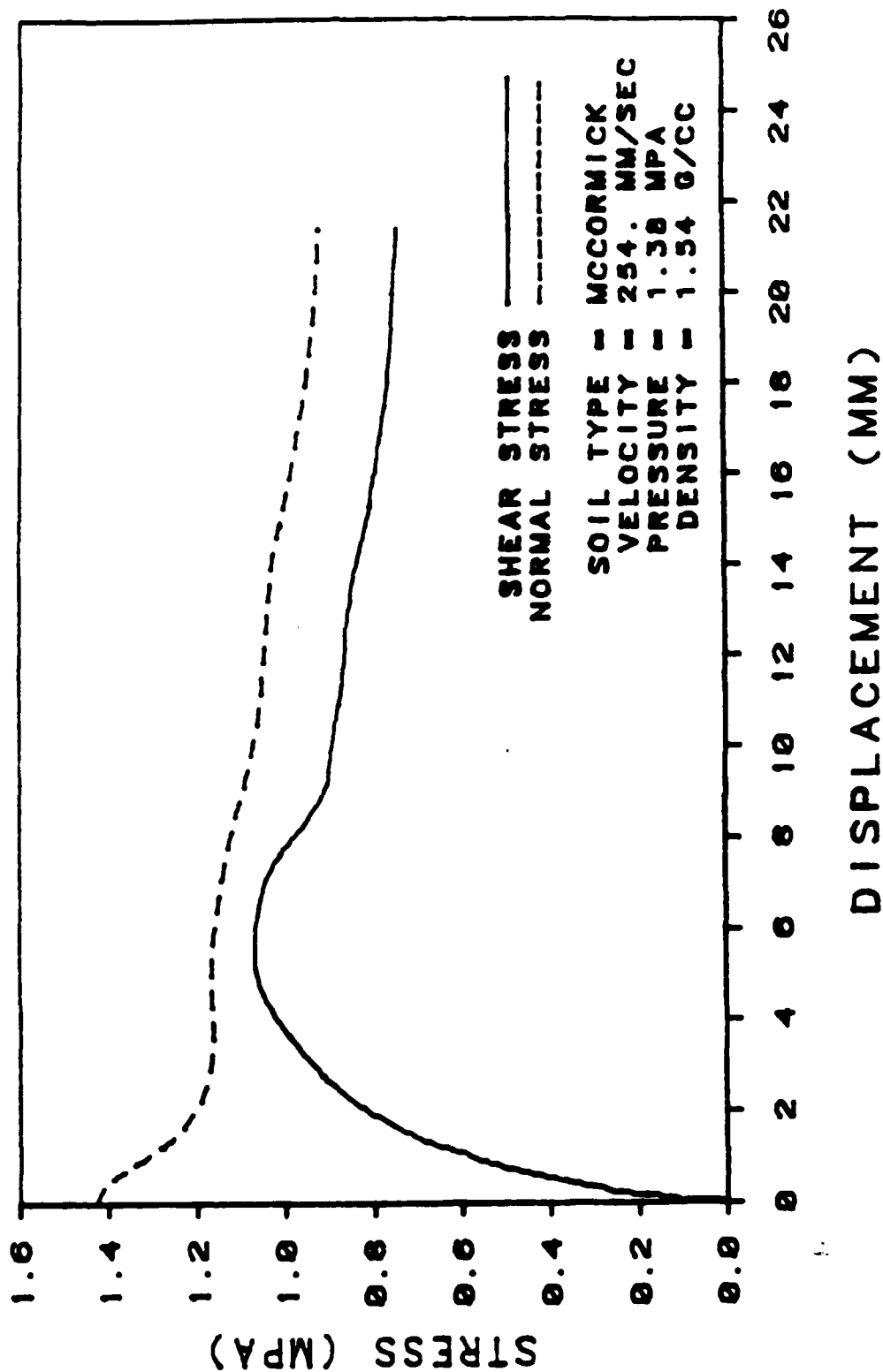


Figure A.40 McCormick Sand/Concrete, $V=254$ mm/s, $P=1.38$ MPa, 2nd Repetition.

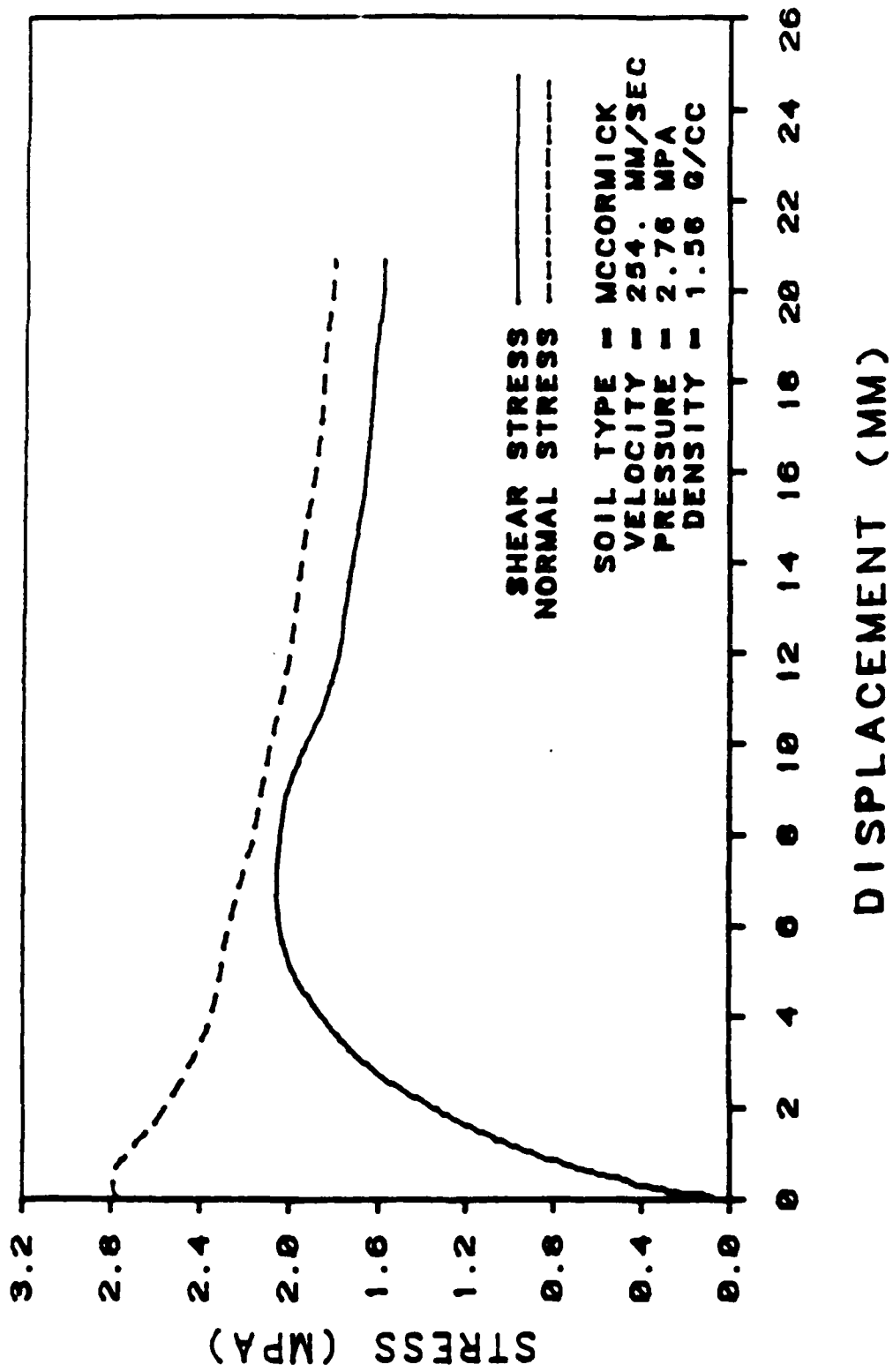


Figure A.41 McCormick Sand/Concrete, $v=254$ mm/s, $p=2.76$ MPa, 1st Repetition.

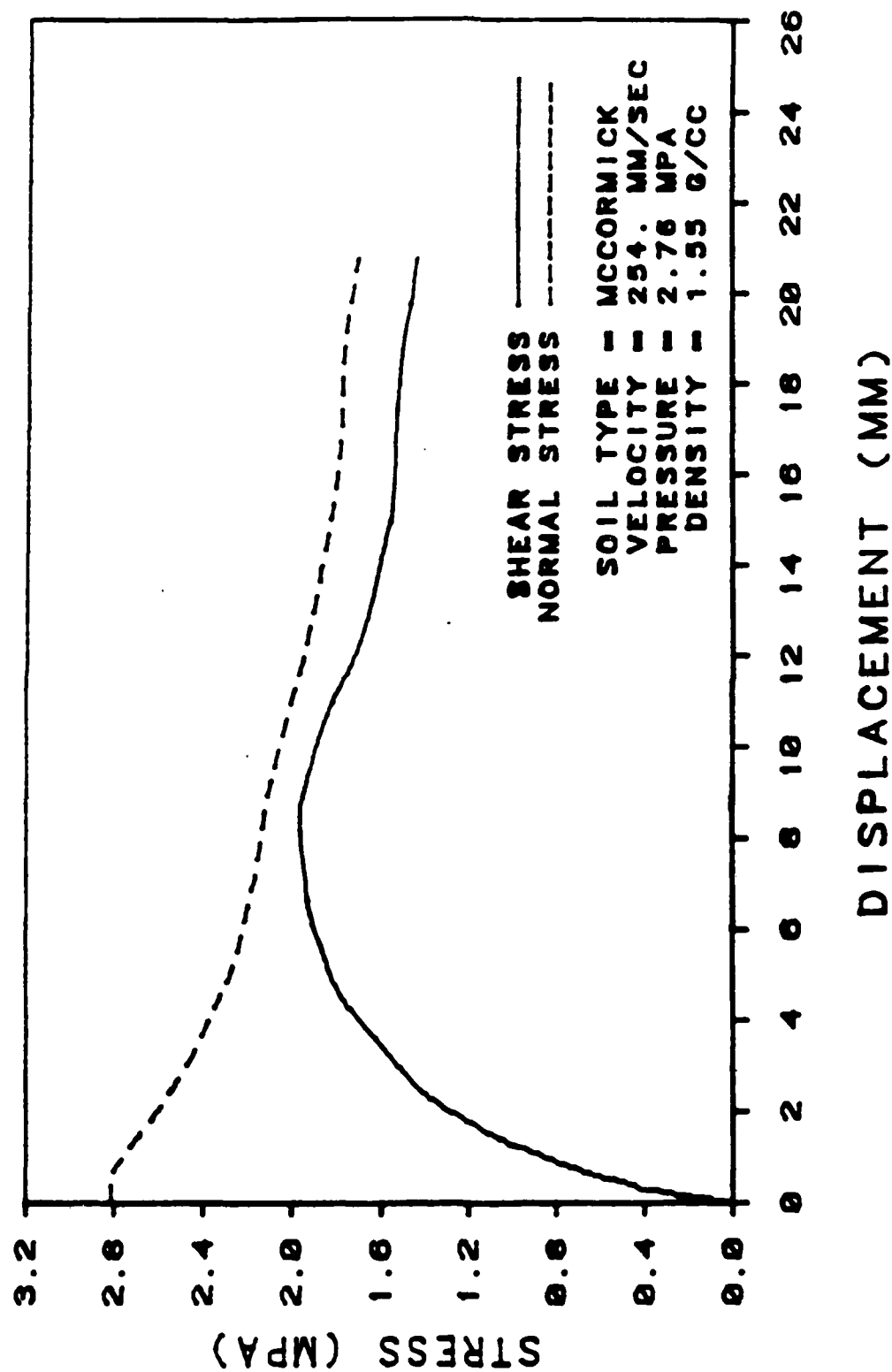


Figure A.42 McCormick Sand/Concrete, $V=254. \text{ mm/s}$, $P=2.76 \text{ MPa}$, 2nd Repetition.

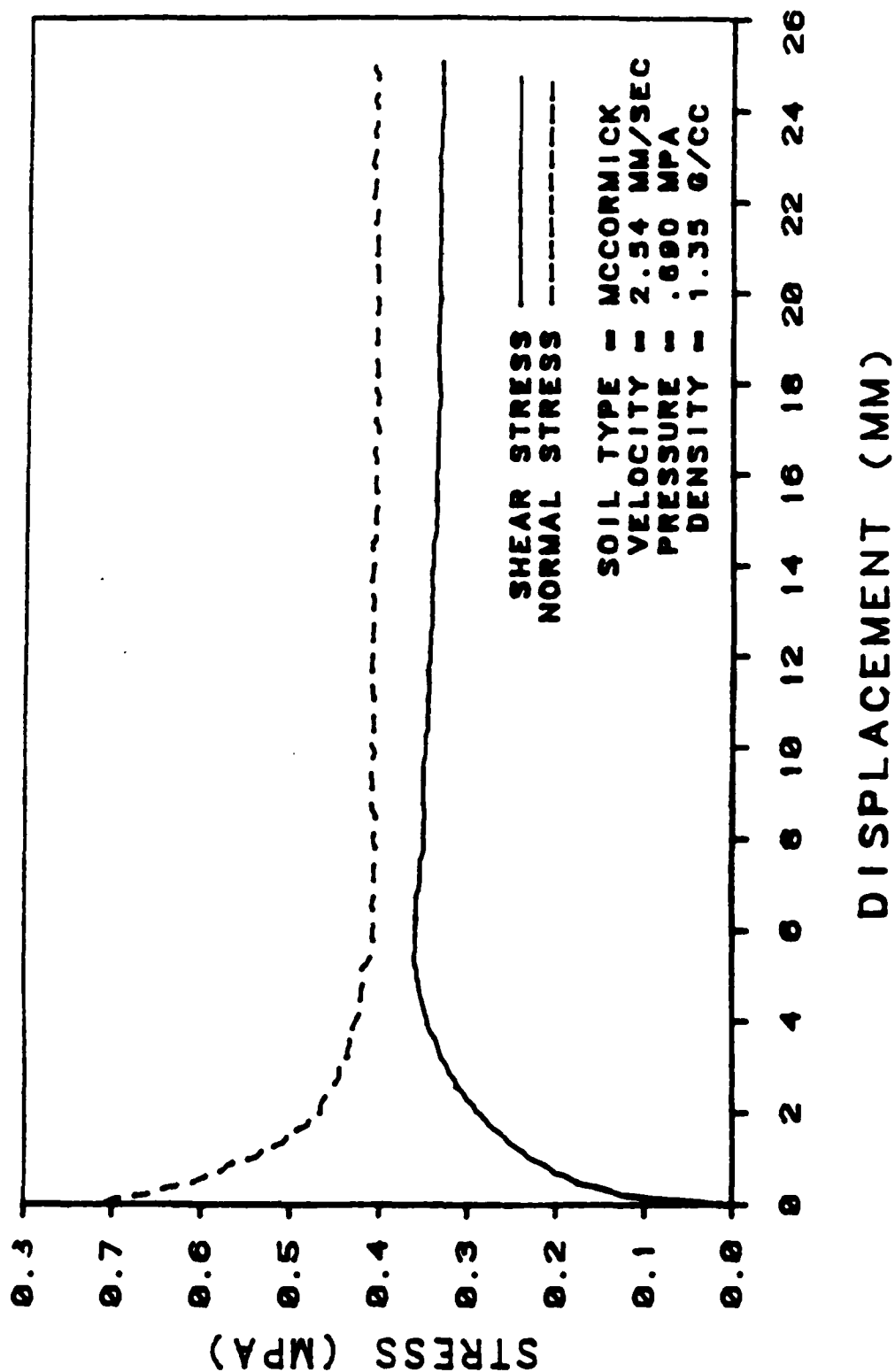


Figure A.43 Loose McCormick Sand/Concrete, $V=2.54$ mm/s, $P=0.69$ MPa.

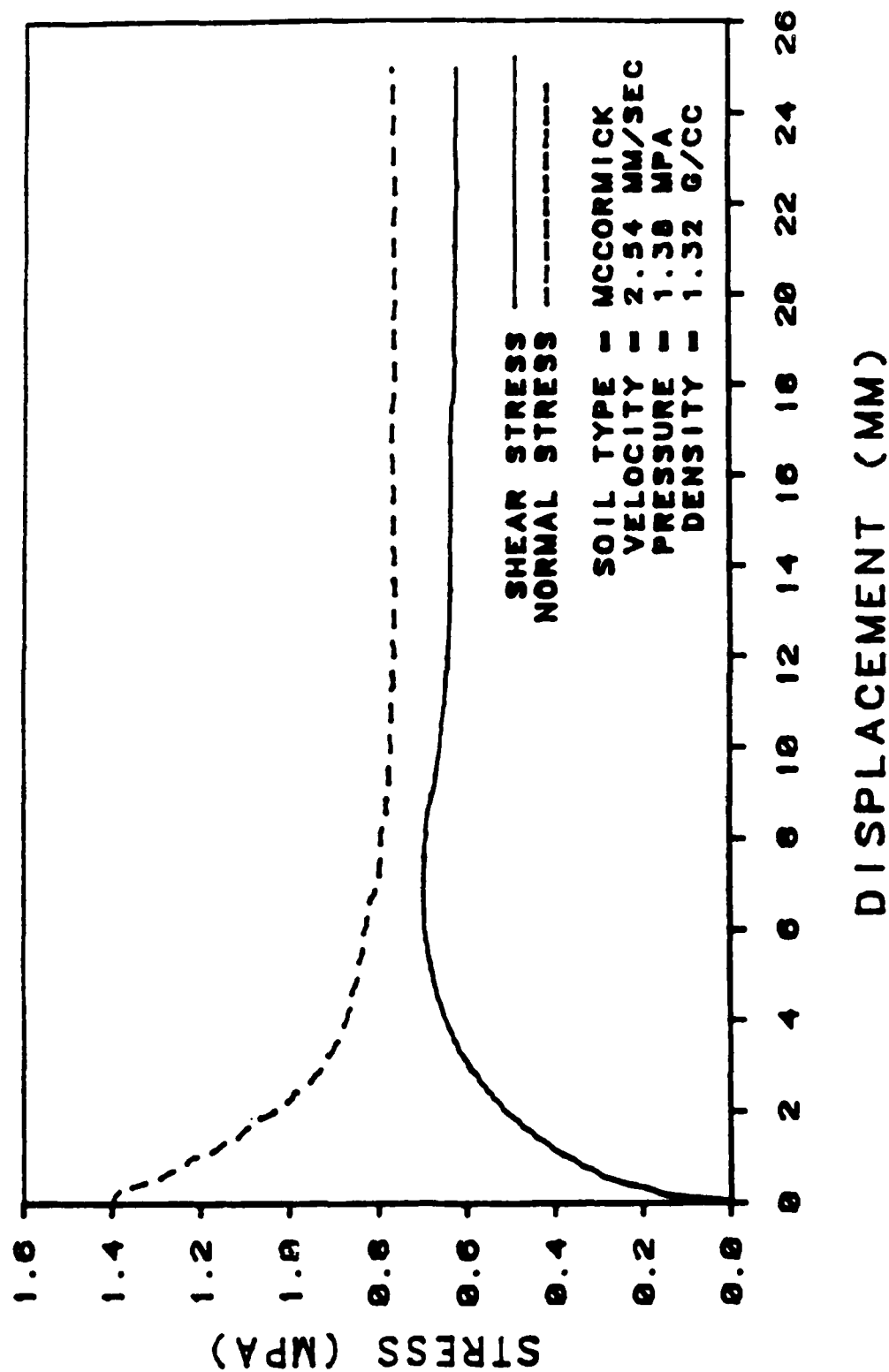


Figure A.44 Loose McCormick Sand/Concrete, $V=2.54$ mm/s, $P=1.38$ MPa.

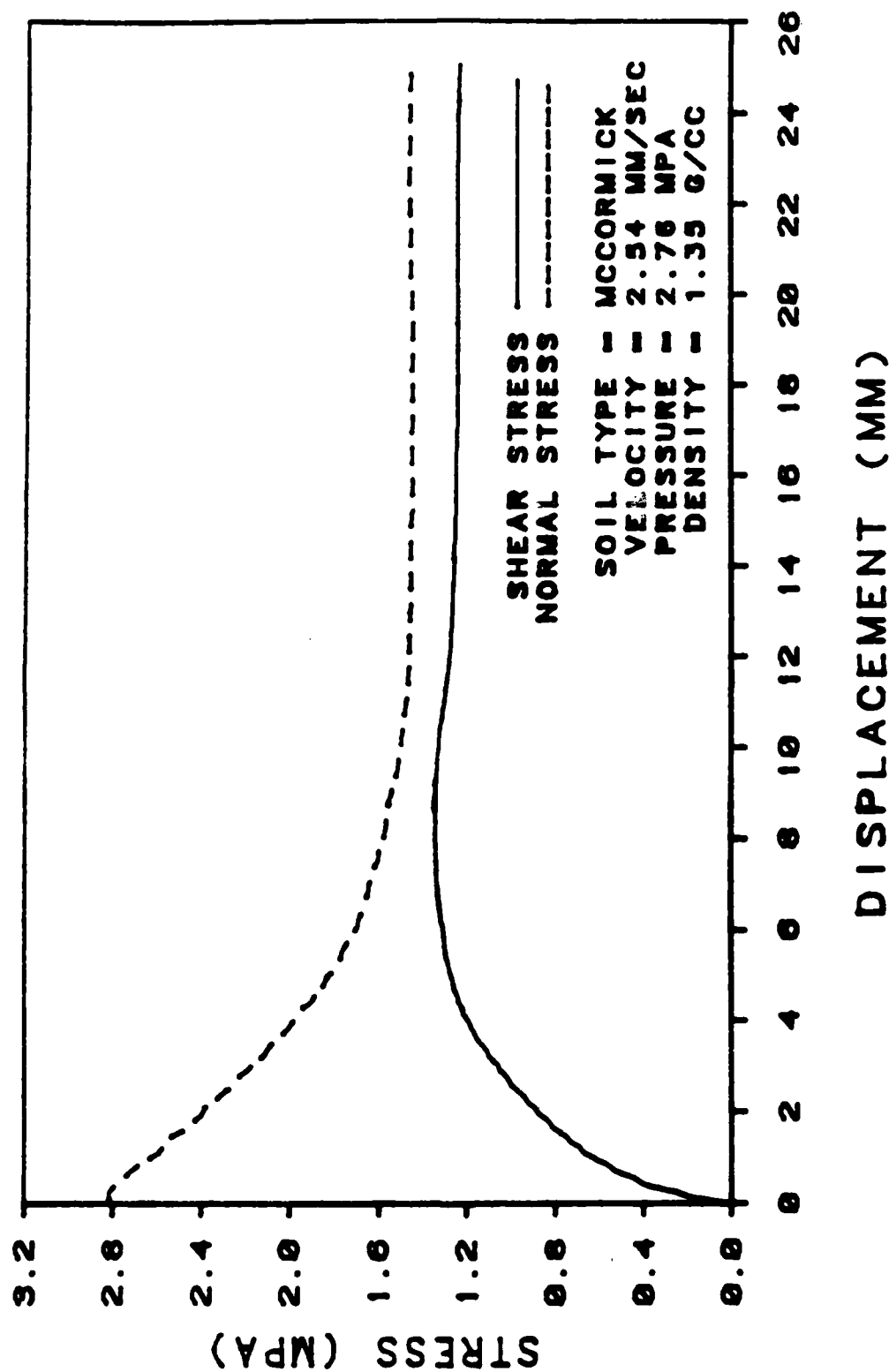


Figure A.45 Loose McCormick Sand/Concrete, $V=2.54$ mm/s, $P=2.76$ MPa.

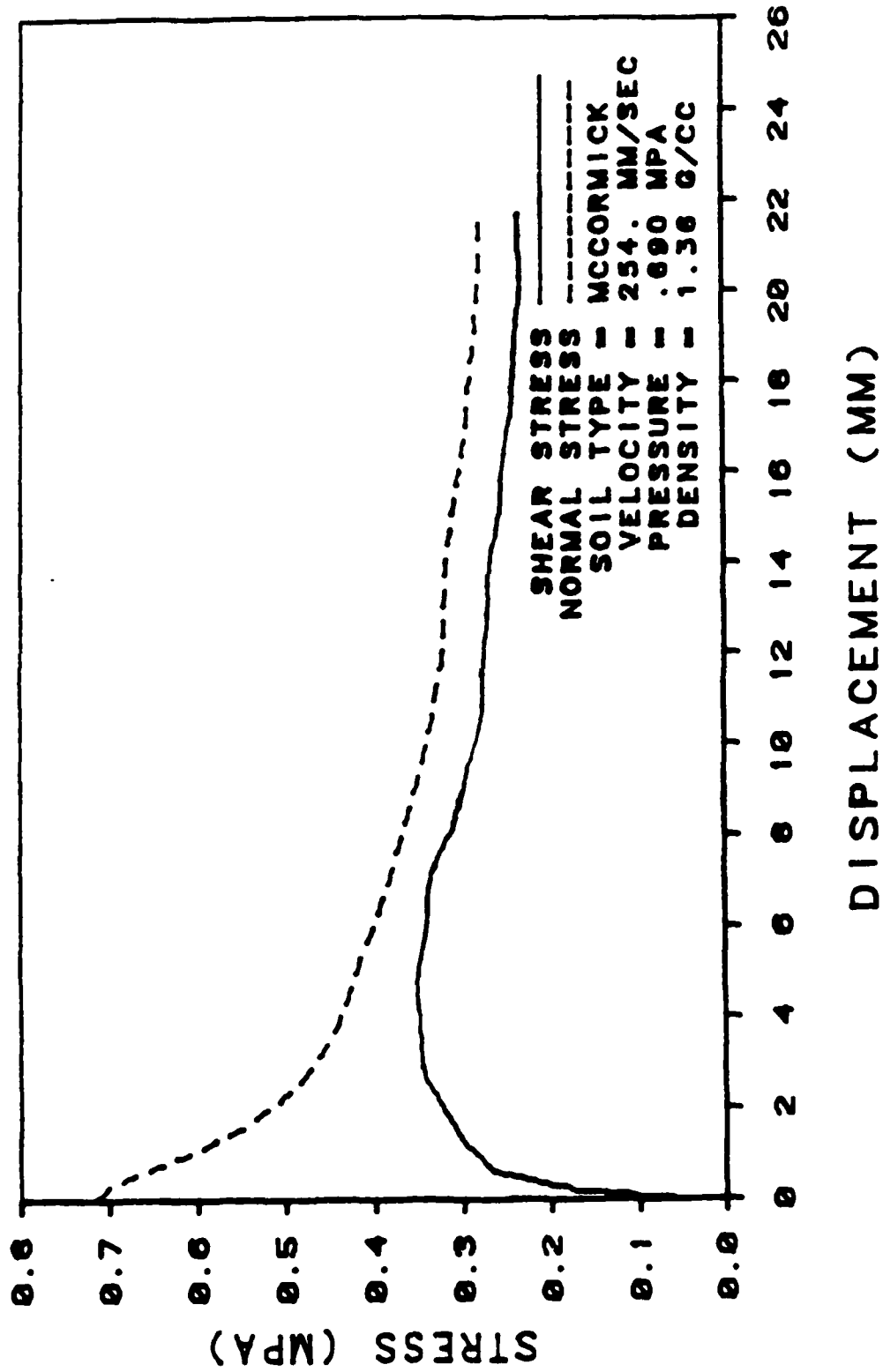


Figure A.46 Loose McCormick Sand/Concrete, V=254. mm/s, P=0.69 MPa.

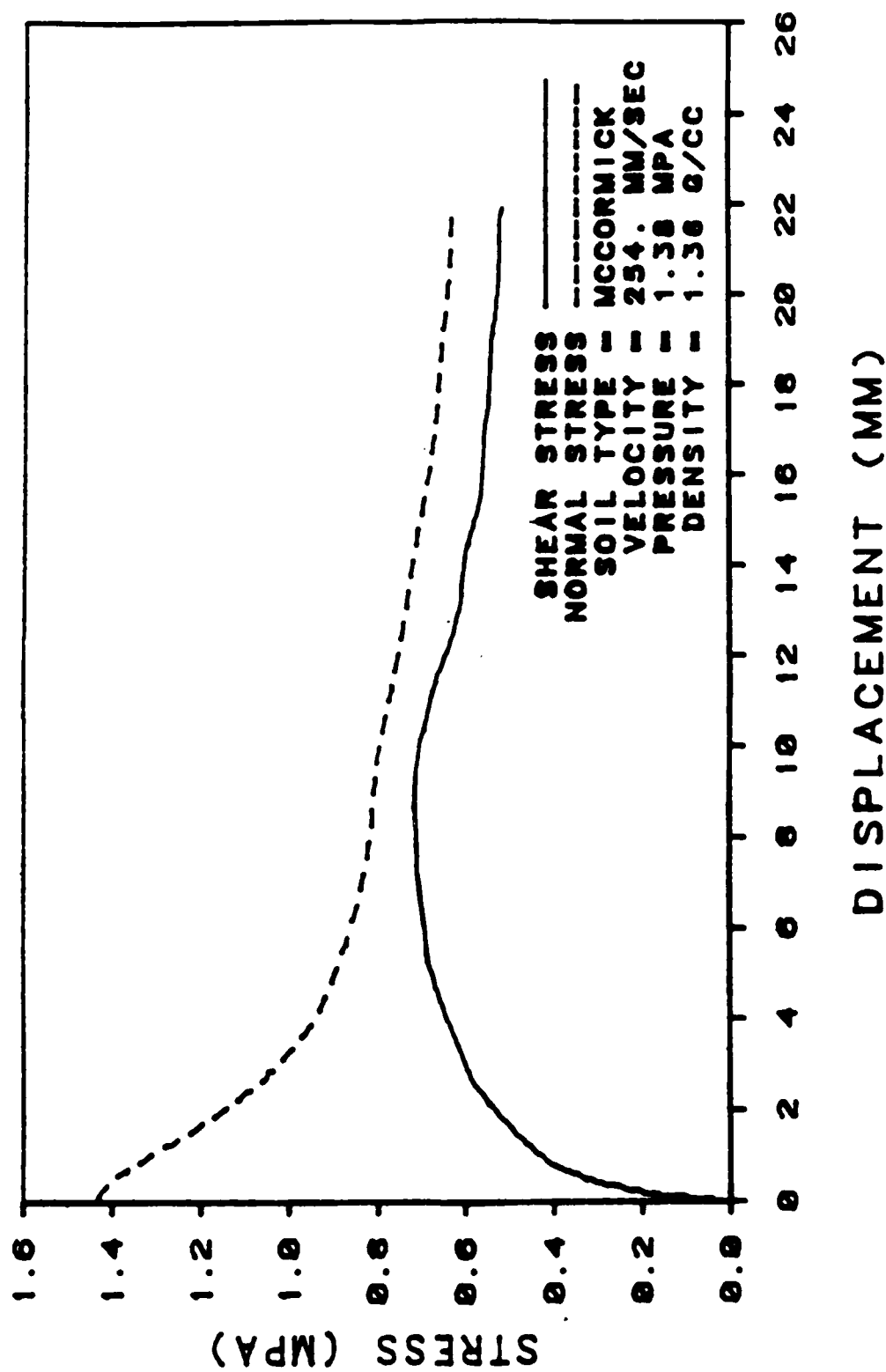


Figure A.47 Loose McCormick Sand/Concrete, $V=254.$ mm/s, $P=1.38$ MPa.

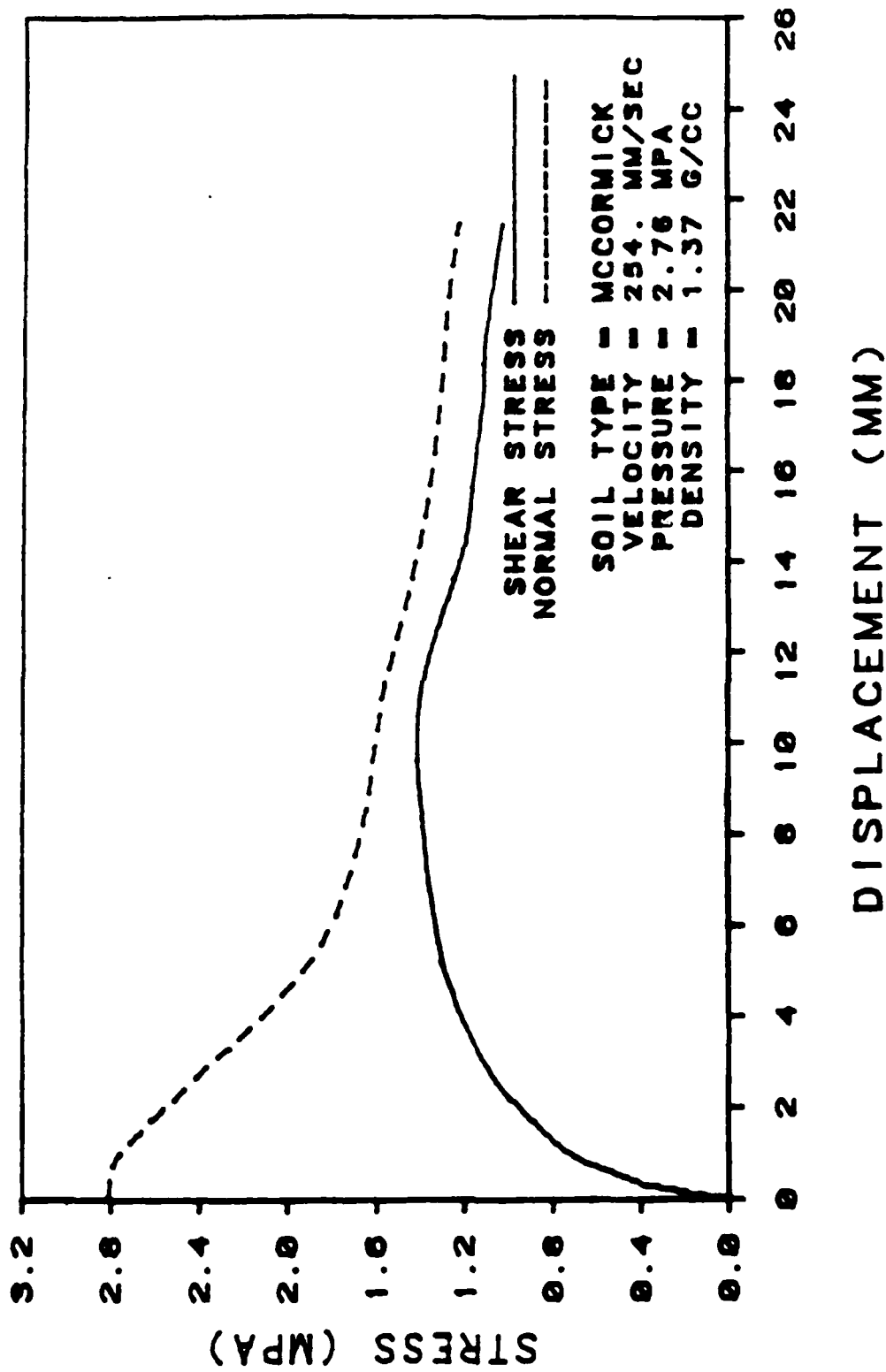


Figure A.48 Loose McCormick Sand/Concrete, $V=254$. mm/s, $P=2.76$ MPa.

END

DATE

FILMED

7-88

Dtic